ABSTRACT

ZHU, YIYING. Synthesis of Bi-Functional Activated Carbon for Removal of *p*-Cresol and Ammonia. (Under the direction of Dr. Praveen Kolar.)

p-Cresol and ammonia are two major pollutions generally present in industrial, agricultural, and domestic wastewaters, which pose a significant threat to the environment as well as public health. Especially, North Carolina ranks second in swine production in the US and the enormous amount of feces, urine, and unconsumed feed are prone to microbiologically decompose into *p*-cresol and ammoniacal nitrogen. It is of great importance to minimize these pollutants in the wastewater prior to their release to the environment. The adsorption using activated carbon is highly efficient and easy to adopt compared to other treatment techniques.

Hence, the present research was focused on the use of the agricultural residues to convert into efficient low-cost activated carbons for *p*-cresol and ammonia uptake. The objectives were to (1) synthesize a highly active alkaline activated carbon for removal of *p*-cresol in aqueous single-solute systems, (2) synthesize an effective acidic activated carbon for adsorption of ammonia in aqueous single-solute systems, and (3) explore a bi-functional activated carbon capable of adsorbing *p*-cresol and ammonia simultaneously in aqueous double-solute systems.

For the first objective, a coconut shell-based activated carbon (CSAC) was first synthesized via physiochemical activation of zinc chloride. Batch experiments were conducted for *p*-cresol adsorption to evaluate the performance of the activated carbon. The effects of different operation parameters such as initial adsorbate concentration (25-500 mg L^{-1}), agitation speed (0-200 rpm), solution pH (2-12), and adsorbent dosage (0.50-3 g 100 mL^{-1}) were examined. Kinetic and equilibrium studies were also carried out. The maximum

monolayer *p*-cresol adsorption capacity for CSAC was found to be 30.23 mg g^{-1} at 293 K, 31.57 mg g^{-1} at 303 K, and 32.77 mg g^{-1} at 313 K.

To improve the adsorption capacity for *p*-cresol further, a coconut shell-based activated carbon (CSAC-SH) was prepared using sodium hydroxide. The characterization of CSAC-SH via Brunauer-Emmitt-Teller (BET) surface area analyzer, scanning electron microscope (SEM), and Boehm titration indicated that CSAC-SH has a well-developed microporous/mesoporous structure with a relatively high surface area of 520.16 m^2 g^{-1} and rich in basic surface functional groups. A maximum monolayer *p*-cresol adsorption capacity of 256.9 mg g^{-1} (298 K) indicated that CSAC-SH was effective in *p*-cresol uptake.

For the second objective, an avocado seed based-activated carbon (AAC-MA) was synthesized using methanesulfonic acid. The effects of pH (3-9), adsorbent dosage (1-20 g L^{-1}), initial ammonia concentrations (50-450 mg L^{-1}) and contact time (0-6 h) on ammonia mitigation were investigated. The pseudo-second order kinetic model and Langmuir isotherm model were found to give the best data correlation to the kinetic and equilibrium data, respectively. A maximum monolayer adsorption capacity of 5.446 mg g^{-1} was found of ammonia on AAC-MA at 298 K.

For the third objective, the previously obtained activated carbon AAC-MA was further investigated by adsorption of *p*-cresol from aqueous single-solute systems. AAC-MA showed reasonably well adsorption capacity for *p*-cresol of 88.03 mg g^{-1}. Further, the same adsorbent was used for simultaneous adsorption of *p*-cresol and ammonia in the binary mixture system. Equilibrium studies were conducted to determine the adsorption behavior and extended Langmuir isotherm model was found to best suitable to describe the experimental data of both *p*-cresol and ammonia. Negligible competitive adsorption between

p-cresol and ammonia was deduced and 87.79 and 3.393 mg g^{-1} maximum monolayer adsorption capacities were determined for *p*-cresol and ammonia in the double solute systems, respectively.

The results indicate that removal of ammonia and *p*-cresol may be effectively accomplished via activated carbons prepared from agricultural residues. If applied to animal agricultural waste management treatment systems, the odor and other pollutants can be minimized, thereby making animal agricultural sustainable and environment friendly.

Synthesis of Bi-Functional Activated Carbon for Removal of *p*-Cresol and Ammonia

by
Yiying Zhu

A dissertation submitted to the Graduate Faculty of
North Carolina State University
in partial fulfillment of the
requirements for the degree of
Doctor of Philosophy

Biological and Agricultural Engineering

Raleigh, North Carolina

2016

APPROVED BY:

_____	_____
Dr. Praveen Kolar Committee Chair	Dr. Sanjay B. Shah
_____	_____
Dr. Jay J. Cheng	Dr. Phooi K. Lim

DEDICATION

This dissertation is gratefully dedicated to my dear parents Lidi Zhu, Chunling Yang, and my beloved husband Shijing Lu, whose endless love, support and encouragement helped me throughout the years.

BIOGRAPHY

Yiying Zhu was born and grew up in a beautiful city of Linhai, Zhejiang, China. She earned her bachelor's degree in Chemical Engineering in 2009 from China. In 2010, she moved to United States to pursue her master's degree at Syracuse University and earned her MS degree in Chemical Engineering in 2012. Soon after she began working on her doctoral studies at North Carolina State University and will receive her Ph.D. in Biological and Agricultural Engineering with a minor in Chemical Engineering in May 2016.

ACKNOWLEDGMENTS

This dissertation would not have been accomplished in present form without the invaluable help and support from others. I would like to take this opportunity to express my immeasurable appreciation and gratitude to the following persons and organizations.

First of all, I want to thank my advisor, Dr. Praveen Kolar, for his continuous support, guidance and help over the years during my stay at North Carolina State University. This dissertation would not have been completed without his constant feedback and advices.

Special thanks and gratitude go to Drs. Sanjay B. Shah, Jay J. Cheng, and P.K. Lim for serving on my committee and providing valuable comments and suggestions.

I sincerely acknowledge Solid Waste Association of North America (SWANA) of North Carolina Chapter and Air & Waste Management Association (AWMA) for awarding me several scholarships. Thanks are also given to the engineering honor society of Tau Beta Pi for inducting me as a top student. These honors gave me tremendous confidence and encouragement to face difficulties in research.

Thanks are due to Drs. Ratna Sharma-Shivappa, Walter Weare, Thomas B. Whitaker, Chuanzhen Zhou, Dhana Savithri, Weizong Xu, Tao Huang, Ms. Rachel Huie, and Mr. Charles Mooney for lab analysis, discussion and help.

I am grateful to Lalitendu Das for his help hands in lab and sharing valuable experiences and thoughts. I would like to thank my other lab mates Yane, Han, Brianna and all the other dear friends and faculties in BAE department. Thanks are also due to Nicole Dobbs, Kevin Koryto, and Jessie Fears for giving me helpful comments on this dissertation.

I would like to express my most precious gratitude to my beloved parents, Mr. Lidi Zhu and Ms. Chunling Yang, for their selfless love, support, patience, and encouragement. Without them, this work could not have been possible. No matter how badly I failed, I always knew that they would treat me like a winner. And no matter how down I was, their hugs and warm words always magically wiped out my frowns. Thank them for being there day after day to make sure my life is on a right track and surround by happiness. I would also like to thank all my other dear family members and a group of best friends for being so supportive.

My deepest appreciation and dearest love go to my cherished, talented husband, Dr. Shijing Lu, for his endless love, support and always being there for me during this meaningful journey. Pursuing a doctorate degree had considerably more difficulties than I had ever expected. I strived, he supported. I flinched, he encouraged. I cried, he reassured. Without his company, love, guidance, and help, I would not have overcome these problems and have gone this far in academics and thanks him for giving me the wings.

TABLE OF CONTENTS

LIST OF TABLES

LIST OF FIGURES

CHAPTER 1

INTRODUCTION

1.1 Background

In today's society, the treatment of wastewater has been drawing more and more attention due to increasing water pollution. Industrial effluents from metal, plastic, food, and pharmaceutical industries are important causes of water pollution, since most industrial wastewaters contain some hazardous and noxious pollutants such as phenols which are very harmful to living beings (Viraraghavan and de Maria Alfaro, 1998).

Animal agriculture, especially, pork and poultry farming are also important sources of water pollution and odor emissions. Pork and poultry populations have expanded tremendously over the years, to meet the rising demand of the increasing human population. The United States is the largest poultry producer and the second-largest pork producer, exporting over 4 billion pounds of pork since the beginning of the 21st century which accounted for 39% of the world pork export (USDA NASS 2012). North Carolina is the second-largest pork producing state in the US (USDA NASS 2010).

The environmental concerns associated with the livestock facilities are related to the increased production of farm waste and odor. In hog farming, wastes including urine, faces and waste water stored in the pits or lagoons generate unpleasant odorants from the metabolism by microorganism (Cook et al., 2010). Phenols and indoles are present in the highest concentrations among the volatile organic compounds produced from swine slurry.

From the evaluation of odor intensity, *p*-cresol, skatole, 4-ethylphenol and acetic acid were the most significant contaminants associated with the malodor (Blanes-Vidal et al., 2009).

As one important source of the pollutants, the presence of phenols is also one of the main contributors to the unpleasant odor and taste of drinking water. From a report by Akbal (2005), when phenols are present, chlorophenols are generated during the chlorination process of disinfection of potable water. Calace et al. (2002) reported that even minute concentrations of phenols were deleterious to organisms. In addition, Dąbrowski et al. (2005) pointed out that most of the phenolic compounds were identified to be toxic carcinogens. In order to ensure the quality of drinking water, stringent legislations have been proposed. The European Union (EU) stated that the total concentration of phenols should be reduced to less than 0.5 ug/L, and individual compounds should be kept below 0.1 µg/L in drinking water (Rodríguez et al., 2000).

p-Cresol $(CH_3)C_6H_4(OH)$ is a volatile organic compound (VOC) which is a member of the large family of the phenols. It is identified to be significantly responsible for the malodor in hog farming operation and is also found in industrial effluents (Yasuhara, 1980). It is very harmful to water and air quality. Even in trace amounts, it has negative effects on human skin, eyes and mental health (Singh et al., 2008; Das et al., 2012).

Ammonia nitrogen, as another harmful pollutant, can harm aquatic animals and plants due to eutrophication, decrease atmospheric visibility, and increase soil acidification (Love et al., 2011). Ammonia is characteristic of pungent smell which is an odor nuisance. The release of the ammonia is an important contributor to the malodor of the swine slurry. The

concentration of ammonia in swine lagoon usually ranges from 100 to 1000 mg/L (Love et al., 2011).

Removal of toxic and recalcitrant pollutants in wastewater and improving animal waste storage and handling to minimize their negative effects on the environment is of great importance. Otherwise, the wastewater will be a serious problem that can lead to large scale damage to humans and aquatic life. This research will focus on mitigating two important contaminants, namely, *p*-cresol and ammonia from aqueous solutions.

1.2 Research needs, proposed work and significance

Adsorption using, using activated carbon, is highly efficient and easy to perform compared to other pretreatment techniques. Studies have only been conducted to synthesize activated carbon for removal of ammonia and *p*-cresol separately.

This research will not only focused on preparing high-performance absorbents from low-cost agricultural waste materials to mitigate *p*-cresol and ammonia separately, but also to fill the gap to synthesize a bi-functional activated carbon capable of adsorbing them simultaneously. Synthesis of activated carbon mainly involves the activation step with either acid or alkali and followed by carbonization. The activated carbon is conditioned by different synthesis parameters such as raw materials, activating agents, carbonaceous temperature, time, and impregnation ratio, and these effects will be adjusted to fulfill the goals.

Batch adsorption experiments will be performed to determine the adsorption capacity of the activated carbons. The concentration changes of *p*-cresol and ammonia after exposure to activated carbon for a certain time will be quantified by UV spectrometer, Nesslerization

or automated phenate method, respectively. Characterization of the activated carbons will be conducted by different technologies of BET surface area analyzer, scanning electron microscope (SEM), time-of-flight secondary ion mass spectrometer (TOF-SIMS), and Fourier transformation infrared spectroscopy (FTIR) as screening methods for selection of high quality adsorbents. Different factors that affect adsorption, such as, contact time, agitation speed, adsorbent dosage, temperature and pH will be discussed. Studies of the kinetics, isotherms, thermodynamics, and mechanism of adsorption will also be carried out. Whether the presence of *p*-cresol and ammonia will inhibit the adsorption of one other due to competition between them on the activated sites will also be examined.

Lab-scale production of high quality bi-functional adsorbents might be scaled up for practical use with more efforts of investigations in the future. This application of bi-functional technology has a favorable prospect and could be extended in other domains such as for production of bi-functional catalysts in petrochemical and biofuel areas. Taking the production of biodiesel fuel as an example, conventional alkaline catalyst will be consumed and lose effectiveness due to the saponification reaction with free fatty acids (FFAs), which reduces the yield. However, if the bi-functional catalyst is invented, its acidic nature will help prevent the saponification reaction. Besides, the production could be enhanced by conversion of the FFAs to biodiesel compounds-fatty acid methyl esters (FAMEs).

1.3 Organization of this dissertation

This dissertation consists of 7 chapters. Chapter 2 is literature review, which endeavors to provide readers an overview of the technology of the adsorption by activated

carbon as well as problems and challenges encountered in using this means for removal of *p*-cresol and ammonia. Chapter 3 presents the results of the adsorption of *p*-cresol by a prepared coconut shell based-activated carbon (CSAC) activated by zinc chloride. Chapter 4 examines the removal of *p*-cresol using another highly active coconut shell-activated carbon (CSAC-SH) activated by sodium hydroxide. Chapter 5 summarizes the observations of the mitigation of ammonia in aqueous solutions using a prepared avocado seed based-activated carbon (AAC-MA) activated via methanesulfonic acid. Chapter 6 presents the results of the investigations of adsorption of *p*-cresol using AAC-MA, and also the simultaneous removal of *p*-cresol and ammonia by AAC-MA. Chapter 7 discusses the future direction and ideas based on this study.

REFERENCES

Akbal, F., 2005. Sorption of phenol and 4-chlorophenol onto pumice treated with cationic surfactant, J. Environ. Manage. 74, 239-244. doi: 10.1016/j.jenvman.2004.10.001.

Blanes-Vidal, V., Hansen, M.N., Adamsen, A.P.S., Feilberg, A., Petersen, S.O., Jensen, B.B., 2009. Characterization of odor released during handling of swine slurry: Part I. Relationship between odorants and perceived odor concentrations, Atmos. Environ. 43, 2997-3005. doi: 10.1016/j.atmosenv.2008.10.016.

Calace, N., Nardi, E., Petronio, B.M., Pietroletti, M., 2002. Adsorption of phenols by papermill sludges, Environ. Pollut. 118, 315-319. doi: 10.1016/S0269-7491(01)00303-7.

Cook, K.L., Rothrock Jr., M.J., Lovanh, N., Sorrell, J.K., Loughrin, J.H., 2010. Spatial and temporal changes in the microbial community in an anaerobic swine waste treatment lagoon, Anaerobe 16, 74-82. doi: 10.1016/j.anaerobe.2009.06.003.

Dąbrowski, A., Podkościelny, P., Hubicki, Z., Barczak, M., 2005. Adsorption of phenolic compounds by activated carbon—a critical review, Chemosphere 58, 1049-1070. doi: 10.1016/j.chemosphere.2004.09.067.

Das, L., Kolar, P., Osborne, J.A., Classen, J.J., 2012. Adsorption of *p*-cresol on granular activated carbon. Agric. Engin. Int.: CIGR Journal 14.

Love, C., Kolar, P., Classen, J., Das, L., 2011. Adsorption of ammonia on ozonated activated carbon, T. ASABE 54, 1931-1940.

Rodríguez, I., Llompart, M.P., Cela, R., 2000. Solid-phase extraction of phenols, Journal of Chromatography A 885, 291-304. doi: 10.1016/S0021-9673(00)00116-3.

Singh, R. K., Kumar, S., Kumar, S., and Kumar, A., 2008. Development of parthenium based activated carbon and its utilization for adsorptive removal of p-cresol from aqueous solution. J. Hazard. Mater. 155, 523-535. doi:10.1016/j.jhazmat.2007.11.117

Viraraghavan, T., de Maria Alfaro, F., 1998. Adsorption of phenol from wastewater by peat, fly ash and bentonite, J. Hazard. Mater. 57, 59-70. doi: 10.1016/S0304-3894(97)00062-9.

Yasuhara, A., 1980. Relation between odor and odorous components in solid swine manure, Chemosphere 9, 587-592. doi: 10.1016/0045-6535(80)90077-6.

CHAPTER 2

LITERATURE REVIEW

In this Chapter, a review of adsorption using activated carbon related to this study is presented. The effects of various process parameters on preparation of activated carbon and adsorption are discussed. An overview on adsorption kinetics, isotherms and mechanism is also provided. Finally, various regeneration methods of spent activated carbon are also reviewed.

2.1 Wastewater treatment by adsorption

Generally, people will face some difficulties with regard to wastewater treatment since some pollutants are volatile, not easily biodegradable during secondary (biological) treatment, or exist in small concentrations. Treatment methods can be broadly classified as physical, chemical, and biological processes. Ion exchange, electrolysis, filtration, adsorption, coagulation, solvent extraction, and foam floatation are different wastewater technologies (Bhatnagar and Sillanpää, 2010). However, most of them are restricted by the cost factors since they are in a demand of considerable financial input, which makes the pollution control less favorable. Among all the treatment processes, adsorption is proved to be highly efficient, and easy to perform.

Adsorption is an accumulation process where certain chemicals are extracted from one phase and bonded onto the surface of another phase (Dąbrowski, 2001). Adsorption involves two different types of interactions, physical adsorption and chemical adsorption.

Physisorption is caused mainly by weak van der Waals forces and is reversible. It can consist of multilayers of adsorbate on the adsorption surface. Chemisorption is characterized by covalent bonding, which is single layer adsorption. Adsorption techniques are commonly applied to remove organic or inorganic contaminants from wastewater such as phenols, Cu (II), and Nickel (II).

In the adsorption process, as illustrated in Fig. 2.1, adsorbates such as ammonia and *p*-cresol in the original aqueous solution will first transport from the bulk to the external surface of adsorbents, then further transport into pores for internal adsorption.

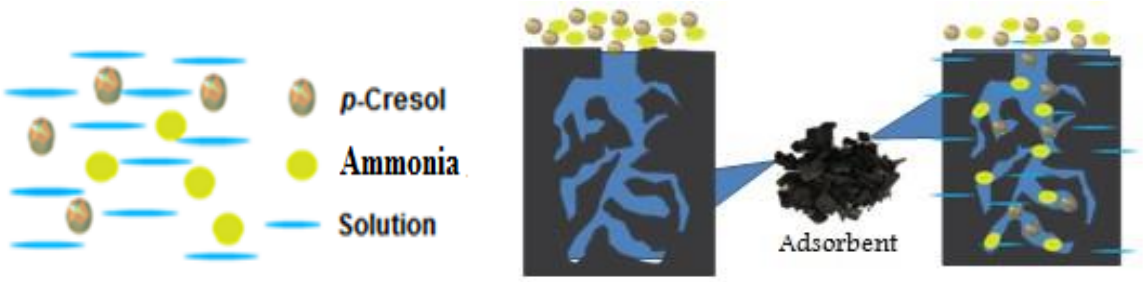

Fig. 2.1: Illustration of adsorption phenomenon.

2.2 Activated carbon (AC) as favored adsorbent

Adsorption for reducing pollutant concentrations in wastewaters before final discharge calls for effort to explore some effective adsorbents. A variety of adsorbents have been used in selective adsorption studies, for instance, activated carbon, biological materials,

synthetic resins, and mineral oxides (Mohan and Singh, 2002). Among these, activated carbon (AC) is the best and most widely used adsorbent for a certain class of pollutants. It is acknowledged to be an efficient adsorbent for organic compounds removal, especially the comparatively low molecular weight compounds such as phenols (Dąbrowski et al., 2005).

Activated carbon is a class of highly carbonaceous materials. They are also named activated charcoal, or activated coal, and they are similar to a char in appearance. Activated carbons own their high adsorption capacities to their high micro pore structure, extremely large surface areas and adjustable nature as affected by different chemical or physical treatments.

Activated carbon is generally made with particle sizes up to a few millimeters. In addition, Streat et al. (1995) stated that the surface area of activated carbon ranges from 600 m^2/g up to 2000 m^2/g and the average opening pore is as small as 1.5 nm. These qualities are vital for the activated carbon to adsorb and accumulate pollutants from the aqueous phase into the interface of that phase and the adsorbent (solid) phase.

2.2.1 Raw materials for activated carbon production

Activated carbons can be produced from a wide range of raw materials which include most of the carbonaceous materials. Conventional activated carbons are derived from some natural materials such as coal, lignite, and wood (Streat et al., 1995).

Amongst all these materials, coal is the most popular precursor for activation carbon manufacture due to its broad availability, inherent microstructure, and comparatively low

price (Ahmaruzzaman, 2008; CarrascoMarin et al., 1996). Coal is a blend of carbonaceous and mineral materials stemming from the degradation of plants.

However, for the activated carbon production from coal, existence of mineral content is the most serious defect since it will remain in the coal's structure and increases the inert part of the activated carbon samples (IllanGomez et al., 1996; Sun et al., 1997). Rodríguez-Reinoso (1998) stated that the unwanted ash content of the resulting activated carbon was as high as 10% to 15%. Another drawback is pointed out by Ehrburger et al. (1986) who said that in chemical activation process, minerals like SiO_2, FeS, Al_2O_3 will consume the alkaline activating agents like KOH or K_2CO_3, and thereby inhibit the formation of activated sites and porosity.

Although conventional materials play an important role in the activated carbon industry, there is a trend to replace them. High initial cost and expensive regeneration of activated carbon motivates the search for some lower cost, disposable ACs from other feedstocks. Madhava et al. (2006) perceived that this imperious need had created a growing interest in deriving the activated carbon from the locally and cheaper available waste materials.

Correspondingly, different studies have being conducted for producing activated carbon from some solid agriculture wastes, such as, Ahmadpour and Do (1997) with macadamia nutshell, Mohan and Singh (2002) with bagasse, Boudrahem et al. (2009) with coffee residue, Foo and Hameed (2012) with orange peel, and Ma et al. (2015) with banana peel. Sud et al. (2008) quoted various other agriculture wastes like sawdust, rice husk, black

gram husk, waste tea leaves, and bark of trees. These low-cost materials are very attractive; for example, Ahmaruzzaman (2008) mentioned that bark is a rich forest residue and rice husk is an abundant byproduct from the rice milling industry with about more than 100 million tonnes.

Adsorption effectiveness and performance is another important screening criterion for choosing feedstock other than cost effectiveness, carbon content, and availability. Activated carbons from different types of raw materials possess different adsorption properties. For example, Colella et al. (1998) studied the adsorption isotherms of a wood-based (Chemviron carbon) and a lignite-based activated carbons for chlorinated phenols removal. Their result indicated that wood-based activated carbon had stronger adsorption ability compared to the lignite-based one. Besides, the presence of additional inorganic solutes had almost no effect on adsorption. Sun et al. (1997) stated that because lignite was less aromatic in structure, its produced surface area and micropore volume of ACs were lower. The influence of substrate on the performance of AC is presented in Table 2.1.

The following criteria should be considered in relation to the selection of materials:

- Low cost and easy availability
- Low mineral and high carbonaceous content
- Ease of activation (e.g., calcined coke is very hard to activate while wood char is quite easy)
- Low degradation during storage
- High adsorption capacity

Table 2.1: Properties of activated carbon manufactured from different feedstocks (Dąbrowski et al., 2005). Reused with Elsevier's permission (attached in Appendix A).

Raw material	Carbon (mass %)	Volatiles (mass %)	Density ($cm^3 g^{-1}$)	Ash (mass %)	Texture of activated carbon
Soft wood	40–45	55–60	0.4–0.5	0.3–1.1	Soft, large pore volume
Hard wood	40–42	55–60	0.55–0.8	0.3–1.2	Soft, large pore volume
Lignin	35–40	58–60	0.3–0.4	–	Soft, large pore volume
Nutshells	40–45	55–60	1.40	–	Hard, large micropore volume
Lignite	55–70	25–40	1.0–1.35	5–6	Hard, small pore volume
Soft coal	65–80	20–30	1.25–1.5	2–12	Medium hard, medium pore volume
Petroleum coke	70–85	15–20	1.35	0.5–0.7	Medium hard, medium pore volume
Semi-hard coal	70–75	10–15	1.45	5–15	Hard, large pore volume
Hard coal	85–95	5–15	1.5–1.8	2–15	Hard, large pore volume

2.2.2 Procedures for activated carbon preparation

Activated carbons are prepared mainly via two procedures-one is thermal pyrolysis process while another is activation step. Pyrolysis of the feedstock is typically carried out at a low temperature between 400 ^oC and 700 ^oC (Mui et al., 2004). This process helps the raw materials get rid of the light portions and leave the heavier fraction to turn into a charred, highly carbonaceous solid residue. Nitrogen or helium is used to assist the breakdown of the raw materials. The pores are initially formed during this treatment. The experiments conducted by Illan-Gomez et al. (1996) proved that the produced activated carbon possess a wider pore size distribution after treatment at 700 ^oC than at 500 ^oC. Another finding from their work is that the pyrolysis time does not influence microporosity formation.

The activation step furthers the microporosity and passage development of the activated carbon with high surface area via oxidation of the charred residue. In practice, the porosity of the final activated carbons is determined by the extent of activation. Rodríguez-Reinoso (1998) summarized the classification of the pores formed in activated carbon: micropores (up to 2nm), mesopores (2-50 nm) and macropores (> 50 nm). Although adsorption takes place predominantly in the micropores, the mesopores and macropores take in charge of permitting and controlling the adsorbents to get access to the micropores. Despite the fact that there are only a few of mesopores and macropores present on the outer surface of the AC, Rodríguez-Reinoso (1998) emphasized that their function as passages cannot be overlooked.

There are two different types of activation: physical activation and chemical activation. Physical activation includes carbonization of the carbonaceous precursor followed by partial gasification of the resulting char. This method is usually conducted at a much higher temperature range than pyrolysis, i.e., 800 ^{o}C to 1000 ^{o}C. High activation temperature is required to maintain a high reaction rate. Generally the temperature is raised up to 900 ^{o}C to ensure the burn-off level. In this process, air, steam or carbon dioxide is used as the activating agent. The activating agent has a significant effect on the carbon properties as well as the degree of the activation. For example, Mui et al. (2004) studied the activated carbon produced from waste tyres. This investigation demonstrated that carbon dioxide-activated carbon displayed a lower micropore volume and larger external surface area.

Chemical activation, is process that yields activated carbon via integration of pyrolysis and activation in the presence of activating agents (Mui et al., 2004). The low temperature operation helps the pore development in the carbon structure in this single step process. Dehydrating agents, such as, H_3PO_4, H_2SO_4, and KOH are widely used as chemical activating agents (Girgis et al., 2002). The alkali KOH was considered to be a highly attractive activating agent (Mui et al., 2004).

2.3 Influence of different factors on activated carbon preparation

In general, different process variables will yield activated carbon with different properties like carbon yield, density or pore width. Knowledge of the effects of different process variables is of great importance for optimizing activated carbon production. Considerable research has been performed in this area that serves as a good reference for carbon preparation.

2.3.1 Physical or chemical activation

According to the work of Illan-Gomez et al. (1996), the chemical activation process is preferred to the physical activation process to make coal-based activated carbon. Compared with physical activation, chemical activation will lower the inherent mineral content of the coal and it will produce activated carbon with much lower ash content. Another obvious advantage of chemical activation method is that the yields of carbon are usually very high in the presence of the chemicals. Also, surface area of the activated carbon via the chemical activation is usually much higher. Furthermore, Teng et al. (2000) proposed that chemical

activation can cut energy consumption compared with physical activation process. Because there is no need to heat the activating agent, and also pyrolysis and the activation are combined into one stage in chemical activation.

2.3.2 Carbonization temperature

Ahmadpour and Do (1997) and Wigmans (1989) indicated that the pore volume evolution was highly correlated with carbonization temperature. When KOH is used as the activating agent, the activated carbon exhibited higher surface area and micropore volume at higher temperature (800 ^{o}C), whereas, lower temperature (500-600 ^{o}C) is preferred in the case of $ZnCl_2$ as the chemical agent (Ahmadpour and Do, 1997). Teng et al. (2000), who measured the production of activated carbon from waste tires, confirmed that maximum pore volume was achieved at 800 ^{o}C in the presence of KOH. Pore volume decreased with further increase in temperature (Teng et al. (2000)), as shown in Table 2.2. The authors stated that this phenomenon could be attributed to the breakdown of cross-links in carbon matrix because of severe thermal stress. The breakdown will result in the rearrangement of the carbonaceous matters and the collapse of pores. Another potential reason is the destruction of pore structures during the gasification process due to the high temperature.

Table 2.2: The influence of the pyrolysis temperatures on the surface properties of activated carbon from waste tires impregnated with KOH [a] (Teng et al., 2000). Reused with permission (attached in Appendix A).

Pyrolysis Temp. (°C)	Carbon Yield (%)	BET SA (m^2/g)	Pore Vol. (cm^3/g)	Pore Size Distribution		Average Pore Diam. (nm)
				Micropore (cm^3/g)/(%)	Mesopore (cm^3/g)/(%)	
600	26	116	0.22	0.051/23	0.17/77	7.7
700	16	474	0.38	0.23/60	0.15/40	3.2
800	12	411	0.57	0.19/33	0.38/67	5.5
900	11	306	0.45	0.11/24	0.34/76	5.9

[a]The pyrolysis was performed by impregnating the tires with a KOH/tire ratio of 4, followed by heating the sample to the pyrolysis temperature and then cooling.

From Table 2.2, it is clear that the final carbon yields varied with the pyrolysis temperature. High pyrolysis temperature reduced carbon yield but increased pore volume and surface area. These trends can be mainly attributed to the gasification of the carbon to form and release CO_2. Greater gasification occurred at higher temperature causing more extensive breakdown of pore walls, therefore, enlarging the pore volume as well as the surface area. This revealed that the extent of carbon removal by gasification dominated pore development. This tendency is similar to that of physical activation.

2.3.3 Impregnation ratio

Impregnation ratio is another parameter found to extensively affect the production of activated carbon. It was found that during chemical activation with the activating agent of KOH, the total pore volume of activated carbon increased with the amount of agent impregnated (Teng et al., 2000).

This can be well seen in the scanning electron micrographs of carbons treated with different impregnation ratios in Fig. 2.2 from the publication of Teng et al. (2000). The activated carbon exhibited an intact external surface without KOH treatment (Fig. 2.2(a)). However, Fig. 2.2(b) and Fig. 2.2(c) vividly displayed the rugged external surfaces of the activated carbon after exposure to KOH in chemical pyrolysis. The extent of erosion increased with the impregnation ratio. Since it is prone to form void structure, to guarantee the mechanical structure of the carbons, the amount of the KOH should be controlled.

Although the surface area was found to increase in parallel with the increase in KOH, Teng et al. (2000) also found out that it will decrease after a maximum value with a higher degree of gasification.

Ehrburger et al. (1986) pointed out that KOH reacted with carbonaceous matters to form potassium salt complexes at a low temperature (~ 650 K). These complexes behave as activated sites during gasification. As a result, increase in the amount of KOH impregnated will result in a higher microporosity.

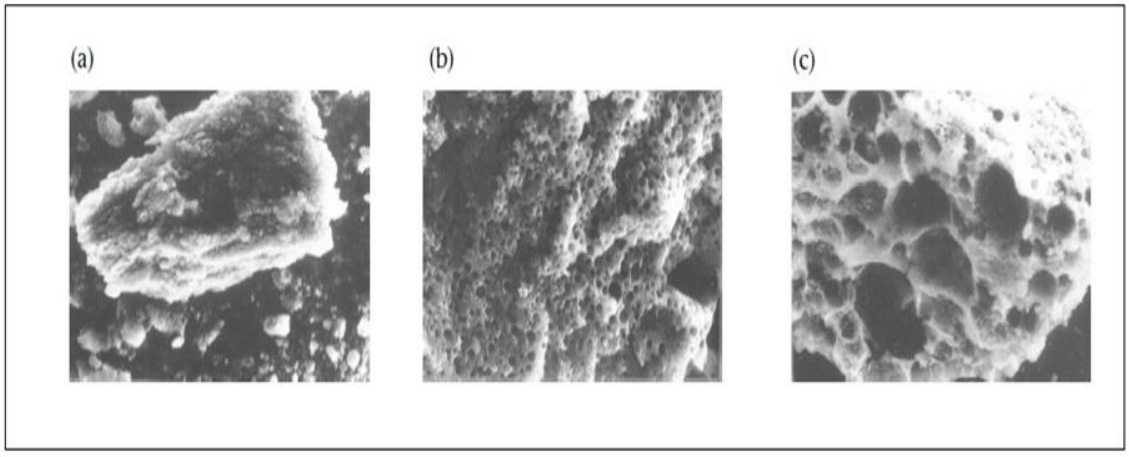

Fig. 2.2: Scanning electron micrographs of activated carbons produced from pyrolysis at 700 ^{o}C impregnated with different KOH/tire ratio: (a) 0, (b) 4 and (c) 6 (Teng et al., 2000). Reused with permission (attached in Appendix A).

2.3.4 Carbonization time

Carbonization time is reported to have a noticeable impact on the properties of activated carbon. Ahmadpour and Do (1997) studied the characteristics of activated carbon made from bituminous coal in KOH and $ZnCl_2$ series. They pointed out that prolonged time is recommended for these series, especially KOH, since the weight loss, the BET surface area, micropore volume, and benzene adsorption can be boosted.

2.4 Methods to improve adsorptive capacity of activated carbon

Activated carbons are frequently tailored physically and chemically for various adsorptive needs. It is true that both the porous structure and the chemical nature of the surface crucially affect the adsorption behavior.

2.4.1 Tailoring the physical properties of activated carbon

Basically, activated carbon can be altered in shape to meet different needs. Forms like granules, pellets, powders, fibers, and cloth are taken into account as adjustable options commonly. Granular activated carbon is often used in adsorption columns, and powdered AC is for direct addition.

Adsorption onto activated carbon is a mass transfer process, which implies that interaction between the carbon surface with the adsorbates is decisive. Owing to the fact that the structure and pore size distribution are responsible for the access of the adsorbates to the activated carbon, they can be tailored for the aim of selectivity. For example, 0.4 nm carbon molecular sieves (CMS) are able to adsorb the disk-like benzene molecule whereas zeolite with the same size fails to adsorb benzene (shown in Fig. 2.3) (Rodríguez-Reinoso, 1998). Benzene has difficulty in entering the zeolite pores because of the incompatible shapes. In comparison, the pore shape of the CMS allows the benzene molecules to penetrate and occupy the pores.

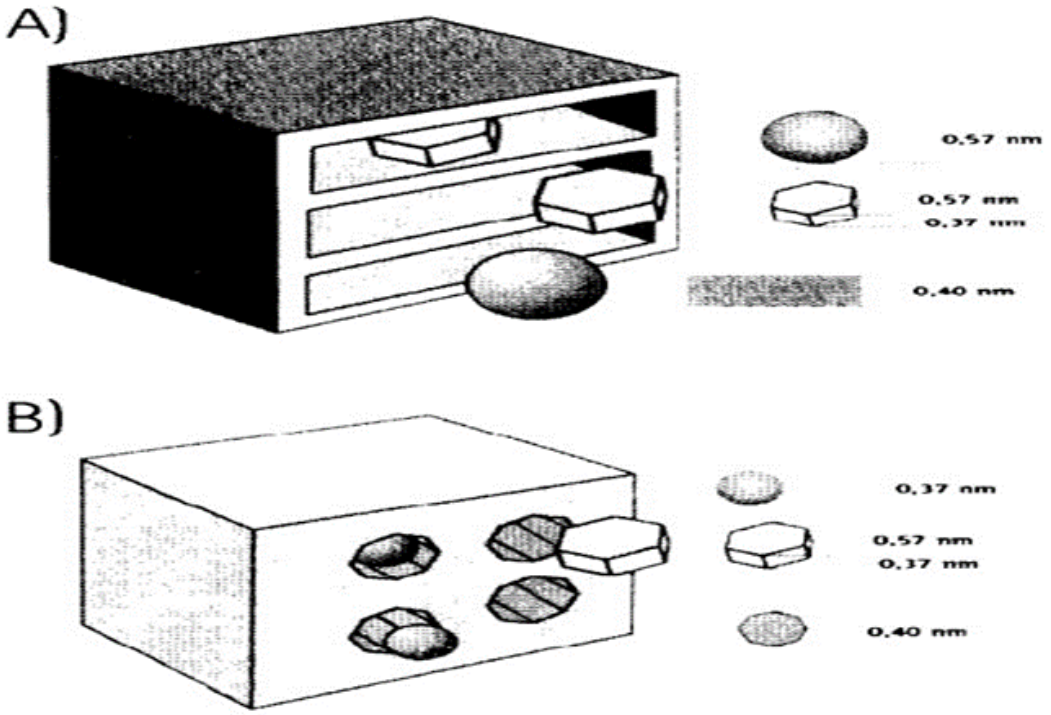

Fig. 2.3: Schema of the porosity and accessibility of micropores of: (a) a carbon (b) a zeolite (Rodríguez-Reinoso, 1998). Reused with Elsevier's permission (attached in Appendix A).

2.4.2 Surface chemical properties of activated carbon

The adsorption characteristics of activated carbons are determined greatly by the chemical nature of the carbon on its surface. Rodriguez-Reinoso (1998) mentioned that the importance of chemical nature was recognized is in the middle 1970s since some adsorptive behavior cannot be sufficiently explained by the physical properties of the adsorbents. As a consequence of a large number of studies of the carbon surface chemistry, people gained

much better understanding of the carbon adsorption behaviors. Acid base characteristics and functional groups were found to contribute to the adsorption properties.

The surface of the activated carbon can be modified using various treatments according to different objective adsorbates. That means that the carbon structure is altered so as to meet different requirement; for instance, the pH of the surface is found to be increased with larger extent of activation. Functional group like the aromatic ring was also indicated to have potential to affect the adsorption property.

The presence of oxygen and hydrogen has remarkable effects on the surface characterizers and adsorption behaviors of the activated carbon. It can be derived from the original raw material directly, through the activation method or by introduction after preparation via post-treatment. Therefore, even though some carbons are produced free of oxygen from phenol-formaldehyde or other polymers, the oxygen surface group will be formed afterwards by chemisorption of oxygen.

The oxygen in surface group is discovered to be largely responsible for the adsorptive properties of the activated carbon (Ahumada et al., 2002). The methods to form carbon-oxygen surface groups are not limited to the reaction with oxygen; many other oxidizing gases (nitrous oxide, nitric oxide, carbon dioxide, etc.) and oxidizing solutions (nitric acid, sodium hypochlorite, hydrogen peroxide, etc.) can be utilized for this oxidization purpose. The functionality of the oxygen groups is influenced by the carbonaceous temperatures, surface area, particle size and ash content as well.

Furthermore, the oxygen-carbon surface functional groups can be acidic, basic or neutral. The acidic functional groups will serve as the proton donors in the solutions, while the basic ones will act as electron-pair donors. There are a variety of forms of the amphoteric groups. The acidic surface functional groups include carbonyl, carboxyl, phenolic, hydroxyl and lactonic, while examples of the basic functional groups are pyrone, chromene, and quinine.

Boehm (2002) stated that the surface functional groups of AC could be analyzed by acid-base titration. Fourier transformed infrared spectroscopy (FTIR), temperature-programmed desorption (TPD), infrared, thermal desorption and X-ray photoelectron spectroscopy (XPS) and so on can also be employed to provide the information of surface functionality.

Some types of oxygen-carbon structures identified by Rodríguez-Reinoso (1998) are shown in Fig. 2.4. The acid-base characteristic can be established by the existence of these surface groups.

Based on the statement of Rodríguez-Reinoso et al. (1998), it is clear that the physical property, i.e., pore size distribution is highly relevant and important for the adsorption of non-polar molecules like N_2 and benzene. Yet oxygen surface complexes are the key for the adsorption of polar compounds. Since carbon is generally hydrophobic and the structure has a resistance to the acidic or basic media, it is indispensable for the treatment of carbons. The addition of oxygen groups not only increases the hydrophilicity but also enhances the surface charge density.

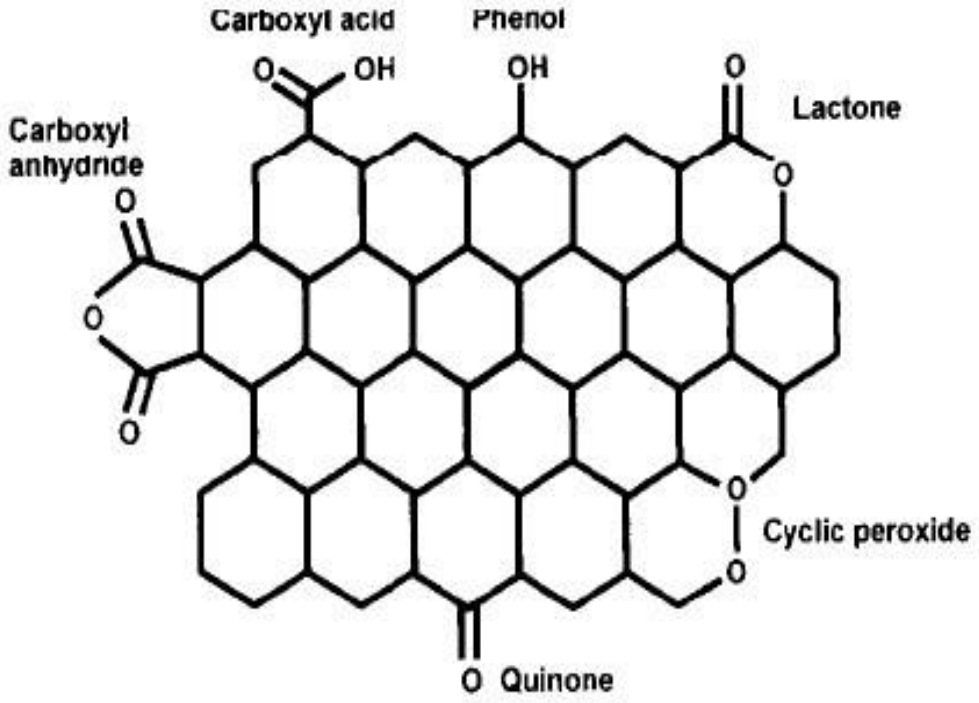

Fig. 2.4: Types of oxygen functional groups in activated carbons (Rodríguez-Reinoso, 1998). Reused with Elsevier's permission.

For adsorption of phenolic compounds which serves as the weak acids, a basic surface is recommended by Laszlo et al. (2003). For removal of ammonia which is a weak alkali, acidic surface groups are desirable (Le Leuch and Bandosz, 2007; Love et al., 2011).

A lot of research has been carried out to improve the adsorption performance of the adsorbent for specific adsorbates. Kurniawan et al. (2011) employed different treatments to optimize adsorptive effectiveness of carbon derived from coconut shell for 4-chlorophenol (4-CP) removal from waste water. Three oxidization methods were evaluated using strong oxidizing agent (HNO_3), alkaline material (NaOH), and impregnation of TiO_2, respectively to

attach oxygenated complexes onto carbons. The resulting carbons showed that while NaOH treated one had roughness and scragginess in morphology which represented the macropores, the HNO_3 treated surface had acute erosion, however the TiO_2 treated one had only pores on the surface (Kurniawan et al., 2011).

Kurniawan et al. (2011) generalized the experimental results that the NaOH treated activated carbon was the most effective for the remove of 4-chlorophenol (4-CP) among the three treatments. As high as 91% of the 4-CP can be transferred from the aqueous solution, however HNO_3 treated activated carbon was only able to adsorb 60%, and TiO_2 treated carbon adsorbed 72%. This study also indicated that the intact interior or too much erosion of the adsorbent might inhibit its adsorption capacity to some extent.

2.5 Factors affecting activated carbon (AC) adsorption

Based on the work of other researchers, the crucial dependent factors for adsorption by activated carbon are summarized below (Boudrahem et al., 2009; Dąbrowski et al., 2005; Mohd Din et al., 2009).

- Starting materials and preparation method
- The nature of adsorbent: ash content, surface area, pore distribution, pore volume, particle size (granular, powered), functional groups, polarity
- The nature of adsorbate: molecular size, pKa, functional groups, polarity.
- Adsorption conditions: pH, temperature, ironic strength, adsorbent dosage, contact time and the initial adsorbate concentration

Due to the acidic and/or basic functional groups, the nature of the activated carbon is amphoteric (Dąbrowski et al., 2005). pH of the solution medium is considered as one of the controlling parameters of the adsorption since it is found to be correlated with the surface charge of the active carbon. pH_{pzc} is a value to determine the nature point when the surface charge is zero. In general, when the pH > pKa, the adsorbates will dissociate into ionic forms. If pH is lower than pH_{pzc}, the surface of the activated carbon will be positively charged, which will result in uptake of the negatively charged adsorbate ions from the solution. If pH is higher than pH_{pzc}, it will be negatively charged and will attract positively charged particles.

Increase in adsorbent dosage will result in higher removal of the adsorbate from the aqueous phase. However, dosage should be controlled to some limit, since the higher adsorbent dosage might lead to lower adsorption capacity, which is undesired from the economic point of view.

Adsorption is a dynamic process and the adsorption rate will be faster at the beginning due to the availability of more activate sites for adsorption as well as the higher concentration gradient (Love et al., 2011). Over time, adsorption will reach equilibrium because of the saturation of the active sites and the decreased adsorbate concentration.

2.6 Mechanism of adsorption by activated carbon

To facilitate adsorption by activated carbon for the removal of target contaminants from aqueous solution, it is important to tailor the physical and chemical properties of activated carbon and enhance their affinity towards adsorbate molecules. To adjust the nature of activated carbon, it is important to recognize the mechanisms by which the

activated carbon interacts with the pollutants. Although considerable research has been directed toward studying the mechanism of adsorption of activated carbon (AC), it is still undefined and controversial. (Dąbrowski et al., 2005). Previous researchers have proposed several mechanisms of phenol adsorption onto activated carbon. Since the surface of activated carbon is heterogeneous, not only geometrically (different sizes, shape of pores, cracks et al.), but also chemically (different functional groups, mainly oxygen groups), it is difficult to predict the mechanism (Dąbrowski et al., 2005; Franz et al., 2000).

2.6.1 The π-π dispersion interaction mechanism

The π-π dispersion interaction mechanism was first proposed by Coughlin and Ezra (1968). They pointed out that activated carbon adsorbed the aromatic compound through dispersive interactions between π electrons of the graphitic rings of the carbon basal planes and those of the aromatic ring of the adsorbates. However, oxidation and reduction of oxidized-treated AC will form some electron withdrawing acidic surface oxygen groups, mostly carboxyl and hydroxyl. These groups will remove the π electrons from the graphite layers of carbon, increase its affinity towards water and therefore weaken the π-π dispersion interaction with phenols and inhibit the adsorption capacity (Rivera-Utrilla et al., 2011).

2.6.2 Electron donor-acceptor complex mechanism

Contrary to the impacts of the carboxyl and hydroxyl functional groups, Mattson et al. (1969) pointed out that carbonyl groups can enhance the uptake of phenols from aqueous solutions by activated carbon. They explained that the carbonyl groups (donor) on the surface

of activated carbon and aromatic ring of the phenol (acceptor) will generate an electron donor-acceptor complex which enhances adsorption of phenol.

2.6.3 Hydrogen-bonding mechanism

Coughlin and Ezra (1968) observed another mechanism which also plays a role in the adsorption process, hydrogen bonding formation. It was suggested that surface oxygen groups such as carboxylic and carbonyl on activated carbon are capable of H-bonding with aromatic compounds with a functional group, such as phenol. These oxygen groups are located at the entrance of the carbon pores, especially carboxylic groups, are highly accessible, hydrophilic and polar, which means that they are also able to attract water molecules through H-bonds between them. It was found that water was more preferential and easy to have this interaction with these oxygen groups, it will form water clusters to hinder the adsorption of the larger phenol molecules. According to this mechanism, water adsorption is dominant on the surface oxygen groups through hydrogen boding effect compared to more hydrophobic phenol compounds.

To eliminate or test the competitive adsorption effect of water for the available adsorption sites, Franz et al. (2000) stated that cyclohexane could be used as the adsorption medium. In the absence of water, the activated carbon will be more efficient in adsorbing the phenol molecules. If the adsorption capacity of the activated carbon are similar in aqueous and in the cyclohexane solution, the influence of water adsorption can be ignored (Franz et al., 2000).

2.7 Adsorption of *p*-cresol and ammonia

2.7.1 Removal of p-cresol

Although some researchers have studied adsorption of *p*-cresol on activated carbon, it is still not well-understood. Ravi et al. (1998) performed the adsorption experiments of phenol, o, m, *p*-cresol, and benzyl alcohol on activated carbon at 278, 298, and 323K respectively. The adsorption data for the cresol isomers were in agreement with the type I isotherms, which implied chemisorption or adsorption in micropores. When the temperature was raised from 278 to 298 K, there was an increase in the adsorption of cresol isotherms. However, from 279 to 232 K, the uptake of o, m, *p*-cresol decreased. From the result of the desorption experiment, it showed that the adsorption of cresol isotherms were irreversible at lower concentrations (Ravi et al., 1998).

Haghseresht et al. (2003) studied the influencing factors of surface chemistry and pH on the adsorption of *p*-cresol. The adsorption of *p*-cresol was investigated on different activated carbons. The oxidized activated carbon chemically treated with nitric acid had a suppression in the uptake of *p*-cresol, whereas the basic activated carbon prepared with 6% H_2 in N_2 mixture at 900 °C for 1 hour resulted in an increase in the *p*-cresol adsorption. The authors indicated that the H_2-treated carbon was more hydrophobic compared to untreated and oxidized activated carbons due to the removal of the surface oxides. The authors further mentioned that the H_2 treated carbon was more positively charged, which also contributed to the higher adsorption capacity of *p*-cresol. The surface of the oxidized activated carbon was more hydrophilic and more negatively charged which would attract water molecules and

repel the *p*-cresol into the interior pores. Hence Haghseresht et al. (2003) demonstrated that oxidation of the surface was undesirable for *p*-cresol uptake, which agreed with some other observations (Coughlin and Ezra, 1968; Franz et al., 2000; Mahajan et al., 1980).

Taking into account the possible effect of pH, Hadjar et al. (2011) and Haghseresht et al. (2003) performed adsorption experiments at pH between 2 and 12. They found that the *p*-cresol was preferentially adsorbed from its neutral form (~10.2). The rate of *p*-cresol adsorption kept nearly constant within the pH range of 2 to 10 and decreased as the solution became more basic. When the pH was below the pKa value of *p*-cresol (10.2), adsorption of the molecular was dominant. As the pH increased above 10.2, the dissociating *p*-cresol existed primarily in ionic forms. The electrostatic repulsive forces between the negatively charged activated carbon and anionic form of *p*-cresol reduced *p*-cresol adsorption (Hadjar et al., 2011).

2.7.2 Removal of ammonia

Adsorption of ammonia using activated carbon has not been studied extensively. Love et al. (2011) used ozone to oxidize the activated carbon to improve its adsorption capacity. Adsorption capacity significantly increased from 0.47 mg/g to 1.02 mg/g after oxidation treatment for 30 minutes owing to the increased surface acidic oxygen groups. The correlation between the acidity of the surface and ammonia removal was similar to the metal-supported activated carbon (Le Leuch and Bandosz, 2007). Their adsorption kinetic study showed that the uptake of ammonia on ozonated activated carbon followed the Elovich model, which suggested that adsorption is controlled by chemisorption (Love et al., 2011).

2.8 Equilibrium and kinetic studies

To investigate the affinity and capacity of the adsorbents for some special adsorbents, equilibrium and kinetic analyses are fundamental and indispensable.

2.8.1 Adsorption isotherms

Equilibrium is established between adsorbent and adsorbate after enough adsorption time. The concentration of the adsorbate on the adsorbent surface is a function of the concentration in solution. Studies have been performed to develop adsorption isotherms to describe the equilibrium relationships. The isotherms provide information on how adsorbates interact with adsorbents at a given temperature. The maximum or ultimate capacity of the adsorbents for a particular adsorbate can also be evaluated by equilibrium isotherms. Some well-established isotherms such as, Freundlich, Langmuir, Redlich-Peterson, and BET isotherms are frequently used (Lin and Juang, 2009).

Considering that different combinations of adsorbates-adsorbents have different relationships and a single correlation could not account for all the cases, the development of different isotherms is essential. To identify the most appropriate equilibrium isotherm for certain adsorption, experimental data should be fitted to different isotherm models. The shape of the isotherm is important information for diagnosing the nature of a particular adsorption phenomenon. Equilibrium isotherms are of great importance and the correlation of the equilibrium data between either theoretical or empirical equations is essential for the adsorption system application.

2.8.1.1 Freundlich isotherm

Freundlich (1906) proposed an empirical equation of heterogeneous adsorption. The Freundlich model is not limited to represent adsorption of single component, and it is also suitable for multiple compounds. This model can be written as:

$$q_e = K_F \, C_e^{\,1/n} \tag{2-1}$$

The Freundlich isotherm can be rearranged to the linear form as:

$$log \; q_e = log \; K_F + \frac{1}{n} log \; C_e \tag{2-2}$$

where q_e is the equilibrium amount of adsorbate adsorbed per unit mass of adsorbent (mg/g), C_e is the equilibrium concentration of adsorbate in bulk solution (mg/L), K_F is a coefficient (function of energy of adsorption and temperature). $1/n$ is a constant, which measure the strength of adsorption. If the adsorption can be described by this model, K_F and $1/n$ can be easily determined through the linear regression. $1/n < 1$ represents the strong adsorption bond for that adsorbate.

2.8.1.2 Langmuir isotherm

Compared to Freundlich's empirical model, the Langmuir isotherm (Langmuir, 1916) has a theoretical justification. Another main difference between these two models is that the Langmuir isotherm is based on some assumptions whereas the Freundlich made no assumption in his isotherm (Langmuir, 1916).

One assumption of Langmuir isotherm is that adsorption is reversible, which means that desorption coexists with adsorption. This indicates that the adsorption is a dynamic

process at any moment. Another assumption is that the active sites on the surface of the adsorbent have the same solute affinity without affecting their adjacent sites. In addition, the Langmuir isotherm is based on the assumption that the adsorption occurs only in a single layer of adsorbate. Further, the molecules do not move on the surface once they are adsorbed.

This model can be well applied to the adsorption of single compounds. The Langmuir isotherm is given by:

$$q_e = \frac{Q_0 K_L C_e}{1 + K_L C_e} \tag{2-3}$$

where Q_0 is the maximum absorbable amount in a monolayer (mg/g), C_e is the equilibrium concentration of adsorbate in bulk solution (mg/L), K_L is a constant (L/mg) which is a function of enthalpy of adsorption and temperature.

2.8.1.3 Redlich-Peterson isotherm

Redlich and Peterson (1959) developed a three parameter empirical equilibrium isotherm that incorporates the characteristics of both Langmuir and Freundlich models (two parameters). Several studies (e.g., Bilgili, 2006; Haimour et al., 2005; Wu et al., 2010) showed that the Redlich-Peterson equation was more accurate than the Langmuir and Freundlich isotherms. This isotherm can be expressed as:

$$q_e = \frac{AC_e}{1 + BC_e^{\beta}} \tag{2-4}$$

where C_e is the equilibrium concentration of adsorbate in bulk solution (mg/L), A is the Redlich-Peterson constant (L/g), B is a constant ((L/mg)$^{\beta}$). β is an exponent which lies between 0 and 1.

2.8.1.4 Brunauer-Emmett-Teller isotherm

The Brunauer-Emmett-Teller (BET) isotherm (Riccardo et al., 2002; Sheshdeh and Khosravi, 2013) assumes that the physical adsorption is multilayer instead of monolayer, which is an extension of the Langmuir theory. In BET theory, the active sites of a layer do not need to be completely occupied before the next layer works. Furthermore, the layers do not interact and influence each other. The BET isotherm is derived by further assuming that the Langmuir theory is applicable for each layer. The resulting equation is as follows:

$$q_e = \frac{Q_O K_B C_e}{(C_S - C)[1 + (K_B - 1)\frac{C_e}{C_s}]} \tag{2-5}$$

where q_e (mg/g) is the adsorbed amount of adsorbate onto adsorbent under equilibrium condition. K_B is a reaction rate constant which is a function of energy of adsorption and temperature). C_e (mg/L) is the equilibrium concentration of adsorbate in bulk solution, and C_s (mg/L) is the saturated concentration for all layers.

The BET equation can be rearranged to give that:

$$\frac{C_e}{(C_S - C_e)q_e} = \frac{1}{K_B q_m} + (\frac{K_B - 1}{K_B q_m})\left(\frac{C_e}{C_s}\right) \tag{2-6}$$

where q_m (mg/g) denotes the adsorbed amount of adsorbate to form a complete monolayer. Accordingly, the linear plot of $C_e/[(C_s - C_e)q_e]$ versus C_e/C_s will be obtained.

2.8.2 Kinetic studies of adsorption

Other than adsorption capacity, the adsorption rate is another important factor for wastewater purification. Besides, an understanding of the mechanism of adsorption and the potential rate determining steps is required to find the optimum operating condition. Hence, kinetics should also be taken into account for the optimization of the adsorption process.

Kinetic studies commonly result in determination of the reaction order. Some kinetic models have been developed for the determination of adsorption rate. Kinetic models, such as, Lagergren pseudo-first-order kinetic reaction model, chemisorption pseudo-second-order reaction model, Elovich kinetic, liquid film diffusion model, and intra-particle diffusion model are widely used (Bilgili, 2006; Demirbas et al., 2009). The first, second, and Elovich models are reaction-based models while others are mass transport models.

2.8.2.1 Lagergren pseudo-first-order reaction model

The pseudo-first-order reaction model is a linear relationship and it can be written as (Demirbas et al., 2009; Lagergren, 1898):

$$log(q_e - q_t) = log(q_e) - \frac{k_1}{2.303}(t) \tag{2-7}$$

where the q_e and q_t are the equilibrium amount and the amount adsorbed at time t, respectively (mg/g). k_1 is the adsorption reaction rate constant (min^{-1}). The values of k_1 and q_e can be determined from the slope and intercept of the plot of $\log(q_e - q_t)$ against t.

2.8.2.2 Chemisorption pseudo-second-order reaction model

It can be inferred from this model that the chemisorption is vital in the rate determining step (Ho and McKay, 1999). The linear form of pseudo-second-order model can be expressed as (Ho and McKay, 1998; Singh et al., 2008):

$$\frac{t}{q_t} = \frac{1}{k_2 q_e^2} + \frac{1}{q_e}(t) \tag{2-8}$$

where k_2 is the reaction rate constant (g mg^{-1}min^{-1}). The plot of t/q_t against t gives a linear relationship, and the slope and intercept can be used to derive q_e and k_2.

2.8.2.3 Elovich kinetic model

The Elovich kinetic model (Chien and Clayton, 1980) is another model can be applied for the study of the chemisorption. In the absence of desorption, the reaction rate will decrease owing to the increasing surface coverage (Juang and Chen, 1997). The equation can be shown as

$$\frac{dq_t}{dt} = \alpha \exp(-\beta q_t) \tag{2-9}$$

where α (mg g^{-1}min^{-1}) and β (g mg^{-1}) are constants. α can be considered as the initial adsorption rate because $\frac{dq}{dt} \rightarrow \alpha$ as $q_t \rightarrow 0$. β is the desorption constant. Given the boundary conditions $q_t = 0$ at $t = 0$ and $q_t = q_t$ at $t = t$, the equation can be simplified to

$$q_t = \frac{1}{\beta}\ln(\alpha\beta) + \frac{1}{\beta}\ln(t) \tag{2-10}$$

A linear plot of q_t against $\ln(t)$ can be obtained from this equation.

2.8.2.4 Liquid film diffusion model

If the transport of the solute adsorbates from the liquid phase to the solid adsorbents is slow and controlling the reaction, the liquid film diffusion model (Boyd et al., 1947; Khan et al., 2012) could be put into use. The form is arranged as follows:

$$\ln(1 - F) = -K_{fd}t \tag{2-11}$$

where F is the fraction of q_t/q_e and K_{fd} is the rate constant (min^{-1}). A linear plot of the $\ln(1 - F)$ versus t suggests that the kinetics of the adsorption process is dominated by diffusion through the liquid film.

2.8.2.5 Intra-particle diffusion

The intra-particle diffusion model (Khan et al., 2012) considers the case when the diffusion of the solute molecules into the interior of the pores of the adsorbents is rate limiting. The equation can be written as

$$q_t = k_{id}\, t^{0.5} + C_i \tag{2-12}$$

where the k_{id} is the reaction rate constant (mg m^{-1} $t^{-0.5}$) and C_i refers to the boundary layer thickness. It can be derived from the slop of the plot of q_t versus $t^{0.5}$.

2.9 Thermodynamic study

In thermodynamics, the Gibbs free energy change indicates a reaction is favorable or not. The spontaneity of the adsorption process can be inferred if the Gibbs free energy

change is negative. The Gibbs free energy change (ΔG^o) of the adsorption process is defined as (Kilic et al., 2011):

$$\Delta G^o = -RTInK_e \tag{2-13}$$

The K_e value is calculated from:

$$K_e = \frac{q_e}{C_e} \tag{2-14}$$

From this equation, the distribution coefficient K_e at different temperatures can be calculated.

Relation between ΔG^o, ΔH^o and ΔS^o can be expressed as:

$$\Delta G^o = \Delta H^o - T\Delta S^o \tag{2-15}$$

where ΔH^o and ΔS^o are enthalpy change and entropy change, respectively. T is the absolute temperature in Kelvin.

Eq. (2-15) can be derived as:

$$\ln K_e = -\frac{\Delta G^o}{RT} = -\frac{\Delta H^o}{RT} + \frac{\Delta S^o}{RT} \tag{2-16}$$

where R is the universal gas constant with the value of 8.314 J mol^{-1} K^{-1}. The standard enthalpy and entropy change can be determined from the plot of $\ln k$ against $1/T$. Also, the Gibbs free energy change can be calculated.

To gain a better understanding of the adsorption process, thermodynamic study should be conducted. Either the Gibbs free energy change or the enthalpy change will provide information of the adsorption system. The negative value of ΔG^o suggests that the

adsorption process is spontaneous. The negative value of ΔH^o indicates that the process is exothermic, while a positive value shows its endothermic nature.

2.10 Regeneration technology of saturated activated carbon

Even though regeneration of saturated activated carbon was not emphasized in this research, it has played a significant role in development of the activated carbon. Different regeneration methods are reviewed here with respect to their advantages, disadvantages, and application for better understanding of the whole adsorption system. Restoring the activity of the exhausted activated carbon has been highly attractive due to several reasons (Leng and Pinto, 1996; Sufnarski, 1999; Toledo et al., 2003). First of all, the production cost of the activated carbon is relatively high in general. The cost of using the reactivated carbon is much cheaper than that of the original AC sometimes due to the relative ease of the operating process. After the activated carbon adsorbs the contaminants and reaches its adsorption capacity, it turns into the noxious solid waste that requires proper treatment or disposal. Incineration, as one means to eradicate this hazardous waste, is undesirable since the activated carbon is not recycled and some air pollutants with even higher toxicities might be emitted during the incineration process (Toledo et al., 2003). Similarly discharge of the depleted activated carbon via landfill will also add pollutants to the environment.

Hence different technologies have been studied to regenerate the exhausted activated carbon for subsequent use. The aim of regeneration of the AC is to desorb the accumulated adsorbents, recover the characteristics of the adsorbent, maintain the pore structure and reduce mass losses (San Miguel et al., 2001).

Since adsorption involves two different types of interactions, physical adsorption and chemical adsorption. Physisorption is caused mainly by weak van der Waals forces and is reversible. It can form multilayers of adsorptions. In this case the recovery of the spent AC can be accomplished by heating, reducing the pressure or rinsing with solvent (Sufnarski, 1999). Chemisorption is characterized by covalent bonding and has a single layer of adsorption and is irreversible. Under these circumstances, energy supply in excess of the sorptive force is needed to break the ionic or covalent bond to reinstate the AC's activity level. Different technologies for regeneration of the AC will be discussed and reviewed in the following sections.

2.10.1 Thermal regeneration

Among the methods operated today to reuse AC, thermal regeneration is most widely used. Moreover, it is the only reactivation means applied at the industrial scale (Sabio et al., 2004). Thermal regeneration has been regarded as economically-attractive alternative to disposal of AC (San Miguel et al., 2001). It is a technology that utilizes the inert gas/steam and elevated temperatures to desorb and destroy the adsorbates mainly by volatilization and oxidation (Martin and Ng, 1984; Sabio et al., 2004; San Miguel et al., 2001).

Generally, the processing steps involved in the thermal regeneration method to treat wet AC removed from the adsorption columns include (Sabio et al., 2004; San Miguel et al., 2001; Suzuki et al., 1978): (1) drying to temperature of ~105 ^{o}C; (2) elevating the temperature up to 800 ^{o}C under inert conditions, thereby, pyrolysis occurs to eliminate the volatile compounds and thermally decompose the less-volatile compounds; and (3) utilizing

mildly oxidizing gas such as steam or carbon dioxide or a mixture of both to gasify the charred remnants and residual organics at around 800 ^{o}C and restore the original carbon pore structure. The second step is considered to be intricate as it includes thermal decomposition, thermal cracking, desorption of decomposition products, partial cracking, and the partial polymerization of the residues afterwards (Suzuki et al., 1978). This step deserve close study because the controlled gasification following it is significantly influenced by the residue and coke. Zhang (2002) reported that the oxidation temperature for thermal regeneration is between 800 ^{o}C to 850 ^{o}C.

Restoration of the carbon's characteristics greatly depends on the conditions employed in the oxidation process (San Miguel et al., 2001). The amount of the residual char generated from the adsorbed organic compounds governs the amount of substance that needs to be oxidized. They also emphasized that appropriate oxidation condition will leads to maximal residue removal, minimal carbon loss and least original carbon structure destruction. The use of excessively mild oxidation conditions will lead to incompletion oxidation of the charred residue, while the application of excessively severe conditions will result in carbon damage and greatly impede the successful regeneration of AC due to carbon loss.

Moreno-Castilla et al. (1995) studied thermal regeneration of AC made from a Spanish bituminous coal independently saturated with four substituted phenols, namely, phenol, *p*-cresol, m-amino-phenol as well as *p*-nitrophenol. They found that part of the phenols was removed from the AC through water evaporation in the course of the drying

process. Lower amount of *p*-nitrophenol than phenol was released due to the stronger interaction with the carbon surface. They also discovered that during the thermal treatment, more CO than CO_2 was desorbed due to the basic nature of the carbonaceous materials and they explained that the light gas might originate from the surface groups such as pyrone, quinone and carbonyl. From their study, it seems that a part of the physisorbed phenolic compounds either released from the AC by itself or deposited as heavy compound. In the meantime, part of the physisorbed compounds can be transformed into chemisorbed phenols and then converted to light gases or heavy products such as the carbonaceous residue or polymers. Results reported demonstrated that thermal regeneration helped to restore the adsorption characteristics of the exhausted ACs, with the AC-*p*-cresol system being most effective (Moreno-Castilla et al., 1995). However, the results also showed that adsorption capacity decreased with increasing number of thermal regeneration cycles.

Similarly, Ferro-García et al. (1993) studied the thermal regeneration of the olive-stone AC exhausted with the chlorophenols. Carbon monoxide is found to be the main gaseous product with other light gases such as H_2, CH_4 (trace), H_2O, and CO_2, which in a good agreement with the conclusion reached by Moreno-Castilla et al. (1995). Furthermore, Ferro-García et al. (1993) pointed out that no other chlorinated compounds such as hydrogen chloride or chlorine were observed during the thermal treatment. The majority of the chlorine of the chlorophenol was observed as a waxy product. Ferro-García et al. (1993) also indicated that the oxygen surface complexes (the carbonyl groups) are greatly involved in the decomposition of the chemisorbed adsorbates, functioning as cracking centers in the

production of the light gases, which is consistent with the conclusion drawn by Moreno-Castilla et al. (1995). The results suggested that thermal regeneration is effective in adsorbate removal and activated carbon regeneration.

The results presented by San Miguel et al. (2001) showed a high recovery rate of up to 95% of the field-spent AC after thermal treatment. But the degrees of the regeneration greatly varied at different process parameters such as the types of the adsorbate, the regeneration time, etc. They indicated that the impact of the regeneration of the carbons can be investigated as regards the recovery of the porosity, surface area, and adsorption characteristics. Nevertheless, thermal regeneration is not effective in restoring the narrow microporosity that exists in the original carbons. On the contrary, the pores will become larger, especially in the presence of the catalytic metals. Therefore, they drew the conclusion that regenerated activated carbons had a reduction in the uptake capacity for small molecular-sized compounds such as phenol, with an increase in the capacity to reduce the larger molecular size compounds such as methylene blue from aqueous solutions.

Sabio et al. (2004) also demonstrated that saturated carbon can be regenerated considerably by thermal treatment and the extent of regeneration was influenced by the process conditions. They examined the effects of the gasifying agents in the air and CO_2 on the recovery of the initial adsorption properties. They discovered that air-gasification led to a lower regeneration capacity (around 90%) than complete regeneration by the CO_2-gasification. But they stated that air was an attractive alternative to conventional CO_2 gasifying agent due to its low cost, short regeneration time and easy accessibility. From their

results, the processes of the thermal regeneration can be simplified to a single step of direct gasification keeping the identical recovery effects so as to reduce operation cost. They also reported that the thermal regeneration brought about the surface chemistry modification of the spent AC. They suggested that surface oxygen-containing groups were developed by the reaction of the reactive gases formed during the thermal stressing with the carbon. The presence of these groups hindered the retention of the organic pollutants attributed to the decreased carbon affinity toward the adsorbates.

Even though thermal regeneration is a reliable means to restore the adsorption characteristics of the AC, it is still insufficiently understood and hence the design parameters and operating conditions are not optimum (Sabio et al., 2004; Suzuki et al., 1978). Actually, it would be very difficult to specify the optimal operating conditions. San Miguel et al. (2001) investigated different field-spent granular ACs under the same thermal treatment conditions in order to optimize the regeneration conditions. However, the spent ACs of similar commercial grades obtained from different water treatment plants presented different characteristics in terms of porosity, reactivity, etc. As a result, it is challenging to define the optimum operating conditions due to the diverse behavior of these exhausted ACs during regeneration treatment. In addition, the influence of the metals on thermal regeneration of activated carbon presents another aspect of the problem in practice (Cannon et al., 1994; San Miguel et al., 2001). It was suggested that the metals had the potential to chemisorb the water or carbon dioxide and catalyze the gasification reactions between the solid carbon and the oxidizing agent therefore impacts the effects of the thermal regeneration (Cannon et al.,

1994; San Miguel et al., 2001). It was discovered that the presence of the metals promoted the formation of increasingly wider porosity in an undesirable way (San Miguel et al., 2001). Moreover, another disadvantage of the thermal regeneration is that carbon loss (~5-10%) owing to the gasification, attrition, and washout occurred in each cycle of the process, and gradually reduced adsorption capacity due to the consecutive regeneration cycles (Cannon et al., 1994; Cooney et al., 1983; Moreno-Castilla et al., 1995; Zhang, 2002). Another drawback that necessitates consideration is the high cost of the energy for maintaining the operation temperature at around 800 ^{o}C, the cost for a steam generator or inert gas supply, and the transport expense of delivering the spent ACs to the special thermal regeneration plant (Yuen and Hameed, 2009; Zhang, 2002). Other than these issues, air emissions of the effluent gases and the incompatibility of some special adsorbates such as the explosive TNT pose additional challenges for this method (Lyman, 1978; Sufnarski, 1999).

2.10.2 Chemical regeneration

Chemical regeneration is a method that removes the adsorbates on the surface of the exhausted AC by reactions with proper chemical reagents or modification of the adsorption equilibrium (Berenguer et al., 2010; Sufnarski, 1999). In comparison to the thermal volatilization method, the chemical regeneration approach has the following advantages: (1) in-situ treatment saves on the costs related to unloading, transportation and repacking of the activated carbons; (2) there is no carbon loss; (3) it is feasible to recover the valuable adsorbates; and (4) reuse of the regenerants is possible via the consequent process of distillation (Leng and Pinto, 1996; Sufnarski, 1999).

Two primary categories of the chemical reagents are associated with the chemical regeneration technology: organic solvents with solubilizing abilities and inorganic chemicals with oxidizing properties (Leng and Pinto, 1996; Martin and Ng, 1984; Sufnarski, 1999). Successive washing with water is needed to remove the regenerants (Sufnarski, 1999). Generally speaking, organic reagents are more effective than inorganic solvents in restoration of the AC (Leng and Pinto, 1996). Martin and Ng (1984) have tested the efficacy of regeneration of the ACs saturated with mono-substituted benzene compounds, i.e., aniline, phenol, benzyl alcohol, benzaldehyde, and nitrobenzene, using the organic chemical reagents (i.e., carboxylic acids, amines, chloromethanes, acetone, benzene and alcohols) and inorganic regenerants (i.e., $KMnO_4$, $K2Cr_2O_7$, and NaOCl). From their studies, organic regenerants were much more effective than the inorganic chemicals. Ineffective oxidizing inorganic solutions will even form oxides on the surface of the active carbon, and hence, decrease its re-adsorptive capacity for phenols and other pollutants. They also stated that the water-soluble organic regenerants gave higher efficiencies when not diluted with water due to the elimination of binding of the organic solvents with water while insoluble organic chemicals were not influenced by the presence of water on the efficacy of the regeneration (Martin and Ng, 1984). Beyond those results, another conclusion was summarized by them that the regeneration efficiencies of the ACs decreased as the molecular weights and sizes of the organic solubilizing regenerants increased (Martin and Ng, 1984). They stated that is was likely that the chemical regeneration of the AC was achievement by the displacement of the adsorbates by the reagents, as a result, the lower weight regenerants can further penetrate into

the micropores of the AC and enhance the desorption of the adsorbates (Martin and Ng, 1984). Therefore, they recommended using chemical reagents with the lower molecular weights than the adsorbate (Martin and Ng, 1984).

A parallel study was performed by Leng and Pinto (1996) to examine the mechanisms of the chemical regeneration through five different chemical regenerants of the ACs exhausted with four diverse aromatic adsorbates, i.e., phenol, aniline, benzoic acid, and nitrobenzene. The results demonstrated that the solubility of the adsorbate in the regenerant is of great significance in the regeneration of the carbons. Adding the micellers (surfactants of aggregated amphiphilic molecules) or production of soluble forms achieved through pH control or the utilization of reactive regenerants can increase the solubility of the adsorbate, this technology had higher efficacy. They pointed out that the acid-base characteristics as well as the potential reactivity of the adsorbate should be taken into account when selecting between the methods. This conclusion was supported by the finding that low regeneration of the aniline was obtained with basic solution due to limited solubility but almost complete regeneration is attained by using HCl to form soluble salt (Leng and Pinto, 1996). For strongly adsorbed compounds, such as nitrobenzene, they observed that the chemical regeneration was effective until a very acidic solution was used. They demonstrated that pH control was very effective since the carbon surface charge characteristics can be controlled; for example, the protonation of the surface occurred at very low pH and the hydrophobic molecules are inclined to desorb and realize the regeneration (Leng and Pinto, 1996).

In the wide spectrum of the inorganic chemical reagents, 4% sodium hydroxide (NaOH) has been proved to be applicable in regeneration of GAC in commercial applications (Himmelstein et al., 1973; Leng and Pinto, 1996). The effectiveness of NaOH was mainly attributed to the formation of sodium phenate, which can be easily desorbed from the carbon surface. Another factor facilitating the desorption of the adsorbates might be due to the changes in the porosity of carbon surface oxides caused by the high pH of sodium hydroxide, and hence, the changes in the force of attraction between the adsorbates and adsorbent.

It was also found that the existence of the dissolved oxygen in the adsorbate solution will bring about polymerization reactions, and therefore promotes the uptake of the phenols on the carbon surface; however this form of chemisorption increases the difficulty of the regeneration and reduces the lifespan of the GAC (Leng and Pinto, 1996). Nakhla et al. (1994) studied extraction experiments on phenol-saturated GAC using methanol and methylene chloride as the chemical reagents; their results suggested that the extraction efficiency was about 80% in anoxic solvent while it was only about 25% in the oxic case. This finding is in an excellent agreement with other studies (e.g., Grant and King, 1990; Vidic and Suidan, 1991).

In spite of the aforementioned merits, chemical regeneration has some apparent disadvantages. The main problem is that the recovery of the adsorption capacity by chemical regeneration does not provide complete restoration and this is the main reason for the paucity of publications available on this technology (Martin and Ng, 1984). Berenguer et al. (2010) reported that chemical regeneration had 20% lower regeneration efficiency than that attained

by thermal regeneration of phenol-exhausted ACs. In addition, restoration of porosity through chemical regeneration method is very low, regardless of the NaOH concentration employed.

2.10.3 Catalyzed coupling regeneration

Other than the conventional thermal and chemical regeneration methods discussed above, the catalyzed coupling technology has great potential to be applied in regeneration of depleted GACs. The coupling reactions present an innovative, simple and economical separation method for extraction of specific substances via conversion into insoluble coupling products upon dimerization and oligomerization catalyzed by the binuclear copper compounds or enzymes (Cha et al., 1986; Giles et al., 1986). The common products generated from these reactions include dimers, oligomers, and occasionally polymers, even though hydroxylation and other higher oxidation products might be produced under alkaline condition (Cha et al., 1986).

Lim et al. (1983) proposed a novel dephenolization scheme using coupling reactions of soluble phenol under facile aerobic reaction conditions using cuprous chloride as the catalyst ($T < 60\ ^{o}C$, $P_{O_2} < 1$ atm). The insoluble solid organic coupling complex can be easily separated from the solution and used as a fuel (Lim et al., 1983). This novel method has a promising application due to the low cost of the catalyst and oxygen, ease of use, the moderate operating conditions employed, and the fuel value of the recuperated coupling products.

A later cost analysis of the dephenolization scheme conducted by Chin et al. (1985) demonstrated that this technology was more economical than traditional dephenolization schemes based on biooxidation and solvent extraction. To remove 99% of the phenols from a wastewater with a phenol concentration of 4 g/L, the cost was around $\$8.6/10^3$ gal of the synthetic natural gas produced in the industrial-scale coal gasification plant whilst the biooxidation scheme cost around $\$12.9/10^3$ gal and the solvent extraction method cost about $\$12.8/10^3$ gal (Chin et al., 1985).

A parallel desulfurization experiment was performed by Giles et al. (1986), in which the mercapto compounds of alkaline thiols were rapidly converted into insoluble disulfides via mild aerobic oxidative coupling reactions. Only trace amount of copper is required for use in the coupling processes. Aqueous solubility of propylthiol drops from about 9.0 g/L to 0.032 g/L when the coupling product of the dipropyl disulfide is formed (Giles et al., 1986). Other similar observations of the fall in the solubility were found of other alkylthiols, glutathione and aryl thiols through coupling reactions (Giles et al., 1986).

Chung et al. (1999) studied the biphasic oxidative coupling of using the 2, 6-mimethylphenol as a substrate, the aqueous-chloroform biphasic mixture, the surface-active coupling catalyst of a cuprous chloride complex of N, N-dibutylethylenediamine, and the surface-active ligand of biphasic mixture to form large molecular weight polymer of poly (2,6-dimethyl-1,4-phenylene oxide) (PPO). The mean molecular weight of the products formed through the process was about 48, 000 amu. From their report, yield of the polymers can reach 95% and the PPO can be used to produce valuable industrial thermoplastics.

Additionally, this method is of great attraction since the catalyst complex can be recycled from the segregation at the middle emulsion layer in a compact form.

From the abovementioned studies, the coupling–dephenolization scheme is a promising method that can be applied to reuse the ACs loaded with phenol, substituted phenols, and the similar coupling-desulfurization method can be used to remove the mercapto and sulfhydryl compounds. Furthermore, other materials are amenable to undergo the aerobic pulling reactions include the diamines, inorganic sulfides and aromatic amines (Cha et al., 1986; Cha and Lim, 1984; Chin et al., 1985; Giles et al., 1986). This technology has the following benefits (Cha and Lim, 1984; Chin et al., 1985; Giles et al., 1986): (1) high-speed reaction rate and effective treatment using mild coupling temperature and pressure; (2) the oxidants and catalysts used are cheap; (3) concurrent removal ability; (4) ease of separation by sedimentation or filtration and disposal of the organic insoluble coupling products by incineration, (5) capable of withstanding process interruptions and (6) ease of recycling of the catalysts from the water-coupling product interface.

However, regeneration efficiency of this coupling-separation scheme is untested for simultaneous extraction of other pollutants from saturated ACs like ammonia, metals and etc. Hence, this technology might be limited in its ability to recover only some pollutants-saturated GACs. Furthermore, its real application in the regeneration of the spent AC via the withdrawal of the adsorbates is still in need. Additionally, the problem that the coupled products cannot recover the adsorbates is a drawback underlying this catalyzed coupling technology. The report from Grant and King demonstrating that the irreversible

chemisorption of the phenol may due to the already existing oxidative coupling of phenolic compounds on carbon surfaces raises another issue with the regeneration of the phenol-saturated activated carbon using the coupling method (Grant and King, 1990). Hence, the proposed oxidative coupling method may only be usable for the removal of the physisorbed phenols or whether it can break the pre-existing coupling bond between the adsorbate and activated carbon still needs examination.

2.10.4 Microwave-assisted regeneration of AC

Owing to its rapid development, the microwave technique has been broadly explored in many areas including food processing, wood drying and polymerization of resins and polymers (Çalışkan et al., 2012; Jones et al., 2002). Microwaves are electromagnetic waves and can create vibrations and rotations in the molecules of countless substrates and consequently produce heat (Robers et al., 2005). Microwave heating has largely replaced electric heating due to its fast heating and easy operation (Çalışkan et al., 2012). Since the carbons have delocalized π-electrons, they can absorb and interact with microwave radiation, therefore effectively transforming the microwave energy into heat (Çalışkan et al., 2012). The microwave radiation is adsorbed by materials denoted by dielectrics and hence microwave heating is also linked to dielectric heating (Jones et al., 2002). Efforts have also been made in the thermal regeneration of ACs using microwaves instead of the conventional electric heating (Ania et al., 2004; Çalışkan et al., 2012). The practical application of the microwave-induced technique should be conducted in an inert environment to prevent spontaneous ignition (Robers et al., 2005).

Ania et al. (2004) performed microwave-assisted regeneration on the phenol-saturated ACs. The microwave method offered several advantages over the conventional electric-furnace process since it allowed the adsorbents to be regenerated without carbon damage or loss in a much shorter period of reaction time, and higher adsorption capacities were achieved even after multiple cycles (Ania et al., 2004). Additionally, microwave technology was able to modify the characteristics of the AC by increasing its surface area, thereby, strengthening its adsorption capacity (Ania et al., 2004; Yuen and Hameed, 2009). The principal difference between the electric heating in rotary kiln or vertical furnaces and the microwave method is the approach by which the heat is provided (Menéndez et al., 1999; Yuen and Hameed, 2009). The heat is generated by conduction and/or convection from the outside of the receptor in the former methods, and the temperature gradient is formed until the steady state is achieved (Menéndez et al., 1999). In the latter approach, microwaves induce the heat from dipole rotation and ionic conduction within the subjects (Menéndez et al., 1999). Similarly, other studies have also confirmed that the microwave-assisted regeneration method can restore the AC with better adsorption performance than other traditional electric heating methods (Cha and Carlisle, 2001; Coss and Cha, 2000).

However, Çalışkan et al. (2012) reported that the microwave-induced technology did not restore the adsorption performance of the ACs. Promethazine-saturated ACs treated with microwave heating resulted in more apparent reduction in regeneration yields upon recycling compared to conventional heating approach. Thermal cracking of this particular pharmaceutical compound of promethazine caused by the microwave energy accounted for

the fall in the adsorption efficiencies of the regenerated carbon samples (Çalışkan et al., 2012). Therefore, close examination of whether the microwave-induced method could perform well to reinstate the AC saturated with some specific pollutants is required.

2.10.5 Selection of appropriate regeneration method

A significant number of references were reviewed regarding the thermal, chemical, catalyzed coupling and microwave-induced regeneration methods of the depleted AC. Every method offers advantages to regenerate the saturated AC as well as disadvantages. Generally speaking, the in situ operation of the chemical regeneration is an attractive alternative to thermal regeneration considering its simplicity, reduced carbon loss and its capacity for recovery of the adsorbates and regenerants. However, this technology is limited by its low recoveries pertaining to both regeneration efficiency and textural properties. Catalyzed coupling reactions provide a novel effective and economical separation means for conversion of the adsorbed phenols and other pollutants into insoluble coupling products. However, this method does not desorb a large spectrum of the pollutants, other than phenols, mercapto compounds, inorganic sulfides and aromatic amines. Additionally, this technology necessitates further testing in the application of the extraction of the pollutants from the spent activated carbon to reinstate the adsorbent. The microwave-assisted regeneration method has been regarded as effective due to its short treatment time, low energy consumption, and high restoration of carbon porosity. However, adsorption performance of the regenerated samples by this technique cannot be guaranteed for different retained pollutants. On the whole, different treatment approaches possess different desirable and undesirable properties. The

choice of the most appropriate regeneration method depends on comprehensive analysis of different factors for specific condition.

Even though scores of contributions on the regeneration the AC have been reviewed in this dissertation, various other undiscussed techniques have been undertaken to desorb and reactivate exhausted ACs such as biological generation, supercritical water oxidation, electrochemical method, ultrasonic desorption, ultrasonic-water desorption (Charinpanitkul and Tanthapanichakoon, 2011; Robers et al., 2005; Yuen and Hameed, 2009; Zhang, 2002). Each method exhibits drawbacks as well as advantages. Therefore, the selection of an appropriate regeneration method should give full considerations to different factors such as cost, regeneration efficiency, application, etc., depending on the situation.

Based on the literature review, it appears that adsorption by activated carbon can serve as an excellent method to remove various types of pollutants from water. Hence in this research, the goal is to systematically synthesize and test activated carbons capable of mitigating *p*-cresol and ammonia from aqueous systems. The following chapters (Chapters 3-6) focus on synthesis, testing of activated carbons from agriculture biomass.

REFERENCES

Ahmadpour, A., Do, D.D., 1997. The preparation of activated carbon from macadamia nutshell by chemical activation, Carbon 35, 1723-1732. doi: 10.1016/S0008-6223(97)00127-9.

Ahmaruzzaman, M., 2008. Adsorption of phenolic compounds on low-cost adsorbents: A review, Adv. Colloid Interface Sci. 143, 48-67. doi: 10.1016/j.cis.2008.07.002.

Ahumada, E., Lizama, H., Orellana, F., Suárez, C., Huidobro, A., Sepúlveda-Escribano, A., Rodríguez-Reinoso, F., 2002. Catalytic oxidation of Fe (II) by activated carbon in the presence of oxygen.: Effect of the surface oxidation degree on the catalytic activity, Carbon 40, 2827-2834. doi: 10.1016/S0008-6223(02)00197-5.

Ania, C., Menéndez, J., Parra, J., Pis, J., 2004. Microwave-induced regeneration of activated carbons polluted with phenol. A comparison with conventional thermal regeneration, Carbon 42, 1383-1387.

Berenguer, R., Marco-Lozar, J., Quijada, C., Cazorla-Amoros, D., Morallón, E., 2010. Comparison among Chemical, Thermal, and Electrochemical Regeneration of Phenol-Saturated Activated Carbon, Energy Fuels 24, 3366-3372.

Bhatnagar, A., Sillanpää, M., 2010. Utilization of agro-industrial and municipal waste materials as potential adsorbents for water treatment—A review, Chem. Eng. J. 157, 277-296. doi: 10.1016/j.cej.2010.01.007.

Bilgili, M.S., 2006. Adsorption of 4-chlorophenol from aqueous solutions by xad-4 resin: Isotherm, kinetic, and thermodynamic analysis, J. Hazard. Mater. 137, 157-164. doi: 10.1016/j.jhazmat.2006.01.005.

Boehm, H.P., 2002. Surface oxides on carbon and their analysis: a critical assessment, Carbon 40, 145-149. doi: 10.1016/S0008-6223(01)00165-8.

Boudrahem, F., Aissani-Benissad, F., Aït-Amar, H., 2009. Batch sorption dynamics and equilibrium for the removal of lead ions from aqueous phase using activated carbon developed from coffee residue activated with zinc chloride, J. Environ. Manage. 90, 3031-3039. doi: 10.1016/j.jenvman.2009.04.005.

Boyd, G. E., Adamson, A. W., and Myers Jr., L. S., 1947. The exchange adsorption of ions from aqueous solutions by organic zeolites. II. Kinetics1. J. Am. Chem. Soc. 69, 2836-2848.

Çalışkan, E., Bermudez, J., Parra, J., Menéndez, J., Mahramanlıoğlu, M., Ania, C., 2012. Low temperature regeneration of activated carbons using microwaves: Revising conventional wisdom, J. Environ. Manage. 102, 134-140.

Cannon, F.S., Knappe, D., Snoeyink, V.L., Lee, R., DeWolfe, J., Dagois, G., 1994. Effect of Metals on Thermal Regeneration of Granular Activated Carbon, AWWAR.

CarrascoMarin, F., AlvarezMerino, M., MorenoCastilla, C., 1996. Microporous activated carbons from a bituminous coal, Fuel 75, 966-970. doi: 10.1016/0016-2361(96)00043-9.

Cha, J., Berry, K., Lim, P., 1986. Aerobic coupling of aqueous phenols catalyzed by binuclear copper: Ring substituent effect and the kinetics of the coupling of o-methylphenol, AIChE J. 32, 477-485.

Cha, C.Y., Carlisle, C.T., 2001. Microwave Process for Volatile Organic Compound Abatement, J. Air Waste Manage. Assoc. 51, 1628-1641. doi: 10.1080/10473289.2001.10464389.

Cha, J.A., Lim, P.K., 1984. A novel separation technique using aerobic coupling reactions, Chem. Eng. Sci. 39, 1522-1524. doi: http://dx.doi.org/10.1016/0009-2509(84)80012-3.

Charinpanitkul, T., Tanthapanichakoon, W., 2011. Regeneration of activated carbons saturated with pyridine or phenol using supercritical water oxidation method enhanced with hydrogen peroxide, J. Ind. Eng. Chem. 17, 570-574.

Chien, S., Clayton, W., 1980. Application of Elovich equation to the kinetics of phosphate release and sorption in soils, Soil Sci. Soc. Am. J. 44, 265-268.

Chin, K.C., Cha, J.A., Lim, P.K., 1985. A novel coupling-dephenolization scheme for full-strength coal-conversion wastewaters: results of wastewater study and a cost analysis, Ind. Eng. Chem. Proc. Des. Dev. 24, 339-343.

Chung, Y., Ahn, W., Lim, P., 1999. Biphasic coupling polymerization of 2, 6-dimethylphenol using surface-active copper complex catalysts, J. Mol. Catal. A: Chem. 148, 117-126.

Colella, L.S., Armenante, P.M., Kafkewitz, D., Allen, S.J., Balasundaram, V., 1998. Adsorption Isotherms for Chlorinated Phenols on Activated Carbons, J. Chem. Eng. Data 43, 573-579. doi: 10.1021/je970217h.

Cooney, D.O., Nagerl, A., Hines, A.L., 1983. Solvent regeneration of activated carbon, Water Res. 17, 403-410.

Coss, P.M., Cha, C.Y., 2000. Microwave Regeneration of Activated Carbon Used for Removal of Solvents from Vented Air, J. Air Waste Manage. Assoc. 50, 529-535. doi: 10.1080/10473289.2000.10464038.

Coughlin, R.W., Ezra, F.S., 1968. Role of surface acidity in the adsorption of organic pollutants on the surface of carbon, Environ. Sci. Technol. 2, 291-297. doi: 10.1021/es60016a002.

Dąbrowski, A., 2001. Adsorption—from theory to practice, Adv. Colloid Interface Sci. 93, 135-224.

Dąbrowski, A., Podkościelny, P., Hubicki, Z., Barczak, M., 2005. Adsorption of phenolic compounds by activated carbon—a critical review, Chemosphere 58, 1049-1070. doi: 10.1016/j.chemosphere.2004.09.067.

Demirbas, E., Dizge, N., Sulak, M.T., Kobya, M., 2009. Adsorption kinetics and equilibrium of copper from aqueous solutions using hazelnut shell activated carbon, Chem. Eng. J. 148, 480-487. doi: 10.1016/j.cej.2008.09.027.

Ehrburger, P., Addoun, A., Addoun, F., Donnet, J., 1986. Carbonization of coals in the presence of alkaline hydroxides and carbonates: Formation of activated carbons, Fuel 65, 1447-1449. doi: 10.1016/0016-2361(86)90121-3.

Ferro-García, M., Utrera-Hidalgo, E., Rivera-Utrilla, J., Moreno-Castilla, C., Joly, J., 1993. Regeneration of activated carbons exhausted with chlorophenols, Carbon 31, 857-863.

Foo, K., Hameed, B., 2012. Preparation, characterization and evaluation of adsorptive properties of orange peel based activated carbon via microwave induced K 2 CO 3 activation, Bioresour. Technol. 104, 679-686.

Franz, M., Arafat, H.A., Pinto, N.G., 2000. Effect of chemical surface heterogeneity on the adsorption mechanism of dissolved aromatics on activated carbon, Carbon 38, 1807-1819. doi: 10.1016/S0008-6223(00)00012-9.

Freundlich, H., 1906. Over the adsorption in solution, J. Phys. Chem. 57, 385-470.

Giles, D.W., Cha, J.A., Lim, P.K., 1986. The aerobic and peroxide-induced coupling of aqueous thiols—I. Kinetic results and engineering significance, Chem. Eng. sci. 41, 3129-3140.

Girgis, B.S., Yunis, S.S., Soliman, A.M., 2002. Characteristics of activated carbon from peanut hulls in relation to conditions of preparation, Mater. Lett. 57, 164-172. doi: http://dx.doi.org/10.1016/S0167-577X(02)00724-3.

Grant, T.M., King, C.J., 1990. Mechanism of irreversible adsorption of phenolic compounds by activated carbons, Ind. Eng. Chem. Res. 29, 264-271.

Hadjar, H., Hamdi, B., Ania, C.O., 2011. Adsorption of *p*-cresol on novel diatomite/carbon composites, J. Hazard. Mater. 188, 304-310. doi: 10.1016/j.jhazmat.2011.01.108.

Haghseresht, F., Nouri, S., Lu, G.Q.M., 2003. Effects of carbon surface chemistry and solution pH on the adsorption of binary aromatic solutes, Carbon 41, 881-892. doi: 10.1016/S0008-6223(02)00437-2.

Haimour, N., El-Bishtawi, R., Ail-Wahbi, A., 2005. Equilibrium adsorption of hydrogen sulfide onto CuO and ZnO, Desalination 181, 145-152. doi: 10.1016/j.desal.2005.02.017.

Himmelstein, K., Fox, R., Winter, T., 1973. In-place regeneration of activated carbon, Chem. Eng. Prog. 69, 65-69.

Ho, Y., McKay, G., 1998. Sorption of dye from aqueous solution by peat, Chem. Eng. J. 70, 115-124.

Ho, Y., McKay, G., 1999. Pseudo-second order model for sorption process. Process biochem. 34, 451-465.

IllanGomez, M., GarciaGarcia, A., deLecea, C., LinaresSolano, A., 1996. Activated carbons from Spanish coals .2. Chemical activation, Energy Fuels 10, 1108-1114. doi: 10.1021/ef950195+.

Jones, D.A., Lelyveld, T.P., Mavrofidis, S.D., Kingman, S.W., Miles, N.J., 2002. Microwave heating applications in environmental engineering-a review, Resour. Conserv. Recycling 34, 75-90. doi: http://dx.doi.org/10.1016/S0921-3449(01)00088-X.

Juang, R., Chen, M., 1997. Application of the Elovich Equation to the Kinetics of Metal Sorption with Solvent-Impregnated Resins, Ind. Eng. Chem. Res. 36, 813-820. doi: 10.1021/ie960351f.

Khan, T.A., Dahiya, S., Ali, I., 2012. Use of kaolinite as adsorbent: Equilibrium, dynamics and thermodynamic studies on the adsorption of Rhodamine B from aqueous solution, Appl. Clay. Sci. 69, 58-66.

Kilic, M., Apaydin-Varol, E., Pütün, A.E., 2011. Adsorptive removal of phenol from aqueous solutions on activated carbon prepared from tobacco residues: Equilibrium, kinetics and thermodynamics, J. Hazard. Mater. 189, 397-403.

Kurniawan, T.A., Lo, W.H., Sillanpaa, M.E.T., 2011. Treatment of Contaminated Water Laden with 4-Chlorophenol using Coconut Shell Waste-Based Activated Carbon Modified with Chemical Agents, Sep. Sci. Technol. 46, 460-472. doi: 10.1080/01496395.2010.512030.

Lagergren, S., 1898. About the theory of so-called adsorption of soluble substances. K. Sven. Vetenskapsakad. Handl. 24(4), 1-39.

Langmuir, I., 1916. THE CONSTITUTION AND FUNDAMENTAL PROPERTIES OF SOLIDS AND LIQUIDS. PART I. SOLIDS. J. Am. Chem. Soc. 38, 2221-2295.

Laszlo, K., Podkoscielny, P., Dabrowski, A., 2003. Heterogeneity of polymer-based active carbons in adsorption of aqueous solutions of phenol and 2, 3, 4-trichlorophenol, Langmuir 19, 5287-5294.

Le Leuch, L.M., Bandosz, T.J., 2007. The role of water and surface acidity on the reactive adsorption of ammonia on modified activated carbons, Carbon 45, 568-578. doi: 10.1016/j.carbon.2006.10.016.

Leng, C., Pinto, N.G., 1996. An investigation of the mechanisms of chemical regeneration of activated carbon, Ind. Eng. Chem. Res. 35, 2024-2031.

Lim, P.K., Cha, J.A., Patel, C.P., 1983. Aerobic coupling of aqueous phenol catalyzed by cuprous chloride: basis of a novel dephenolization scheme for phenolic wastewaters, Ind. Eng. Chem. Proc. Des. Dev. 22, 477-482.

Lin, S., Juang, R., 2009. Adsorption of phenol and its derivatives from water using synthetic resins and low-cost natural adsorbents: A review, J. Environ. Manage. 90, 1336-1349. doi: 10.1016/j.jenvman.2008.09.003.

Love, C., Kolar, P., Classen, J., Das, L., 2011. Adsorption of ammonia on ozonated activated carbon, T. ASABE 54, 1931-1940.

Lyman, W.J., 1978. Applicability of carbon adsorption to the treatment of hazardous industrial wastes, Carbon Adsorption Handbook.Ann Arbor Science Publishers Inc 4, 131-165.

Ma, J., Huang, D., Zou, J., Li, L., Kong, Y., Komarneni, S., 2015. Adsorption of methylene blue and Orange II pollutants on activated carbon prepared from banana peel, J. of Porous Mater. 22, 301-311.

Madhava, R., M., Ramesh, A., Chandra, R., G. Purna, Seshaiah, K., 2006. Removal of copper and cadmium from the aqueous solutions by activated carbon derived from Ceiba pentandra hulls, J. Hazard. Mater. 129, 123-129. doi: 10.1016/j.jhazmat.2005.08.018.

Mahajan, O.P., Moreno-castilla, C., Walker, P.L., 1980. Surface-Treated Activated Carbon for Removal of Phenol from Water, Sep. Sci. Technol. 15, 1733-1752. doi: 10.1080/01496398008055619.

Martin, R.J., Ng, W.J., 1984. Chemical regeneration of exhausted activated carbon—I, Water Res. 18, 59-73. doi: 10.1016/0043-1354(84)90048-4.

Mattson, J.A., Mark Jr., H.B., Malbin, M.D., Weber Jr., W.J., Crittenden, J.C., 1969. Surface chemistry of active carbon: Specific adsorption of phenols, J. Colloid Interface Sci. 31, 116-130. doi: 10.1016/0021-9797(69)90089-7.

Menéndez, J.A., Menéndez, E.M., Iglesias, M.J., García, A., Pis, J.J., 1999. Modification of the surface chemistry of active carbons by means of microwave-induced treatments, Carbon 37, 1115-1121. doi: http://dx.doi.org/10.1016/S0008-6223(98)00302-9.

Mohan, D., Singh, K.P., 2002. Single- and multi-component adsorption of cadmium and zinc using activated carbon derived from bagasse—an agricultural waste, Water Res. 36, 2304-2318. doi: 10.1016/S0043-1354(01)00447-X.

Mohd Din, A., Hameed, B., Ahmad, A., 2009. Batch adsorption of phenol onto physiochemical-activated coconut shell, J. Hazard. Mater. 161, 1522-1529.

Moreno-Castilla, C., Rivera-Utrilla, J., Joly, J., Lopez-Ramon, M., Ferro-Garcia, M., Carrasco-Marin, F., 1995. Thermal regeneration of an activated carbon exhausted with different substituted phenols, Carbon 33, 1417-1423.

Mui, E.L.K., Ko, D.C.K., McKay, G., 2004. Production of active carbons from waste tyres—a review, Carbon 42, 2789-2805. doi: 10.1016/j.carbon.2004.06.023.

Nakhla, G., Abuzaid, N., Farooq, S., 1994. Activated carbon adsorption of phenolics in oxic systems: effect of pH and temperature variations, Water Environ. Res, 842-850.

Ravi, V.P., Jasra, R.V., Bhat, T.S.G., 1998. Adsorption of phenol, cresol isomers and benzyl alcohol from aqueous solution on activated carbon at 278, 298 and 323 K, J. Chem. Technol. & Biotechnol. 71, 173-179. doi: 10.1002/(SICI)1097-4660(199802)71:2<173::AID-JCTB818>3.0.CO;2-N.

Redlich, O., Peterson, D.L., 1959. A useful adsorption isotherm, J. Phys. Chem. 63, 1024-1024.

Riccardo, J., Ramirez-Pastor, A., Romá, F., 2002. Multilayer adsorption with multisite occupancy: an improved isotherm for surface characterization, Langmuir 18, 2130-2134.

Rivera-Utrilla, J., Sánchez-Polo, M., Gómez-Serrano, V., Álvarez, P.M., Alvim-Ferraz, M.C.M., Dias, J.M., 2011. Activated carbon modifications to enhance its water treatment applications. An overview, J. Hazard. Mater. 187, 1-23. doi: 10.1016/j.jhazmat.2011.01.033.

Robers, A., Figura, M., Thiesen, P.H., Niemeyer, B., 2005. Desorption of odor-active compounds by microwaves, ultrasound, and water, AIChE J. 51, 502-510. doi: 10.1002/aic.10334.

Rodríguez-Reinoso, F., 1998. The role of carbon materials in heterogeneous catalysis, Carbon 36, 159-175. doi: 10.1016/S0008-6223(97)00173-5.

Sabio, E., González, E., González, J.F., González-García, C.M., Ramiro, A., Gañan, J., 2004. Thermal regeneration of activated carbon saturated with p-nitrophenol, Carbon 42, 2285-2293. doi: http://dx.doi.org/10.1016/j.carbon.2004.05.007.

San Miguel, G., Lambert, S., Graham, N., 2001. The regeneration of field-spent granular-activated carbons, Water Res. 35, 2740-2748.

Sheshdeh, R.K., Khosravi, M.R., 2013. Evaluation of adsorption kinetics and equilibrium for the removal of benzene by modified diatomite, Chem. Eng. Technol. 36, 1713-1720.

Singh, R.K., Kumar, S., Kumar, S., Kumar, A., 2008. Development of parthenium based activated carbon and its utilization for adsorptive removal of *p*-cresol from aqueous solution, J. Hazard. Mater. 155, 523-535. doi: http://dx.doi.org/10.1016/j.jhazmat.2007.11.117.

Streat, M., Patrick, J.W., Perez, M.J.C., 1995. Sorption of phenol and para-chlorophenol from water using conventional and novel activated carbons, Water Res. 29, 467-72. doi: 10.1016/0043-1354(94)00187-C.

Sud, D., Mahajan, G., Kaur, M.P., 2008. Agricultural waste material as potential adsorbent for sequestering heavy metal ions from aqueous solutions - A review, Bioresour. Technol. 99, 6017-6027. doi: 10.1016/j.biortech.2007.11.064.

Sufnarski, M.D., 1999. The regeneration of granular activated carbon using hydrothermal technology, The University of Texas, Austin, Tex, USA, 1999, http://www.dtic.mil/get-tr-doc/ pdf?AD=ADA362534.

Sun, J., Hippo, E.J., Marsh, H., O'Brien, W.S., Crelling, J.C., 1997. Activated carbon produced from an Illinois Basin coal, Carbon 35, 341-352. doi: 10.1016/S0008-6223(96)00157-1.

Suzuki, M., Misic, D.M., Koyama, O., Kawazoe, K., 1978. Study of thermal regeneration of spent activated carbons: thermogravimetric measurement of various single component organics loaded on activated carbons, Chem. Eng. Sci. 33, 271-279.

Teng, H., Lin, Y., Hsu, L., 2000. Production of Activated Carbons from Pyrolysis of Waste Tires Impregnated with Potassium Hydroxide, J. Air Waste Manage. Assoc. 50, 1940-1946. doi: 10.1080/10473289.2000.10464221.

Toledo, L.C., Silva, A.C.B., Augusti, R., Lago, R.M., 2003. Application of Fenton's reagent to regenerate activated carbon saturated with organochloro compounds, Chemosphere 50, 1049-1054.

Vidic, R.D., Suidan, M.T., 1991. Role of dissolved oxygen on the adsorptive capacity of activated carbon for synthetic and natural organic matter, Environ. Sci. Technol. 25, 1612-1618.

Wigmans, T., 1989. Industrial aspects of production and use of activated carbons, Carbon 27, 13-22. doi: 10.1016/0008-6223(89)90152-8.

Wu, F., Liu, B., Wu, K., Tseng, R., 2010. A new linear form analysis of Redlich–Peterson isotherm equation for the adsorptions of dyes, Chem. Eng. J. 162, 21-27. doi: 10.1016/j.cej.2010.03.006.

Yuen, F.K., Hameed, B., 2009. Recent developments in the preparation and regeneration of activated carbons by microwaves, Adv. Colloid Interface Sci. 149, 19-27.

Zhang, H., 2002. Regeneration of exhausted activated carbon by electrochemical method, Chem. Eng. J. 85, 81-85. doi: 10.1016/S1385-8947(01)00176-0.

CHAPTER 3

ADSORPTIVE REMOVAL OF *P*-CRESOL USING COCONUT SHELL-ACTIVATED CHAR

Yiying Zhu, Praveen Kolar *

Biological and Agricultural Engineering, Campus Box 7625, North Carolina State University, Raleigh, NC, 27695-7625, USA.

E-mail addresses: yzhu15@ncsu.edu, pkolar@ncsu.edu

* Corresponding author contact information: 278 Weaver Labs, Campus Box 7625, North Carolina State University, Raleigh, NC, 27695-7625, USA.

Phone: +1 919 513 9797; Fax: +1 919 515 7760.

E-mail address: pkolar@ncsu.edu

*** This chapter "ADSORPTIVE REMOVAL OF *P*-CRESOL USING COCONUT SHELL-ACTIVATED CHAR" has been published in *Journal of Environmental Chemical Engineering*. Reproduced with permission (attached in Appendix A).**

Abstract

Swine farming is a major contributor to the United States' animal agriculture industry. However, it is also associated with several environmental pollutants, among which, *p*-cresol is one of the most odorous. In order to make swine husbandry more sustainable, its environmental impacts have to be minimized. Among several available environmental control technologies, adsorptive removal is perhaps the most effective, practical, simple, and easiest to retrofit. Hence, in this research, a highly adsorptive activated char was synthesized using coconut shells. Batch experiments were systematically carried out to investigate the adsorption performance of the prepared activated char for the removal of *p*-cresol from aqueous solutions. Effects of initial adsorbate concentration (25-500 mg L^{-1}), agitation speed (0-200 rpm), solution pH (2-12), and adsorbent dosage (0.50-3 g 100 mL^{-1}) were also investigated. Results suggest that the kinetic data followed a pseudo-second-order model and intra-particle diffusion was rate limiting during the entire adsorption process. The equilibrium data were best represented by the Langmuir isotherm model, with maximum monolayer adsorption capacities of 30.23 mg g^{-1} at 293 K, 31.57 mg g^{-1} at 303 K and 32.77 mg g^{-1} at 313 K. Our results suggest that physiochemical-activated coconut char is highly effective in the mitigation of *p*-cresol.

Key words

p-Cresol; Adsorption; Coconut shell; Physiochemical activation; Zinc chloride; Activated char

3.1 Introduction

p-Cresol (4-methylphenol) is a major nuisance responsible for the malodor released from swine farming operations [1]. *p*-Cresol is predominantly derived from the decomposition of swine waste, a mixture including urine, feces, and wash water stored in pits underneath the facility or in lagoons [2]. The number of these concentrated animal feeding operations (CAFOs) is growing, resulting in degradation of the air quality in surrounding communities, especially in rural areas [3]. In addition to swine slurry, *p*-cresol is also widely found in petroleum, petrochemical, refinery, coal conversion, and industrial wastewaters [4, 5] and can impart unpleasant taste and odor to drinking water [6]. Even a low concentration of *p*-cresol is harmful to humans, exerting negative effects on human eyes, skin, lungs, kidneys, stomach, and mental health [7]. Thus, it is of great importance to remove this highly malodorous contaminant from wastewater prior to it being released into receiving water bodies [8].

Adsorption is one of the most suitable methods to mitigate *p*-cresol from wastewater. Past studies have tested peat, bentonite, synthetic resin, and rubber tires as adsorbents for removing *p*-cresol and similar phenols from water [4, 6, 9]. Peat and bentonite were found to remove 40-45% of the phenol from the aqueous solution with the adsorption capacity of around 1 mg g^{-1} [4]. On the other hand, synthetic resin was shown to possess a fairly high adsorption capacity for an uptake of 4-chlorophenol of 27.91 mg g^{-1} [6]. Similarly, the adsorption behavior of the rubber tire-based-activated carbon was found to be almost identical to the conventional activated carbon for mitigating phenol and *p*-chlorophenol from

water [9]. Even though these adsorbents have shown to work well for the removal of the contaminants, their cost and availability override their pollutant removal performance.

At the present time, there is a significant emphasis to reuse, recycle, and add value to agricultural solid wastes. Demirbas et al., Kilic et al., and Mondal et al. [10-12] used agricultural wastes such as hazelnut shells, tobacco residues, and bamboo leaves to remove copper, phenol, and mercury, respectively, from wastewater. Our group is also interested in synthesizing inexpensive adsorbents from agricultural wastes for applications in odor mitigation in animal agriculture. Recently, char-based adsorbents derived from pinewood [13] and swine manure for mitigation of *p*-cresol [14] have been synthesized and tested. Adsorbents obtained from pinewood and char served as good adsorbents for mitigation of *p*-cresol, with an adsorption capacity ranging from 2-14 mg g^{-1}. However, these adsorbents did not possess structural stability. In order to withstand the intense mixing that is expected in a commercial adsorption system, the adsorbent should be physically stable and be able to resist physical disintegration of pellets. Based on literature review and our previous experience, the nature of precursor also plays a very important role on the physicochemical properties and adsorption capacity of the material. Previous research by Din et al., Hu et al., and Cazetta et al. [15-17] suggested that activated char derived from coconut shell had excellent physical strength. However, there is a limited information on adsorption of *p*-cresol on activated char derived from coconut shell despite *p*-cresol being one of the most common pollutants associated with swine industry. Therefore, the goal of this research was to synthesize coconut shells activated char (CSAC) and systematically test its efficiency to remove *p*-cresol from

an aqueous system. After obtaining CSAC, the objectives were to (1) characterize the physical and chemical properties of the CSAC; (2) evaluate kinetics of *p*-cresol removal by studying the effects of initial adsorbate concentration, adsorbent mass, pH, and agitation speed; and (3) determine the adsorption isotherms.

3.2 Materials and methods

3.2.1 Preparation of activated char

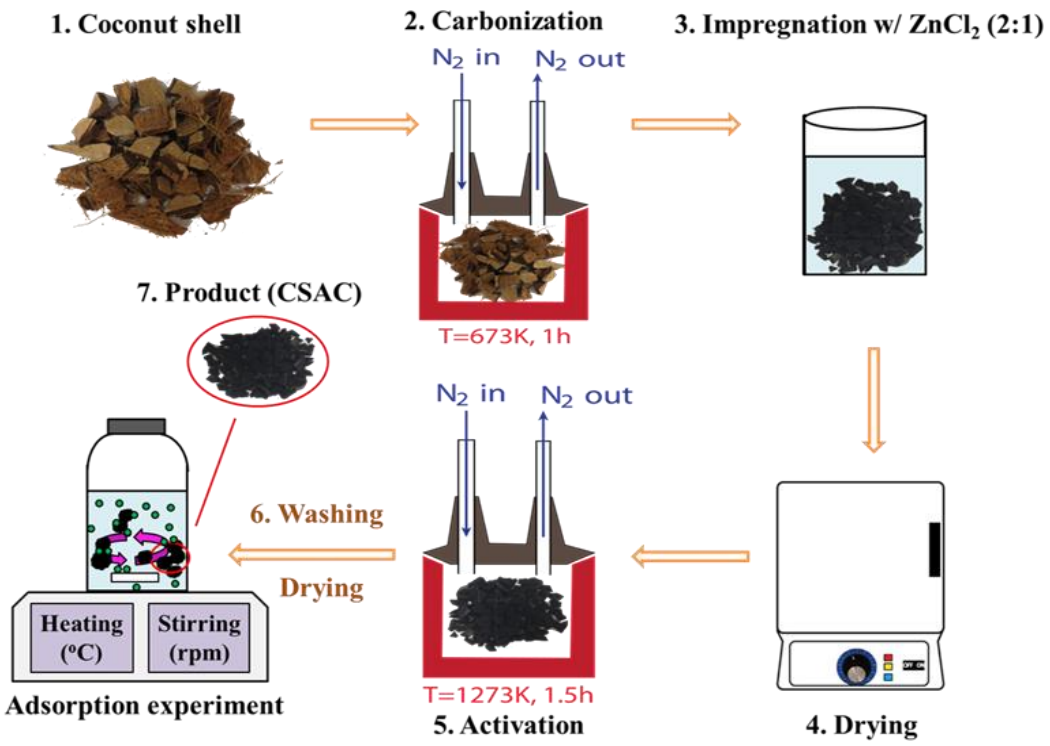

Fig. 3.1: Schematic of the synthesis of CSAC for removal of *p*-cresol.

Locally obtained coconut shells were crushed to a size of 10 mm and carbonized at 673 K for 1 h under an inert atmosphere (nitrogen at 2 L min^{-1} and 10 K min^{-1}). The obtained char was ground and sieved to a size of 2-6 mm, impregnated with zinc chloride (purity 97+%, Acros Organics) (char:$ZnCl_2$: 2:1) for 3 h, and followed by the removal of excess solution and overnight drying at 383 K (Fig. 3.1). The char sample was further pyrolyzed (1273 K for 1.5 h) under a nitrogen flow of 2 L min^{-1}. Subsequently, the cooled samples of CSAC were repeatedly washed via hot deionized water to remove free $ZnCl_2$, tar, fines, and leachable matter followed by overnight drying at 343 K.

3.2.2 Characterization

The yield (%) of CSAC was determined based on the final weight compared to the initial weight of the original shells [18]. Additionally, the CSAC was characterized for its surface physical and chemical properties.

The specific surface area was determined via a Brunauer-Emett-Teller (BET) analyzer (Micrometrics Germini VII 2390p). Prior to the analysis, a certain weight of the CSAC was randomly selected and degassed at 423 K for at least 2 h in a furnace with a N_2 flow of 10 L min^{-1}. The BET surface area was then calculated assuming the monolayer N_2 adsorption at the temperature of liquid nitrogen (77K) and molecular area of 0.162 nm^2 on the activated char surface [19, 20].

A time-of-flight secondary ion mass spectrometer (TOF-SIMS) (ION TOF Inc., Chestnut Ridge, NY) equipped with Bi_3^+ and C_{60}^+ guns was employed to investigate the surface functional groups of CSAC after physiochemical treatment. In this study, a pulsed

Bi_3^+ primary ion beam with an impact energy of 25 kV and 0.4 pA current was used. The beam width was kept below 1ns to ensure high mass resolution.

The acid value of CSAC was determined by measuring the pH of an equilibrated sample of 0.4 g of the dry CSAC mixed with 20 mL of deionized water at 400 rpm for 12 h [21].

The point of zero charge (pzc) of the CSAC was determined by the pH drift method outlined by Babić et al. [22]. Briefly, 0.2 g of CSAC was shaken with 40 mL of 0.1 N and 0.01 N KNO_3 solutions for 24 h at 150 rpm in serum bottles maintained at pH between 2 and 12 (adjusted with 0.1 N KOH or HNO_3 solution). After filtration, the final pH values of the filtrates were recorded and plotted against the initial pH. The pH at which the plotted curve intersected the 45°straight line ($pH_{final} = pH_{initial}$) was recorded as the pH_{pzc} of the CSAC [23, 24].

Boehm titration was performed to determine the type and strength of the functional groups [25]. Briefly, 0.5 g of the CSAC was mixed with 50 mL of 0.05 M HCl, NaOH, Na_2CO_3, and $NaHCO_3$ solutions, respectively, in a series of flasks. These flasks were sealed with a parafilm and placed in a shaking incubator for 24 h at 150 rpm. The solutions were filtered with a Whatman No.42 filter paper, and 10 mL of each filtrate was pipetted to a flask and titrated with 0.05 M NaOH or HCl solution, using phenolphthalein and methyl red indicators for basic and acidic titrants, respectively.

3.2.3 Batch adsorption experiments

One gram of CSAC was mixed with 100 mL of *p*-cresol solution (25-500 mg L^{-1}) at 100 rpm on an isothermal hot plate for 24 h. Liquid samples (0.5 mL) were periodically withdrawn and the residual concentration of *p*-cresol was determined using a UV spectrometer (UV-1700 Pharma Spec, Shimadzu) (277 nm). All batch adsorption experiments were carried out in duplicate under identical conditions in 150 mL serum bottles, as indicated in Fig. 3.1. The data obtained were used to determine the fractional removal, X (%), and equilibrium adsorption capacity, q_e (mg g^{-1}), using the following equations [12]:

$$X\ (\%) = \frac{C_0 - C_t}{C_0} \times 100 \tag{3-1}$$

$$q_e = \frac{(C_o - C_e)V}{W} \tag{3-2}$$

where C_0, C_t, and C_e are the initial, any given time, and equilibrium *p*-cresol concentrations in the aqueous solutions, respectively (mg L^{-1}), V is the volume of the solution (L), and W is the weight of the CSAC (g).

3.2.4 Adsorption kinetics and isotherms

Experiments were performed in duplicates to study the effects of initial adsorbate concentration (25-500 mg L^{-1}), pH (2-12), adsorbent dosage (5-30 g L^{-1}), and agitation speed (0-200 rpm). The data were analyzed to determine the kinetic parameters using non-linear pseudo first-order (Eq. (3-3)), pseudo second-order (Eq. (3-4)), Elovich (Eq. (3-5)), and linear intra-particle diffusion kinetic models (Eq. (3-6)) [10, 17].

$$q_t = q_e[1 - e^{-k_1 t}\,] \tag{3-3}$$

where the q_e (mg g^{-1}) and q_t (mg g^{-1}) are the adsorption of *p*-cresol at equilibrium and the adsorption of *p*-cresol at a time t (min), respectively, and k_1 is the pseudo first-order adsorption rate constant (min^{-1}).

$$q_t = \frac{k_2 q_e^2 t}{1 + k_2 q_e t} \tag{3-4}$$

where k_2 is the pseudo second-order adsorption rate constant (g $mg^{-1}min^{-1}$). In addition, from the values q_e and k_2, the initial adsorption rate $h = k_2 q_e^2$ (mg g^{-1} min^{-1}) was also calculated.

$$q_t = \frac{1}{\beta} In(\alpha\beta) + \frac{1}{\beta} In(t) \tag{3-5}$$

where α (mg $g^{-1}min^{-1}$) and β (g mg^{-1}) are constants. α can be considered as the initial adsorption rate.

$$q_t = K_{id} t^{0.5} + I \tag{3-6}$$

where the k_{id} is the intraparticle diffusion constant (mg $g^{-1}min^{-0.5}$) and I is a constant.

To determine adsorption isotherms, duplicate experiments were performed at 293, 303, and 313 K using *p*-cresol concentrations of 25-500 mg L^{-1}. The data were analyzed using Langmuir (Eq. (3-7)), Freundlich (Eq. (3-8)), Redlich-Peterson (Eq. (3-9)), and Temkin isotherm models (Eq. (3-10)) [26].

$$q_e \quad = \frac{Q_O K_L C_e}{1 + K_L C_e} \tag{3-7}$$

$$q_e = K_F \, C_e^{\,1/n} \tag{3-8}$$

$$q_e = \frac{AC_e}{1 + BC_e^{\beta}} \tag{3-9}$$

$$q_e = \left(\frac{RT}{b_T}\right) In(\alpha C_e) \tag{3-10}$$

where q_e is the equilibrium amount of adsorbate adsorbed per unit mass of adsorbent (mg g^{-1}), C_e is the equilibrium concentration of adsorbate in bulk solution (mg L^{-1}), Q_0 represents the maximum monolayer adsorption capacity of the adsorbent (mg g^{-1}), K_L (L mg^{-1}) and K_F (mg g^{-1}(L $mg^{-1})^{1/n}$) are Langmuir and Freundlich constants associated with the affinity of the binding sites. The constant $1/n$ measures the strength of adsorption, where $1/n < 1$ represents a strong adsorption bond for that adsorbate.

In the empirical Redlich-Peterson adsorption isotherm, A (L g^{-1}) and B (L mg^{-1}) are Redlich-Peterson constants, while β is an exponent between 0 and 1. Similarly, for the Temkin isotherm model, RT/b_T (J mol^{-1}), is the Temkin constant related to the heat of adsorption, whereas R (8.314 J mol^{-1} K^{-1}) and T (K) are the universal gas constant and the absolute solution temperature, respectively. The term α is the equilibrium binding constant related to the maximum binding energy with the unit of liter per gram.

Furthermore, the dimensionless separation factor (R_L) (Eq. (3-11)) was determined using the Langmuir constant K_L (L mg^{-1}) to ascertain the favorability of the adsorption [7].

$$R_L = \frac{1}{1 + K_L C_o} \tag{3-11}$$

where C_0 is the initial concentration of adsorbate (mg L^{-1}).

All data were analyzed using MATLAB and EXCEL to obtain kinetic and isotherm parameters.

3.3 Results and discussion

3.3.1 Characterization of CSAC

The results of the physical and chemical characterization of the CSAC are summarized in Supplementary Table B.1 and B.2, Fig. 3.2 and Supplementary Fig. B.1. The surface of the CSAC consisted of 70.47% of the microporous surface area, which favors adsorption of small molecules such as *p*-cresol. The moderate char surface area was considered to be associated with the low pore volume observed, perhaps due to the prevalence of the micropores that resulted from $ZnCl_2$ treatment [27, 28]. Since adsorption on activated char is governed by mass transfer processes, with the exceptions of the surface area and pore volume, other factors such as pore size distribution, shape and arrangement of the pores, the interaction between adsorbent and adsorbate will also affect the adsorption processes [29-31].

Supplementary Fig. B.1 elucidates that pH_{pzc} of the CSAC is 7.2, which provides the information on surface charge of the adsorbent as a function of the pH of the coexisting liquid bulk solution. pH_{pzc} refers to the pH value at which the surface charge of the activated char is zero and how the surface potential of the activated char changes with pH. In this study, the surface of the activated char is positively charged until the pH value of the solution reaches 7.2, above which the char surface will become negatively charged.

Results from Boehm titration (Supplementary Table B.2) suggest that the basic functional groups are predominant in the produced CSAC with a very low content of the acidic oxygen functional groups, which is preferable for adsorption of *p*-cresol [32]. The presence of the acidic oxygen functional groups such as carboxylic acid is highly undesirable in *p*-cresol adsorption, since it has been reported that these groups will increase the char hydrophilicity and form water cluster through hydrogen bonds, and therefore, hinder the adsorption of phenolic compound [21, 33]. Further, the electron-withdrawing acidic functional groups, mostly carboxyl and phenolic hydroxyl, will remove the π electrons from the graphene layers of char, increase its affinity toward water and therefore weaken the π-π dispersion interaction with phenols and inhibit the adsorption capacity [33, 34]. However, the basic functional groups (e.g., pyrones, chromenes, quinones and ethers) can act as electron acceptors to enhance the adsorption of *p*-cresol from the formation of electron donor-acceptor complexes [15]. Furthermore, the basic sites at π-electron rich regions at the carbon basal plane edges may induce the formation of the electron donor complexes with the aromatic ring of the phenolic compounds, thereby promoting adsorption [15].

The negative ion TOF-SIMS spectrum (Fig. 3.2) shows an increase in O^- and OH^- ion intensities relative to the hydrocarbon fragment groups after physiochemical treatment. However, no significant change in ion intensity for carboxylic functional group CHO_2^- at m/z 45 was detected from the spectrum, presumably due to low concentration, which is consistent with the results obtained from Boehm titration where the carboxylic groups are not detected (Supplementary Table B.2). Other functional groups that are substantially increased

after the physiochemical treatment are F^- (m/z 19) and Cl^- (m/z 35 and 37). C_2H^- (m/z 25) and C_4H^- (m/z 49) showed significantly decreased ion intensities. The relatively higher ion intensities of O^- and OH^- to hydrocarbon fragments suggest that CSAC underwent carbonation and oxidation processes during physiochemical treatment.

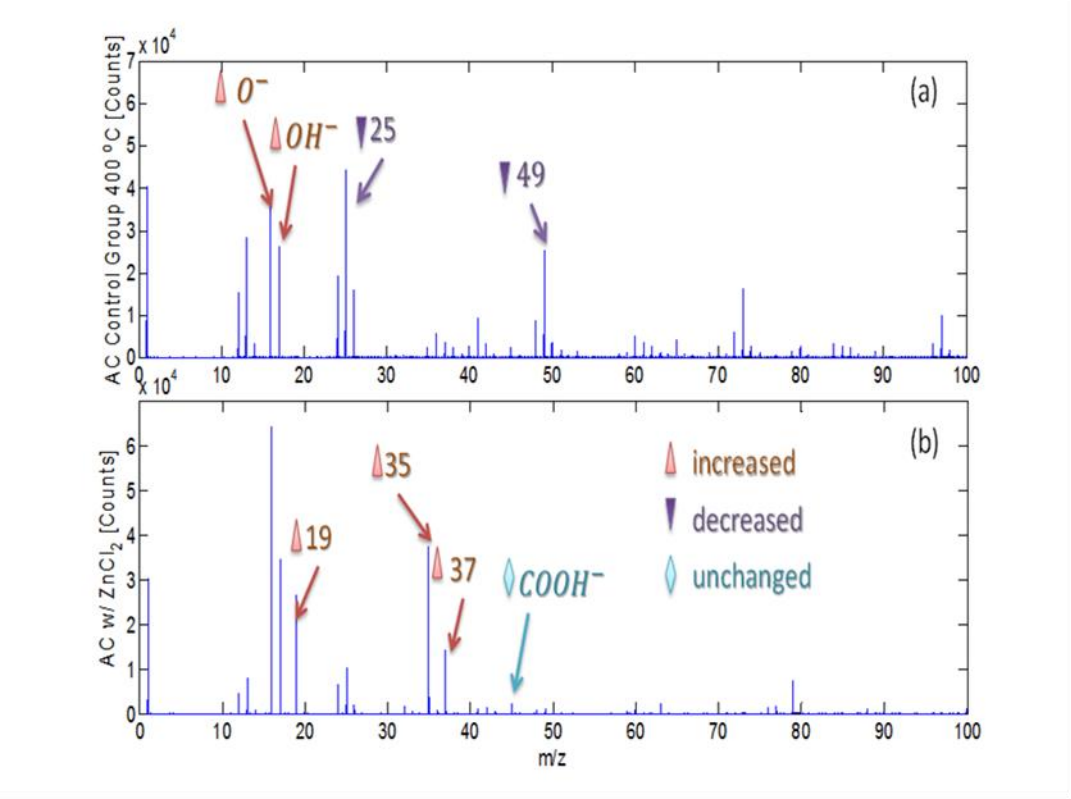

Fig. 3.2: Negative ion TOF-SIMS spectrum for (a) raw material pretreated for 1 h at 313 K; (b) pretreated material that was further physicochemically treated to CSAC.

3.3.2 Kinetic study

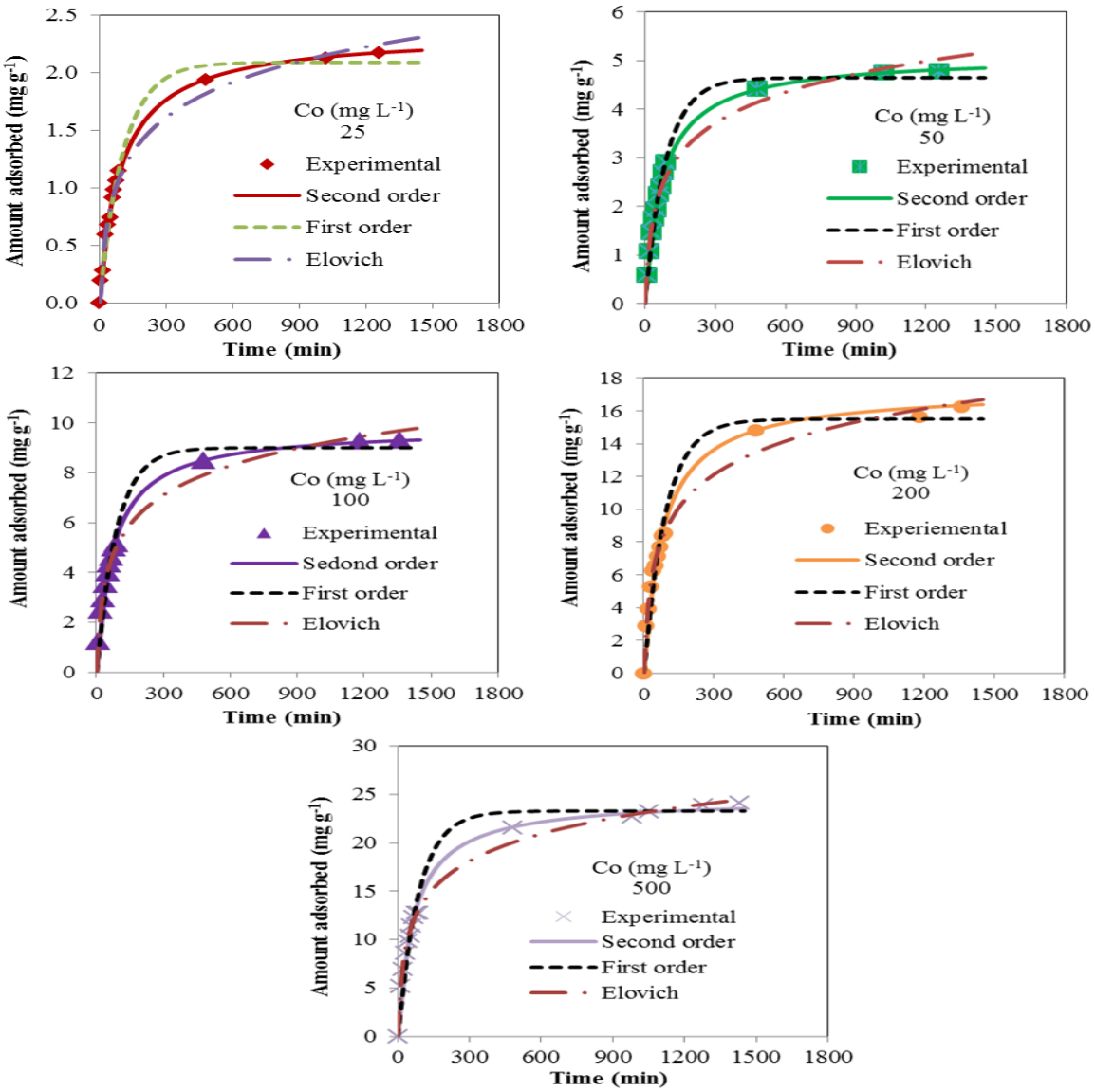

Fig. 3.3: Comparison of non-linear fits of pseudo-first order, pseudo-second order, and Elovich kinetic models for adsorption of *p*-cresol at various initial concentrations (Conditions: 10 g L^{-1} adsorbent dosage, 100 rpm, unadjusted pH, 24-h agitation time at 303 K)

Supplementary Table B.3 and B.4 list the kinetic parameters derived from fitting the experimental data to three kinetic models. Considering the correlation coefficient (R^2), the experimental data presented were in excellent compliance with the pseudo-second-order kinetic model and closer values between $q_{e,exp}$ and $q_{e,cal}$ than pseudo first-order or Elovich models, suggesting a chemisorption-dominated adsorption process. A sample comparison of these fits is presented in Fig. 3.3, which illustrates that the second order kinetic model is most suitable for describing these adsorption systems.

3.3.2.1 Effect of the initial adsorbate concentration on p-cresol adsorption

As shown in Fig. 3.4, the uptake of *p*-cresol on CSAC for a given concentration increased with the initial time period. As expected, adsorption rate was much higher during the initial period because of the availability of the active sites on CSAC, together with a larger concentration gradient between CSAC surface and *p*-cresol solution. As the adsorption proceeded, the removal rate declined as activated sites were occupied and the concentration gradient decreased. Adsorption was found to reach an equilibrium after 24 h.

At higher initial concentrations (50-500 mg L^{-1}), adsorption of *p*-cresol was found to be higher due to the larger driving force as suggested by Killic et al [11]. However, increasing the initial *p*-cresol concentration from 25 mg L^{-1} to 500 mg L^{-1} decreased the second order rate constant (k_2) from 4.33×10^{-3} g mg^{-1} min^{-1} to 6.1×10^{-4} g mg^{-1} min^{-1} while the initial adsorption rate (h) increased from 2.38×10^{-2} mg g^{-1} min^{-1} to 3.70×10^{-1} mg g^{-1} min^{-1}. Similar observations were reported for removal of copper and 4-chlorophenol from

aqueous solutions [10, 35]. Our results demonstrate that the adsorption of *p*-cresol is a function of the initial concentration. Lower adsorbate concentrations may have lower collisions between *p*-cresol and adsorbent, causing the adsorption to be completed in a shorter time, whereas higher solute concentrations have a higher mass transfer driving force that enables more adsorbate molecules to enter the activated sites.

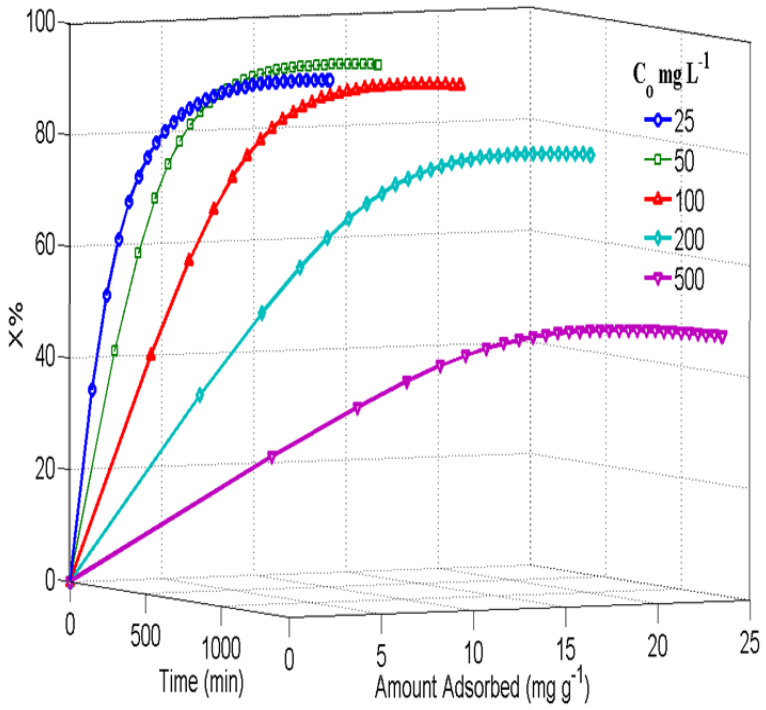

Fig. 3.4: Effect of initial concentration on the adsorption of *p*-cresol by CSAC and percent fractional removal (Conditions: 10 g L^{-1} adsorbent dosage, 100 rpm, unadjusted pH, 24-h contact time at 303 K).

However, Fig. 3.4 exhibits that the fractional removal (after 24 h) decreased from around 95-48% when initial concentrations were increased from 100 mg L^{-1} to 500 mg L^{-1}, indicating the saturation of the activated sites. As the vacant sites on the CSAC are limited, higher initial concentrations result in reduction of percentage removal because available *p*-cresol molecules in solution exceed the adsorption capacity of the CSAC. These findings are consistent with the results of other previously reported adsorption systems for removal of *p*-cresol and phenol [7, 15].

3.3.2.2 Effect of the pH

The solution pH is one of the significant factors governing the uptake process because of its influence on solute dissociation, char surface charge and heterogeneity [32, 36, 37]. As a weak electrolyte, the ionization of the *p*-cresol is pH dependent and the distribution of the surface charge of the amphoteric activated carbon is also found to be a function of the pH [32, 36, 38]. As a result, the electrostatic interactions between the CSAC surface and the *p*-cresol ions and between the adsorbate and adsorbate will change greatly in response to the change in solution pH. Therefore, the effect of the pH is fairly important, and thereby a wide range of pH from 2 to 12 was studied to shed more light on the effect of pH on adsorption. The limiting pH_{pzc} of the liquid bulk solution is the pH at which the adsorbent surface charge is neutral. At this point, the adsorption is simply caused by the diffusion of the adsorbate molecules into the micropores and mesopores of the activated carbon. At $pH < pH_{pzc}$, the carbon surface is positively charged, while it becomes negatively charged at $pH > pH_{pzc}$. Our data clearly show that the acidic environment (pH between 4 and 7) favored the adsorption

with the maximum adsorption capacity at a pH of 4 (Fig. 3.5). This phenomenon can be explained by the electrostatic attraction between positively charged carbon surface and the anionic form of *p*-cresol, since *p*-cresol is more basic in nature due to the methyl and hydroxyl electron-donating functional groups.

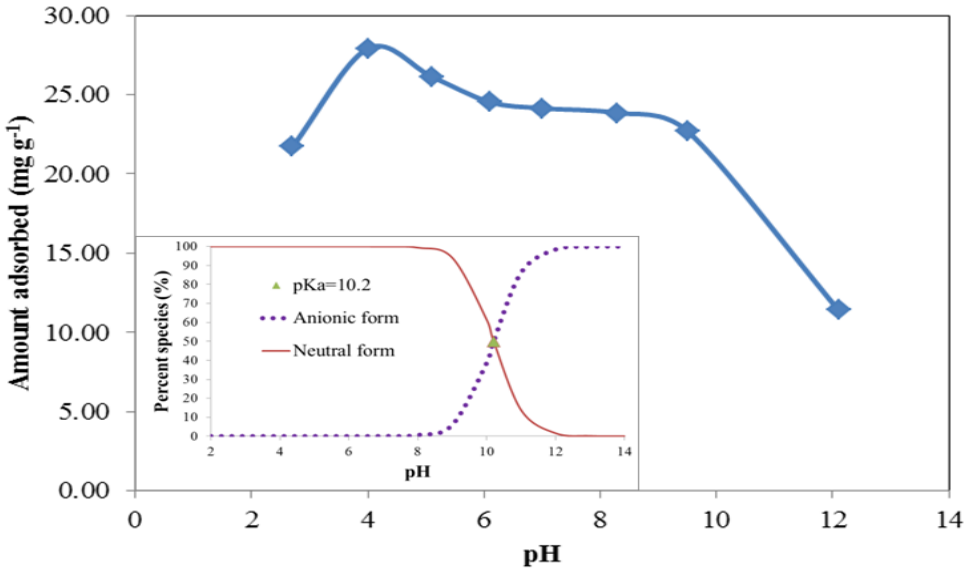

Fig. 3.5: Effect of pH on adsorption of *p*-cresol by CSAC (Conditions: 500 mg L^{-1} concentration, 10 g L^{-1} adsorbent dosage at 303 K, 100 rpm). Inset: Theoretical disassociation pK_a plot for *p*-cresol (adapted from [31]).

Results indicate that the adsorption of *p*-cresol was reduced with incremental pH above 7, and became increasingly pronounced. At pH higher than pH_{pzc} (7.2), the CSAC surface changed to be negatively charged, and the resulting electrostatic repulsion of the

negatively charged *p*-cresol and carbon surface gradually dropped down the adsorption capacity. In addition, using a pK_a value of *p*-cresol of 10.2, a theoretical pK_a plot (Fig. 3.5) is presented similar to the plot previously proposed by Hadjar et al. [31]. The pK_a value implies that the pH value at which the ionizable solute groups are half ionized and half nonionized [39]. At pH higher than 10.2, the ionic *p*-cresol will be dominant over the molecular form, the adjacent molecules of the adsorbed species on the carbon surface will repel each other strongly since they carry the same electrical charge and they cannot be packed densely. The strong electrical repulsion between the *p*-cresol ions on the CSAC surface leads to the impressive decrease in adsorption amount as observed in Fig. 3.5 [39].

Similar to the moderate adsorption at high pH, it is clear from Fig. 3.5 that the low pH will also result in lesser adsorbed *p*-cresol, which is consistent with the results presented in other literatures [31, 40-42]**.** This observation can be explained with the stronger acidic solution (e.g. pH 2.7), the lone pair of electrons in the hydroxyl group are more available for hydrogen bonding and the *p*-cresol becomes positively charged which leads to the reduction in adsorption, also due to the repulsive forces [7, 43].

3.3.2.3 Effect of the adsorbent dosage on p-cresol adsorption

Data presented in Supplementary Table B.3 and Fig. 3.6(a) indicate that as the adsorbent dosage of *p*-cresol increased from 5 to 30 g L^{-1}, adsorption capacity of CSAC decreased from 30.5 to 15.8 mg g^{-1}. As suggested by Kilic et al. [11], excess adsorbents perhaps result in aggregation such that the active sites are not completely occupied by *p*-cresol. Results in this study are similar to other findings from Demirbas et al. and Das et al.

[10, 30], who also reported that increased in adsorbent dosage, resulted in reduction in adsorption capacity owing to more than enough adsorbent used. However, from a kinetic standpoint, the second order rate constant (k_2) increased from 2.3 × 10^{-4} g mg^{-1} min^{-1} to 2.25 × 10^{-3} g mg^{-1} min^{-1} (10-fold increase) with an increase of the adsorbent dosage.

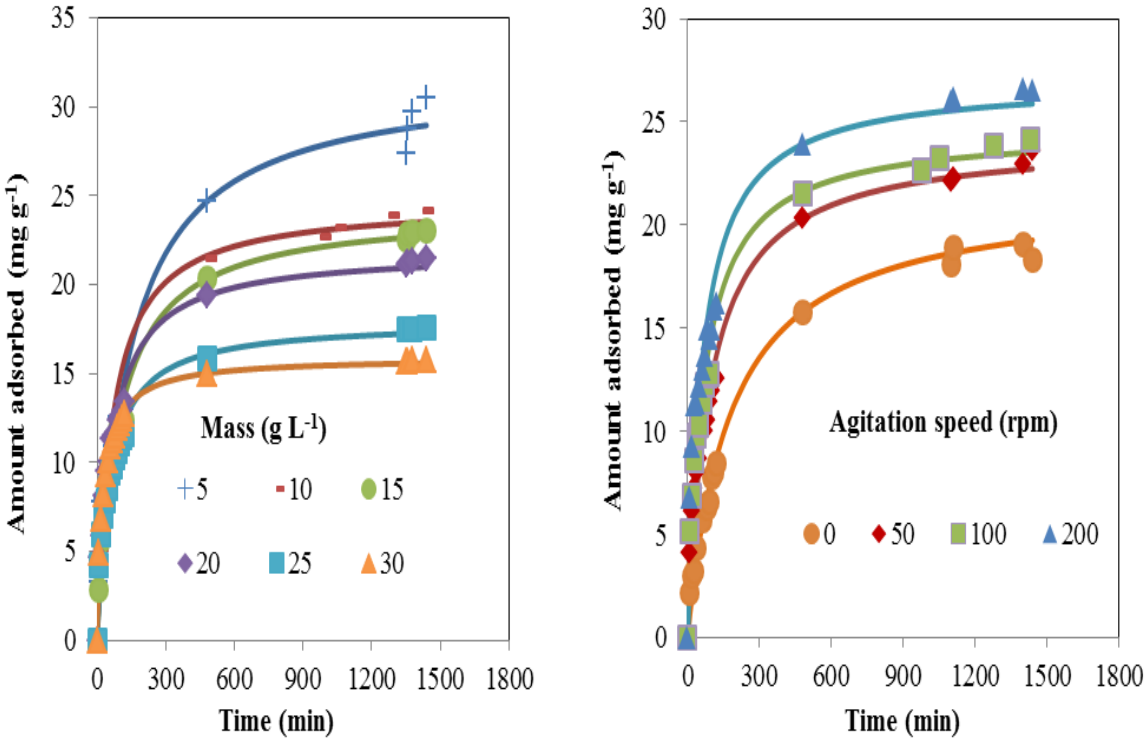

Fig. 3.6: (a) Effect of adsorbent dosage on the adsorption of *p*-cresol by CSAC (Conditions: concentration of 500 mg L^{-1}, 100 rpm, unadjusted pH, 24-h contact time at 303 K); (b) effect of agitation speed (Conditions: concentration of 500 mg L^{-1}, 10g L^{-1} adsorbent dosage, unadjusted pH, 24-h contact time at 303 K).

3.3.2.4 Effect of agitation speed

Our data suggest that the agitation of the system has a significant effect on adsorption capacity (Supplementary Table B.3 and Fig. 3.6(b)). In this study, the unagitated system had an adsorption capacity of 18.4 mg g^{-1}; however, as soon as the agitation was increased (50-200 rpm), the adsorption capacity was significantly increased to 23.6-26.5 mg g^{-1} (an increase of 44%). Gupta et al. [44] also observed a similar trend when studying adsorption of chromium on carbon nanotubes. An analogous tendency was also noticed by Walker et al. [45], who reported increased rate of removal of a reactive dye (Levafix Brilliant Red E-4BA) on dolomite with an increase in agitation rate. In addition, the authors reported up to 90% removal within 60 seconds of agitation. In our work, the turbulence caused by agitation likely enhanced the mass transfer of *p*-cresol from the bulk solution to the CSAC surface, helped adsorbate penetrate into the pores, and thereby facilitated the adsorption process. Beyond 100 rpm, the second order constant remained constant (6×10^{-4} g mg^{-1} min^{-1}), suggesting that the boundary layer thickness around the adsorbent was largely decreased due to the adequate mixing and only the intra-particle diffusion was rate limiting in the adsorption processes.

3.3.3 The mechanism of the adsorption

Supplementary Table B.5 shows the parameters obtained from fitting the intra-particle diffusion model to the data. Fig. 3.7 (q_t versus $t^{1/2}$) shows a combination of two linear segments of the curve with different slopes and intercepts. The first phase, considered to be the instantaneous adsorption phase during which the adsorbent molecules were

transferred to the external surface of the adsorbent via film diffusion, was accomplished in about 3 h. The second phase, regarded as a gradual stage in which the intra-particle diffusion was expected to be rate limiting. However, in our research, neither of the linear segments passed through the origin, suggesting that both the intra-particle diffusion and film diffusion are mechanisms occurring during the adsorption process.

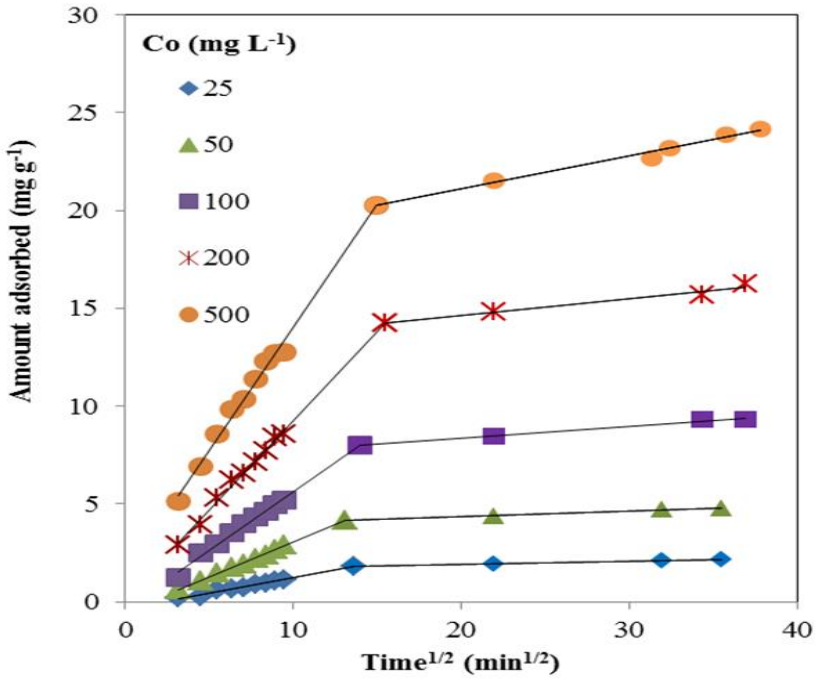

Fig. 3.7: Plot of intraparticle diffusion kinetic model for adsorption of *p*-cresol on CSAC at 303 K.

3.3.4 Isotherm models

The shape of the adsorption isotherm for *p*-cresol on CSAC (Fig. 3.8(a)) suggests a L2 type adsorption process [10]. At low concentrations, there was a rapid increase in the adsorbed amount with the incremental adsorbate concentration due to the large affinity of the surface, which reached a plateau at higher *p*-cresol concentrations indicating a possibility of monolayer adsorption. The L2 type isotherm also suggests that aromatic adsorbate molecules occupied the activated char surface in parallel without strong competitive adsorption of the solvent on char surface. Comparison of different isotherm models at 303K are presented in Fig. 3.8(b) and the isotherm parameters are summarized in Table 3.1. The equilibrium data were best represented by the Langmuir isotherm (R^2 > 0.98) and the monolayer adsorption capacities were estimated to be 30.23 mg g^{-1} (293 K), 31.57 mg g^{-1} (303 K), and 32.77 mg g^{-1} (313 K). When the adsorption data were fitted to the Redlich-Peterson model, the β value was found to be 1.0 and the model was reduced to Langmuir's model supporting the monolayer adsorption. The Freundlich's parameter ($1/n$) was found to be between 0.29 and 0.32, which suggests strong interaction between *p*-cresol and CSAC. This is also corroborated by the estimated separation factors R_L (from Eq. (3-11) (between 0.02 and 0.31)), suggesting that *p*-cresol preferred the solid phase of CSAC over the fluid phase resulting in adsorption of *p*-cresol. With an increase in temperature from 293 K to 313 K, the adsorption capacity was marginally increased. Similar observations were also reported by Al-Degs et al. [46], who observed that as the temperature increased from 298 K to 328 K, the adsorption capacity of reactive dyes on activated carbon increased from 0.27 mmol g^{-1} to

0.77 mmol g^{-1}. Additionally, they explained that it presumably was due to further penetration of the dyes into micropores and the formation of new activated sites [46]. The fitted Temkin model also presents high regression coefficients (R^2 > 0.97), suggesting the decrease in the heat of adsorption at low or medium coverage with increasing coverage due to the adsorbate-adsorbate interactions. The Langmuir model yielded a better fit than the Temkin or the Freundlich model, indicating relatively more homogeneous nature of the CSAC, which was also suggested by Kalavathy et al. [47] in a study that focused on the adsorption of copper on wood sawdust.

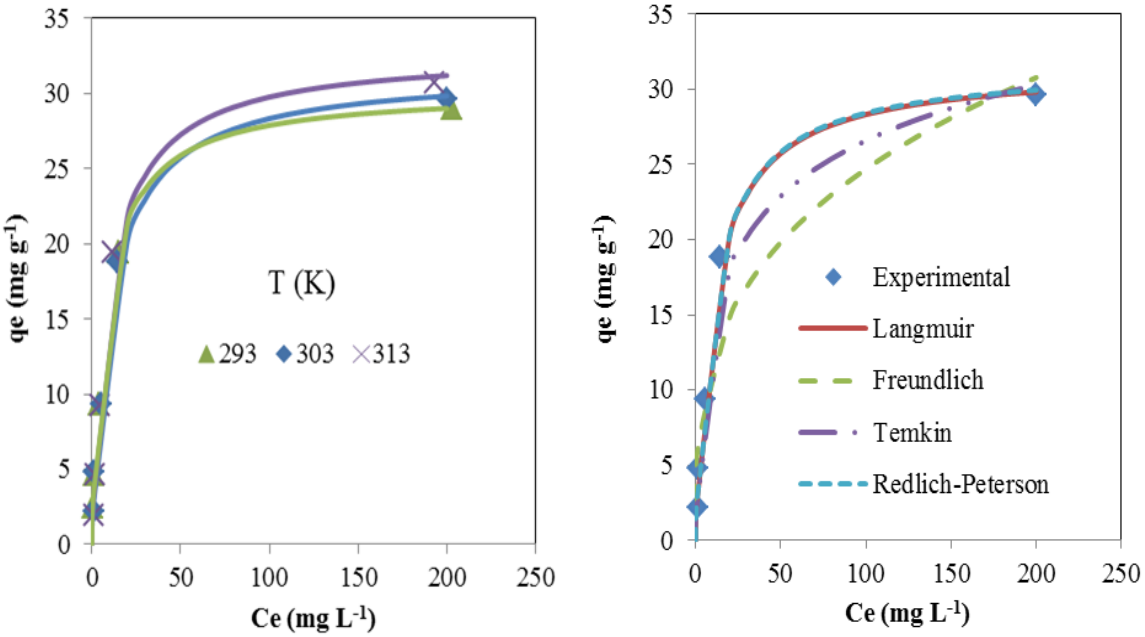

Fig. 3.8: (a) Adsorption isotherms of *p*-cresol on CSAC; (b) comparison of equilibrium isotherms of *p*-cresol on CSAC at 303 K fitted to Langmuir, Freundlich, Redlich–Peterson and Temkin models.

Table 3.1: Isotherm parameters for adsorption of *p*-cresol on CSAC

T (K)	Freundlich isotherm			Langmuir isotherm		
	K_F (mg g^{-1}) (L mg^{-1})$^{1/n}$	*1/n*	R^2	K_L (L mg^{-1})	Q_0 (mg g^{-1})	R^2
293	6.376	0.293	0.906	0.119	30.226	0.999
303	5.711	0.318	0.905	0.089	31.568	0.992
313	5.888	0.321	0.877	0.099	32.768	0.984
T(K)	Redlich-Peterson isotherm				Temkin		
	A (L g^{-1})	B (L mg^{-1})	β	R^2	α (L g^{-1})	ϕ (J mol^{-1})	R^2
293	3.591	0.119	1	0.999	2.218	4.875	0.982
303	2.815	0.089	1	0.992	1.456	5.339	0.978
313	3.241	0.099	1	0.984	1.312	5.78	0.967

The adsorption capacities of *p*-cresol on different adsorbents are compared and listed in Table 3.2. Despite the diversity in use of precursor materials and synthesis conditions, our results show that the coconut shell activated char is a potential adsorbent, which has a relative high adsorption capacity for *p*-cresol. In addition, the rate of adsorption was found to be adequate enough to mitigate *p*-cresol from stagnant wastewater bodies such as swine lagoons. It is also encouraging to note that the coconut shell are easy available, and the synthesis process of CSAC is comparatively simple and is expected to be relatively inexpensive.

Table 3.2: Isotherm parameters for adsorption of *p*-cresol on CSAC

Adsorbent	Maximum adsorption capacity Q_0 (mg g^{-1})	Ref.	Adsorbate	Temperature (K)
Commercial activated carbon	4.74	[48]	Cresol	303
Fly ash	6.7	[48]	Cresol	301
Pine wood activated carbon	6.97	[13]	*p*-Cresol	298
Clay and membrane	8.8	[49]	*o*-Cresol	298
Swine manure char	14.99	[14]	*p*-Cresol	308
Tobacco residue	17.83	[11]	Phenol	Unknown
Amberlite XAD-4 resin	27.59	[6]	*p*-Cresol	308
Coconut-shell activated char	32.77	This work	*p*-Cresol	313
Commercial Activated Alumina	56.61	[50]	*p*-Cresol	298
Phartenium-based activated carbon	62.91	[7]	*p*-Cresol	301
Diatomite/carbon composites	86	[31]	*p*-Cresol	Room temperature

3.4 Conclusion

The present study indicates that the coconut shell-based activated char exhibits high adsorptive performance in mitigating *p*-cresol. The adsorption capacity was determined to be a function of the initial adsorbate concentration, pH, adsorbent dosage, and agitation speed. The physical and chemical characterization of CSAC suggests that the surface chemistry of the char plays a more important role than the specific surface area. The maximum monolayer adsorption capacities were found to be 30.23 mg g^{-1} at 293 K, 31.57 mg g^{-1} at 303 K, and 32.77 mg g^{-1} at 313 K. Our results are expected to add value to agricultural solid waste and improve the design of treatment systems for the removal of *p*-cresol from swine lagoons.

REFERENCES

[1] V. Blanes-Vidal, M.N. Hansen, A.P.S. Adamsen, A. Feilberg, S.O. Petersen, B.B. Jensen, Characterization of odor released during handling of swine slurry: part I. Relationship between odorants and perceived odor concentrations, Atmos. Environ. 43 (18) (2009) 2997–3005.

[2] K.L. Cook, M.J. Rothrock Jr., N. Lovanh, J.K. Sorrell, J.H. Loughrin, Spatial and temporal changes in the microbial community in an anaerobic swine waste treatment lagoon, Anaerobe 16 (2) (2010) 74–82, doi: http://dx.doi.org/ 10.1016/j.anaerobe.2009.06.003. 19539043.

[3] L. Cai, J.A. Koziel, Y. Lo, S.J. Hoff, Characterization of volatile organic compounds and odorants associated with swine barn particulate matter using solid-phase microextraction and gas chromatography–mass spectrometry–olfactometry, J. Chromatogr. A 1102 (1–2) (2006) 60–72, doi: http://dx.doi.org/10.1016/j. chroma.2005.10.040. 16297922.

[4] T. Viraraghavan, F. de Maria Alfaro, Adsorption of phenol from wastewater by peat, fly ash and bentonite, J. Hazard. Mater. 57 (1–3) (1998) 59–70.

[5] F.A. Banat, B. Al-Bashir, S. Al-Asheh, O. Hayajneh, Adsorption of phenol by bentonite, Environ. Pollut. (Barking, Essex: 1987) 107 (3) (2000) 391–398, doi: http://dx.doi.org/10.1016/S0269-7491(99)00173-6. 15092985.

[6] M.S. Bilgili, Adsorption of 4-chlorophenolfromaqueous solutionsbyxad-4 resin: isotherm, kinetic, and thermodynamic analysis, J. Hazard. Mater. 137 (1) (2006) 157–164, doi: http://dx.doi.org/10.1016/j.jhazmat.2006.01.005. 16487655.

[7] R.K. Singh, S. Kumar, S. Kumar, A. Kumar, Development of parthenium based activated carbon and its utilization for adsorptive removal of *p*-cresol from aqueous solution, J. Hazard. Mater. 155 (3) (2008) 523–535, doi: http://dx.doi. org/10.1016/j.jhazmat.2007.11.117. 18207322.

[8] N. Calace, E. Nardi, B.M. Petronio, M. Pietroletti, Adsorption of phenols by papermill sludges, Environ. Pollut. (Barking, Essex: 1987) 118 (3) (2002) 315–319, doi: http://dx.doi.org/10.1016/S0269-7491(01)00303-7. 12009128.

[9] M. Streat, J.W. Patrick, M.J.C. Perez, Sorption of phenol and para-chlorophenol from water using conventional and novel activated carbons, Water Res. 29 (2) (1995) 467–472, doi: http://dx.doi.org/10.1016/0043-1354(94)00187-C.

[10] E. Demirbas, N. Dizge, M.T. Sulak, M. Kobya, Adsorption kinetics and equilibrium of copper from aqueous solutions using hazelnut shell activated carbon, Chem. Eng. J. 148 (2–3) (2009) 480–487.

[11] M. Kilic, E. Apaydin-Varol, A.E. Pütün, Adsorptive removal of phenol from aqueous solutions on activated carbon prepared from tobacco residues: equilibrium, kinetics and thermodynamics, J. Hazard. Mater. 189 (1–2) (2011) 397–403, doi: http://dx.doi.org/10.1016/j.jhazmat.2011.02.051. 21420235.

[12] D.K. Mondal, B.K. Nandi, M.K. Purkait, Removal of mercury (II) from aqueous solution using bamboo leaf powder: equilibrium, thermodynamic and kinetic studies, J. Environ. Chem. Eng. 1 (4) (2013) 891–898, doi: http://dx.doi.org/ 10.1016/j.jece.2013.07.034.

[13] L. Das, P. Kolar, J.J. Classen, J.A. Osborne, Adsorbents from pine wood via K2CO3-assisted low temperature carbonization for adsorption of *p*-cresol, Ind. Crops Prod. 45 (0) (2013) 215–222.

[14] S. Fitzgerald, P. Kolar, J. Classen, M. Boyette, L. Das, Swine manure char as an adsorbent for mitigation of *p*-cresol, Environ. Prog. Sustain. Energy (2014).

[15] A. Mohd. Din, B. Hameed, A. Ahmad, Batch adsorption of phenol onto physiochemical-activated coconut shell, J. Hazard. Mater. 161 (2–3) (2009) 1522–1529, doi: http://dx.doi.org/10.1016/j.jhazmat.2008.05.009. 18562090.

[16] Z. Hu, M.P. Srinivasan, Preparation of high-surface-area activated carbons from coconut shell, Micropor. Mesopor. Mater. 27 (1) (1999) 11–18, doi: http://dx. doi.org/10.1016/S1387-1811 (98) 00183-8.

[17] A.L. Cazetta, A.M.M. Vargas, E.M. Nogami, M.H. Kunita, M.R. Guilherme, A.C. Martins, T.L. Silva, J.C.G. Moraes, V.C. Almeida, NaOH-activated carbon of high surface area produced from coconut shell: kinetics and equilibrium studies from the methylene blue adsorption, Chem. Eng. J. 174 (1) (2011) 117–125.

[18] Y. Diao, W.P. Walawender, L.T. Fan, Activated carbons prepared from phosphoric acid activation of grain sorghum, Bioresour. Technol. 81 (1) (2002) 45–52, doi: http://dx.doi.org/10.1016/S0960-8524 (01) 00100-6. 11708755.

[19] Y. Lee, D. Choi, J. Park, Surface chemical characterization using AES/SAM and ToF-SIMS on KOH-impregnated activated carbon by selective adsorption of NOx, Ind. Eng. Chem. Res. 40 (15) (2001) 3337–3345, doi: http://dx.doi.org/ 10.1021/ie001068q.

[20] S. Brunauer, P.H. Emmett, E. Teller, Adsorption of gases in multimolecular layers, J. Am. Chem. Soc. 60 (2) (1938) 309–319.

[21] Y. El-Sayed, T.J. Bandosz, Adsorption of valeric acid from aqueous solution onto activated carbons: role of surface basic sites, J. Colloid Interface Sci. 273 (1) (2004) 64–72, doi: http://dx.doi.org/10.1016/j.jcis.2003.10.006. 15051433.

[22] B. M. Babić, S. K. Milonjić, M. J. Polovina and B. V. Kaludierović, Point of zero charge and intrinsic equilibrium constants of activated carbon cloth, Carbon 37 (3) (1999) 477–481, doi: http://dx.doi.org/10.1016/S0008-6223(98)00216-4.

[23] C. Tangsathitkulchai, Y. Ngernyen, M. Tangsathitkulchai, Surface modification and adsorption of eucalyptus wood-based activated carbons: effects of oxidation treatment, carbon porous structure and activation method, Korean J. Chem. Eng. 26 (5) (2009) 1341–1352, doi: http://dx.doi.org/10.1007/s11814- 009-0197-4.

[24] M.V. Lopez-Ramon, F. Stoeckli, C. Moreno-Castilla, F. Carrasco-Marin, On the characterization of acidic and basic surface sites on carbons by various techniques, Carbon 37 (8) (1999) 1215–1221, doi: http://dx.doi.org/10.1016/ S0008-6223(98)00317-0.

[25] H. Boehm, Chemical identification of surface groups, Adv. Catal. 16 (1966) 179–274.

[26] B. Hameed, I. Tan, A. Ahmad, Adsorption isotherm, kinetic modeling and mechanism of 2,4,6-trichlorophenol on coconut husk-based activated carbon, Chem. Eng. J. 144 (2) (2008) 235–244, doi: http://dx.doi.org/10.1016/j. cej.2008.01.028.

[27] B.S. Girgis, S.S. Yunis, A.M. Soliman, Characteristics of activated carbon from peanut hulls in relation to conditions of preparation, Mater. Lett. 57 (1) (2002) 164–172, doi: http://dx.doi.org/10.1016/S0167-577X(02)00724-3.

[28] N. Mohamad Nor, L.C. Lau, K.T. Lee, A.R. Mohamed, Synthesis of activated carbon from lignocellulosic biomass and its applications in air pollution control—a review, J. Environ. Chem. Eng. 1 (4) (2013) 658–666, doi: http://dx. doi.org/10.1016/j.jece.2013.09.017.

[29] A. Daifullah, B. Girgis, Removal of some substituted phenols by activated carbon obtained from agricultural waste, Water Res. 32 (4) (1998) 1169–1177, doi: http://dx.doi.org/10.1016/S0043-1354(97)00310-2.

[30] L. Das, P. Kolar, J.A. Osborne, J.J. Classen, Adsorption of *p*-cresol on granular activated carbon, Agric. Eng. Int.: CIGRJ 14 (4) (2012) 37.

[31] H. Hadjar, B. Hamdi, C.O. Ania, Adsorption of *p*-cresol on novel diatomite/ carbon composites, J. Hazard. Mater. 188 (1–3) (2011) 304–310, doi: http://dx. doi.org/10.1016/j.jhazmat.2011.01.108. 21339051.

[32] A. Dąbrowski, P. Podkościelny, Z. Hubicki and M. Barczak, Adsorption of phenolic compounds by activated carbon—a critical review, Chemosphere 58 (8) (2005) 1049–1070, doi: http://dx.doi.org/10.1016/j.chemosphere.2004. 09.067. 15664613.

[33] R.W. Coughlin, F.S. Ezra, Role of surface acidity in the adsorption of organic pollutants on the surface of carbon, Environ. Sci. Technol. 2 (4) (1968) 291–297.

[34] J. Rivera-Utrilla, M. Sánchez-Polo, V. Gómez-Serrano, P.M. Alvarez, M.C.M. Alvim-Ferraz, J.M. Dias, Activated carbon modifications to enhance its water treatment applications. An overview, J. Hazard. Mater. 187 (1–3) (2011) 1–23, doi: http://dx.doi.org/10.1016/j.jhazmat.2011.01.033. 21306824.

[35] F. Akbal, Sorption of phenol and 4-chlorophenol onto pumice treated with cationic surfactant, J. Environ. Manage. 74 (3) (2005) 239–244, doi: http://dx. doi.org/10.1016/j.jenvman.2004.10.001. 15644263.

[36] G. Müller, C. Radke and J. Prausnitz, Adsorption of weak organic electrolytes from aqueous solution on activated carbon. Effect of pH, J. Phys. Chem. 84 (4) (1980) 369–376.

[37] S. Mubarik, A. Saeed, Z. Mehmood, M. Iqbal, Phenol adsorption by charred sawdust of sheesham (Indian rosewood; Dalbergia sissoo) from single, binary and ternary contaminated solutions, J. Taiwan Inst. Chem. Eng. 43 (6) (2012) 926–933, doi: http://dx.doi.org/10.1016/j.jtice.2012.07.003.

[38] C. Hua, R. Zhang, L. Li, X. Zheng, Adsorption of phenol from aqueous solutions using activated carbon prepared from crofton weed, Desalin. Water Treat. 37 (1–3) (2012) 230–237, doi: http://dx.doi.org/10.1080/19443994.2012.661277.

[39] D.O. Cooney, Adsorption Design for Wastewater Treatment, Lewis Publishers, 1999.

[40] V.L. Snoeyink, W.J. Weber Jr, H.B. Mark Jr., Sorption of phenol and nitrophenol by active carbon, Environ. Sci. Technol. 3 (10) (1969) 918–926.

[41] S. Rengaraj, S. Moon, R. Sivabalan, B. Arabindoo, V. Murugesan, Agricultural solid waste for the removal of organics: adsorption of phenol from water and wastewater by palm seed coat activated carbon, Waste Manage. (New York, N. Y.) 22 (5) (2002) 543–548, doi: http://dx.doi.org/10.1016/S0956-053X (01) 00016-2. 12092764.

[42] C. Moreno-Castilla, Adsorption of organic molecules from aqueous solutions on carbon materials, Carbon 42 (1) (2004) 83–94, doi: http://dx.doi.org/ 10.1016/j.carbon.2003.09.022.

[43] S. Nouri, F. Haghseresht, G.M. Lu, Comparison of adsorption capacity of pcresol & p-nitrophenol by activated carbon in single and double solute, Adsorption 8 (3) (2002) 215–223, doi: http://dx.doi.org/10.1023/ A:1021260501001.

[44] V.K. Gupta, S. Agarwal, T.A. Saleh, Chromium removal by combining the magnetic properties of iron oxide with adsorption properties of carbon nanotubes, Water Res. 45 (6) (2011) 2207–2212, doi: http://dx.doi.org/10.1016/ j.watres.2011.01.012. 21303713.

[45] G. Walker, L. Hansen, J. Hanna, S. Allen, Kinetics of a reactive dye adsorption onto dolomitic sorbents, Water Res. 37 (9) (2003) 2081–2089, doi: http://dx. doi.org/10.1016/S0043-1354 (02) 00540-7. 12691893.

[46] Y.S. Al-Degs, M.I. El-Barghouthi, A.H. El-Sheikh, G.M. Walker, Effect of solution pH, ionic strength, and temperature on adsorption behavior of reactive dyes on activated carbon, Dyes Pigm. 77 (1) (2008) 16–23, doi: http://dx.doi.org/ 10.1016/j.dyepig.2007.03.001.

[47] M.H. Kalavathy, T. Karthikeyan, S. Rajgopal, L.R. Miranda, Kinetic and isotherm studies of Cu(II) adsorption onto H3PO4-activated rubber wood sawdust, J. Colloid Interface Sci. 292 (2) (2005) 354–362, doi: http://dx.doi.org/10.1016/j. jcis.2005.05.087. 16040040.

[48] S. Kumar, S. Upadhyay, Y. Upadhya, Removal of phenols by adsorption on fly ash, J. Chem. Technol. Biotechnol. 37 (4) (1987) 281–290.

[49] S. Lin, R. Hsiao, R. Juang, Removal of soluble organics from water by a hybrid process of clay adsorption and membrane filtration, J. Hazard. Mater. 135 (1–3) (2006) 134–140, doi: http://dx.doi.org/10.1016/j.jhazmat.2005.11. 030. 16359788.

[50] I. Bakas, K. Elatmani, S. Qourzal, N. Barka, A. Assabbane, I. Aît-Ichou, A comparative adsorption for the removal of *p*-cresol from aqueous solution onto granular activated charcoal and granular activated alumina, J. Mater. Environ. Sci. 5 (3) (2014) 675–682.

CHAPTER 4

INVESTIGATION OF ADSORPTION OF *P*-CRESOL ON COCONUT SHELL-DERIVED ACTIVATED CARBON

Yiying Zhu, Praveen Kolar *

Biological and Agricultural Engineering, Campus Box 7625, North Carolina State University, Raleigh, NC, 27695-7625, USA.

E-mail addresses: yzhu15@ncsu.edu, pkolar@ncsu.edu

* Corresponding author contact information: 278 Weaver Labs, Campus Box 7625, North Carolina State University, Raleigh, NC, 27695-7625, USA.

Phone: +1 919 513 9797; Fax: +1 919 515 7760.

E-mail address: pkolar@ncsu.edu

*** A modified version of this chapter "INVESTIGATION OF ADSORPTION OF *P*-CRESOL ON COCONUT SHELL-DERIVED ACTIVATED CARBON" is currently under review at *Journal of the Taiwan Institute of Chemical Engineers*.**

Abstract

Mitigation of odorous volatile organic compounds, such as *p*-cresol from wastewater needs simple and practical technologies such as adsorption. In our previous work, we reported adsorptive removal of *p*-cresol on activated carbon synthesized via zinc chloride. Although the activated carbon was reasonably active (maximum monolayer adsorption capacity of *p*-cresol was found to be 31.57 mg g^{-1} at 303 K), the data suggested that the surface functional groups may be enhanced via stronger activation, which may in turn enhance adsorption of *p*-cresol. Hence, in this research, a strong basic activating agent, NaOH, was employed to synthesize an activated carbon from coconut shell (CSAC-SH). The prepared activated carbon was characterized via BET, SEM and FTIR techniques. To evaluate the performance of CSAC-SH, a series of batch experiments were conducted to investigate the effects of contact time (0-24 h), initial concentration (50-1000 mg L^{-1}) and adsorbent dosage (1-20 mg L^{-1}) on adsorption of *p*-cresol. The characterization results suggested that CSAC-SH possessed a well-developed microporous/mesoporous structure. The equilibrium data were found to conform to Redlich-Peterson, Fritz-Schluender, and Langmuir isotherms. The maximum monolayer adsorption capacity of 256.9 mg g^{-1} (298 K) suggested that the prepared adsorbent has a high affinity towards *p*-cresol. The kinetics suggested that the experimental data were best described by a second-order kinetic model and adsorption was governed by intra-particle diffusion. The thermodynamic analysis showed that the adsorption was feasible, spontaneous, and exothermic (298-328 K). Furthermore, the desorption study suggested that chemisorption was dominant in the

adsorption process. It appears that sodium hydroxide-activated carbon is effective in mitigating *p*-cresol from wastewater.

Key words

p-Cresol; Adsorption; Activated carbon; Physiochemical activation; Sodium hydroxide

4.1 Introduction

Odorous emissions from intensive swine operations are an increasing environmental nuisance, particularly in rural areas. *p*-Cresol (4-methylphenol), one of the volatile organic compounds (VOCs), is reported to be the most malodorous among the air pollutants released from swine farming operations [1]. It is also prevalent in wastewaters generated from paint, pesticide, petroleum, coal conversion, polymeric resin and phenol-producing industries [2,3]. As a highly toxic derivative of phenol, *p*-cresol is detrimental even at low concentrations and it has been classified by Environmental Protection Agency (EPA) as a possible carcinogen [4]. As a result, there is a strong interest in mitigating *p*-cresol from water bodies.

Adsorption of contaminants by activated carbon has been identified as one of the most effective and feasible technologies owing to activated carbons' microporous nature, favorable pore size distribution, high degree of surface reactivity, high adsorption capacity, versatility and easy availability [3,5]. There has been an increasing interest in using renewable and environmentally friendly agricultural residues as the starting materials. Coconut shell, as one of the most abundant low-cost lignocellulosic agricultural by-products, has been found to yield inexpensive, microporous, structurally stable and highly adsorptive activated carbons [6-8].

Recently, Martins et al. [9] reported that activated carbon prepared using NaOH as an activating agent provided a high surface area equipped with basic functional groups which resulted in high adsorption capacities for tetracycline reduction. In another study conducted by the same group, Cazetta et al. [10], it was reported that NaOH-activated carbon performed

well for uptake of methylene blue. Moreover, Tan et al. [11] modified commercial activated carbon with NaOH and it was found to be active for CO_2 removal and the authors explained that NaOH was responsible for change in the morphological structural and reduction in acidity of the carbon surface by exchanging carboxylic and phenols ions with Na^+. Based on these studies, we hypothesized that NaOH-activation process is also capable of yielding a highly active adsorbent for mitigation of *p*-cresol. To the best of our knowledge, *p*-cresol has never been reported to be adsorbed onto coconut shell-activated carbon using NaOH as an activating agent in scientific literature.

The objectives of the present work were to characterize the physiochemical-NaOH-activated carbon prepared from coconut shell, investigate the adsorption properties of the adsorbent for removal of *p*-cresol, and study the kinetics, equilibrium, mechanism, and thermodynamics of the adsorption process to determine the feasibility of the adsorbent for uptake of *p*-cresol. A desorption study was also carried out to obtain further insights into the nature of adsorption of *p*-cresol onto the adsorbent.

4.2 Materials and methods

4.2.1 Preparation of coconut shell based activated carbon

The coconut shell used for preparation of activated carbon in this study was obtained locally. The preparation method and instruments employed in the present research were similar to those reported earlier in preparation of $ZnCl_2$ treated coconut shell-activated carbon (CSAC-$ZnCl_2$) by the authors [6]. Initially, the coconut shell was crushed into small

pieces with a particle size of about 10 mm and placed in a horizontal stainless steel reactor and carbonized at 673 K for 1 h with a nitrogen flow rate of 2 L min^{-1} in a horizontal kiln (Sentry Xpress 4.0, Paragon) under a heating rate of 10 K min^{-1}. This semi-finished product was named Char-400. Subsequently, the Char-400 was ground and sieved through a 5 mm screen before mixing with sodium hydroxide pellets (≥ 97.0 %, Acros) with NaOH: char impregnation ratio (IR) of 1:1 for 3 h and dried overnight at 383 K after removing the supernatant liquid. Further, the char sample was pyrolyzed (1273 K for 1.5 h) and allowed to cool down to room temperature under nitrogen atmosphere followed by washing with hot deionized water and overnight dehydration (343 K) to obtain the final product, named CSAC-SH.

4.2.2 Characterization of activated carbon

The structure and morphology of the adsorbents were characterized via scanning electron microscopy (SEM). The SEM images were recorded using a Hitachi Model S-3200N apparatus.

The Brunauer-Emmett-Teller surface area (S_{BET}) of the adsorbents was determined from the nitrogen adsorption isotherms at 77 K using an automatic BET analyzer (Micrometrics Gemini VII 2390p).

The surface functional groups of the activated carbon samples were also studied via Fourier transform infrared spectra (FTIR) recorded at 4 cm^{-1} of resolution and 64 scans min^{-1} between 4000 and 500 cm^{-1} using a Perkin-Elmer RXI FTIR spectrometer. The raw material of coconut shell was analyzed in a Bruker Platinum ATR spectrometer.

The acid value of the activated carbon was measured from the pH of a solution containing 0.4 g activated carbon and 20 mL deionized water after shaking at 400 rpm for 12 h [12].

The surface functional groups of the activated carbon were also determined using the Boehm titration [13]. The procedure was the same as described in a previous paper [6].

4.2.3 Batch adsorption of p-cresol on CSAC-SH

Experimental *p*-cresol solutions of desired concentrations (50-1000 mg L^{-1}) were prepared from the stock solution with appropriate dilutions. 0.5 g of CSAC-SH was weighted and added into 100 mL aliquots of *p*-cresol solutions in 150 mL serum bottles, which were covered with rubber stoppers and sealed with 20 mm aluminum air-tight caps, and were placed on an isothermal hot plate and agitated at 100 rpm. The *p*-cresol concentrations in the supernatant solutions before and after adsorption were determined using a UV spectrophotometer (Genesys 10S, Thermo Scientific) at its maximum wavelength (λ) of 277 nm. All batch adsorption experiments were performed in duplicates. A blank of the same *p*-cresol concentration without adsorbent followed the identical procedure and was monitored in every experiment to confirm that the adsorbate is neither volatilized nor adsorbed on the walls of serum bottles. The equilibrium amount of *p*-cresol amount adsorbed, q_e (mg g^{-1}), and the percent removal, X (%) were calculated by Eq. (4-1) and Eq. (4-2), respectively [3]:

$$q_e = \frac{(C_o - C_e)V}{W} \quad (4\text{-}1)$$

$$X\,(\%) = \frac{C_o - C_t}{C_o} \times 100 \quad (4\text{-}2)$$

where C_o, C_t, and C_e (mg L^{-1}) are the initial, any given time, and equilibrium liquid phase concentrations of *p*-cresol, respectively. V (L) is the volume of the solution, and W (g) is the mass of the dry CSAC-SH used.

4.2.4 Kinetic and equilibrium modeling of p-cresol removal

Experimental data were fitted to different kinetic models and isotherm models, as given in Table 4.1 of Eq. (4-3) to Eq. (4-6) [10,14] and of Eq. (4-7) to Eq. (4-12) [3,4], respectively.

Table 4.1: Kinetic and isotherm models for adsorption

Kinetic model names	Expression	
Pseudo-first-order	$q_t = q_e[1 - e^{-k_1 t}]$	(4-3)
Pseudo-second-order	$q_t = \frac{k_2 q_e^2 t}{1 + k_2 q_e t}$	(4-4)
Elovich	$q_t = \frac{1}{\beta} In(\alpha\beta) + \frac{1}{\beta} In(t)$	(4-5)
Intra-particle diffusion	$q_t = K_{id} t^{0.5} + C$	(4-6)

Table 4.1 Continued

Isotherm model names	Expression	
Freundlich	$q_e = K_F\, C_e^{\,1/n}$	(4-7)
Langmuir	$q_e = \frac{Q_O K_L C_e}{1 + K_L C_e}$	(4-8)
Redlich-Peterson	$q_e = \frac{AC_e}{1 + BC_e^{\beta}}$	(4-9)
Temkin	$q_e = \left(\frac{RT}{b_T}\right) In(\alpha C_e)$	(4-10)
Fritz-Schluender	$q_e = \left(\frac{\alpha_1 C_e^{\beta_1}}{1 + \alpha_2 C_e^{\beta_2}}\right)$	(4-11)
Radke-Prausnitz	$\frac{1}{q_e} = \frac{1}{KC_e} + \frac{1}{kC_e^{\,1/n_1}}$	(4-12)

where q_t (mg g^{-1}) and q_e (mg g^{-1}) = the amount of adsorbate adsorbed at any time and at equilibrium on adsorbent, respectively; $k_1(\min^{-1})$ and k_2(g $mg^{-1}\min^{-1}$) = pseudo-first-order and pseudo-second-order adsorption rate constants; $h(mg\ g^{-1}\min^{-1}) = k_2 q_e^2$ = initial adsorption rate; α $(mg\ g^{-1}min^{-1})$ and β $(g\ mg^{-1})$= Elovich constants; k_{id}(mg $g^{-1}\min^{-0.5}$) = intra-particle diffusion constant; C (mg g-1) = the thickness of the boundary layer. K_F (mg g^{-1}(L $mg^{-1})^{1/n}$) = Freundlich constant; n = constant in Freundlich isotherm; Q_o(mg g^{-1}) = maximum monolayer adsorption capacity; K_L (L mg^{-1}) = Langmuir constant; A(L g^{-1}),B(L mg^{-1}) and β = Redlich-Peterson constants; R (8.314 J $mol^{-1}K^{-1}$) = universal gas constant; T (K) = absolute solution temperature; α(L g^{-1}) = equilibrium binding constant; $\emptyset$ (J mol^{-1}) $= RT/b_T$ = Temkin constant related to the heat of adsorption; $\alpha_1\left((\text{mg g}^{-1})/(\text{mg L}^{-1})^{\beta_1}\right)$, $\alpha_2((\text{mg L}^{-1})^{-\beta_2})$, β_1 and β_2= Fritz-Schluender constants; K(L g^{-1}), k (mg g^{-1})(L $mg^{-1})^{1/n}$) and n_1= Radke-Prausnitz constants.

4.2.5 Thermodynamic modeling

Adsorption thermodynamics were studied with initial *p*-cresol of 500 mg L^{-1} at different temperatures of 298 K, 308 K, 318 K and 328 K with 5 g L^{-1} CSAC-SH and agitated at 100 rpm. The thermodynamic parameters including Gibbs free energy (ΔG^o), enthalpy change (ΔH^o), and entropy change (ΔS^o), were determined from the following equation [3]:

$$\Delta G^o = -RT \ln K_e \tag{4-13}$$

where R (8.314 J mol^{-1} K^{-1}) is the universal gas constant. T (K) is the temperature, and K_e is the distribution coefficient. The K_e value was given by:

$$K_e = \frac{q_e}{C_e} \tag{4-14}$$

where q_e (mg g^{-1}) and C_e(mg L^{-1}) are the equilibrium concentrations of *p*-cresol on adsorbent and in solution, respectively. Relation between ΔG^o, ΔH^o and ΔS^o can be expressed as:

$$\Delta G^o = \Delta H^o - T\Delta S^o \tag{4-15}$$

Eq. (4-15) can be written as:

$$\ln K_e = -\frac{\Delta G^o}{RT} = -\frac{\Delta H^o}{RT} + \frac{\Delta S^o}{R} \tag{4-16}$$

4.2.6 Desorption of p-cresol on CSAC-SH

The spent carbon from previous *p*-cresol adsorption experiment (1000 mg L^{-1}, 5 g L^{-1} CSAC-SH, 298 K) was separated out by filtration and the filtrate was discarded. The carbon was given a gentle wash with deionized water to remove any unadsorbed *p*-cresol. Desorption studies were conducted in duplicates by mixing the carbon with 0.14 N sodium hydroxide solution (100 mL) [15] in a sealed serum bottle and stirred (100 rpm) at 298 K to monitor desorption of *p*-cresol into bulk solution.

4.3 Results and discussion

4.3.1 Physical and chemical characterizations of activated carbon

4.3.1.1 Surface area, and pore structural characterization

The nitrogen adsorption isotherms of the carbon samples are shown in Fig. 4.1(a), including CSAC-SH, as well as starting material, Char-400, CSAC-$ZnCl_2$, and the commercially available coconut shell activated carbon for comparison purposes. From Fig. 4.1(a), the nitrogen isotherm of the prepared CSAC-SH has the shape in between type I and type II according to IUPAC classification [16,17]. This type of isotherm is generally characterized by the well-developed micropore and mesopore structures of the adsorbent [17]. This is also observed in Fig. 4.1(b) that the sharpest peak was detected at the pore diameter between 1.75 nm and 2 nm for CSAC-SH, which is much more pronounced than that of the other samples. The majority of the pores existing in CSAC-SH have the average pore width of 1.84 nm, classified as the secondary micropore region (0.7-2 nm) [16].

Fig. 4.1 together with the results of the physical characterization of CSAC-SH compared with other samples (Table 4.**2**) showed that CSAC-SH was aggregated with micropores (< 2 nm) and mesopores (2-50 nm), which is favorable for uptake of *p*-cresol since the abovementioned two kinds of pores contribute most to the adsorption of small molecules [16,18]. In addition, the distinctive large external surface of the CSAC-SH allows more attachment of the *p*-cresol molecules onto the carbon surface, enables them to enter into the pores for adsorption, and hence provides a high potential for *p*-cresol removal.

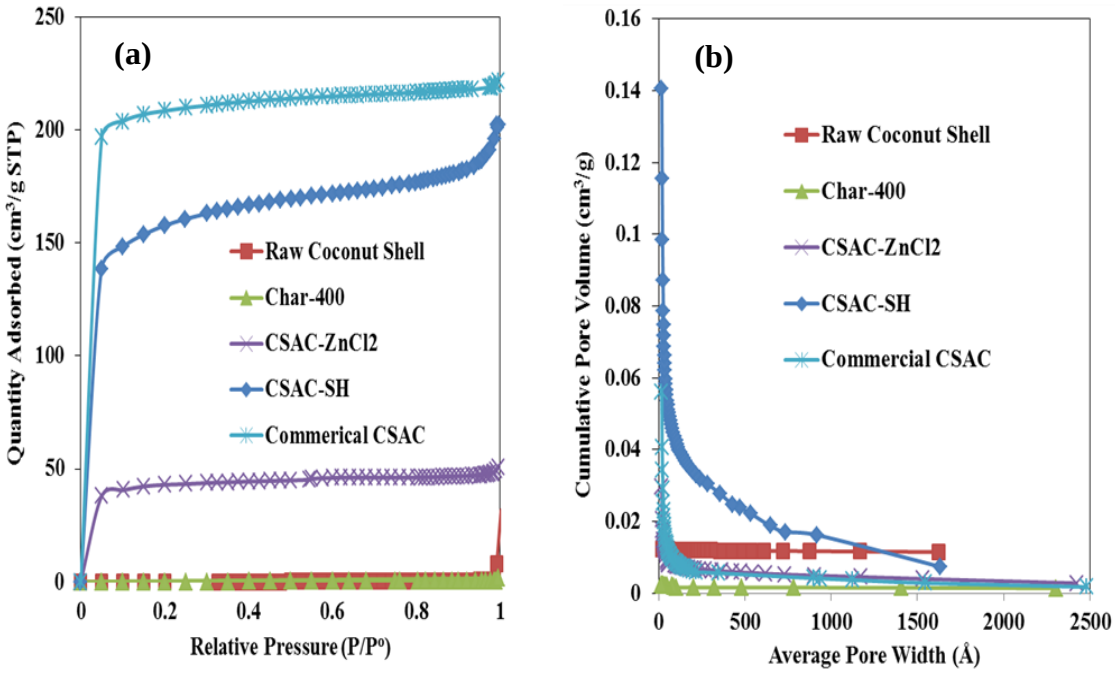

Fig. 4.1: (a) Nitrogen adsorption isotherms at 77K of the activated carbon samples; (b) Pore size distribution.

Table 4.2: Physical characterization of different samples

Sample	S_{BET} ($m^2 g^{-1}$)	S_{mi} ($m^2 g^{-1}$)	S_{ext} ($m^2 g^{-1}$)	V_{tot} ($cm^3 g^{-1}$)	V_{mi} ($cm^3 g^{-1}$)	V_{me} ($cm^3 g^{-1}$)	D_p (Å)	S_{mi}/S_{BET} (%)	V_{mi}/V_{tot} (%)
Raw coconut shell	0.33	0	0.65	0.049	0	0.049	5912.01	0	0
Char-400[a]	0.19	0	0.37	0.002	0	0.10	487.41	0	0
CSAC-$ZnCl_2$[b]	140.02	98.67	41.35	0.079	0.048	0.031	22.49	70.47	60.76
CSAC-SH	520.16	330.46	189.71	0.31	0.16	0.15	23.88	63.53	51.61
Commercial CSAC	669.88	580.25	89.63	0.34	0.28	0.06	20.46	86.62	82.35

[a] Char-400: Physical activated at 673 K for 1 h only.

[b] CSAC-$ZnCl_2$: Physiochemical treated by $ZnCl_2$ [6].

[c] Commercial CSAC (coconut shell activated carbon) (C 270C, Fisher Scientific, Inc.).

where V_{tot} is the total pore volume, S_{mi} is the micropore surface area, S_{ext} is the external surface area, V_{mi} and V_{me} are the micropore volume and mesopore volume, respectively, and D_p is the average pore diameter.

It is also apparent that the use of sodium hydroxide as the activating agent improves the carbon's properties better than zinc chloride. The properties of the CSAC-SH might be attributed to the reaction between NaOH and char during the physiochemical activation as expressed by Eq. (4-17) [19]:

$$6NaOH + 2C \rightleftharpoons 2Na + 2Na_2CO_3 + 3H_2 \quad (4\text{-}17)$$

As described in Eq. (4-17), the generated metallic sodium, in combination with the CO_2 decomposed from the produced sodium carbonate, may penetrate the carbon structure, make drastic changes in the texture and help to develop the porosity of the activated carbon [19]. This explains why the coconut shell-based activated carbon derived from NaOH has much larger surface area, total pore volume, micropore surface area, and micropore volume than that of the adsorbent treated by $ZnCl_2$ [6]. Therefore, we theorize that sodium hydroxide brings about aggressive activation and aids in the enhancement of the porosity of the activated carbon.

4.3.1.2 SEM analysis of the activated carbon

Fig. 4.2 presents the SEM images of the precursor and the activated carbon samples, respectively, which vividly demonstrates the alteration of the physical structure and the transformation of the non-porous precursor as shown in Fig. 4.2(a) to porous adsorbent in Fig. 4.2(d). There is a change in the char surface as it appears to separate into smaller pieces in Fig. 4.2(b), which is attributable to the release of volatile compounds during the carbonization process.

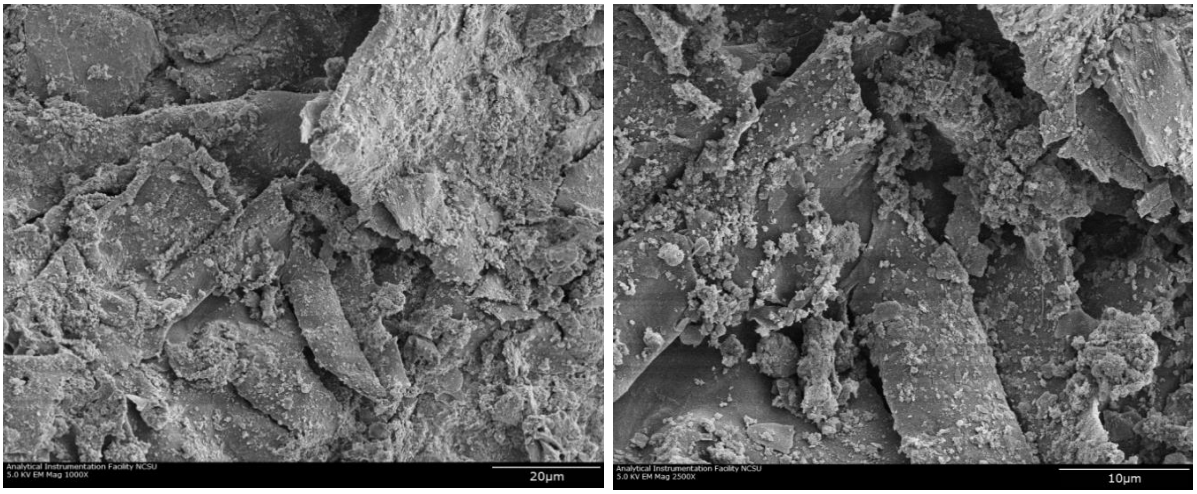

(a)

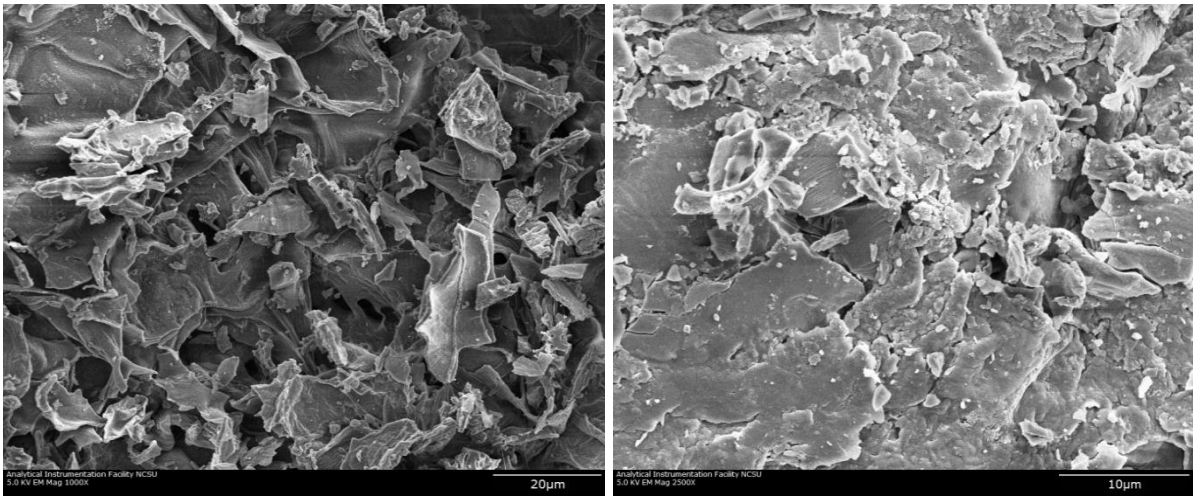

(b)

Fig. 4.2: Scanning electron micrographs of transformation of starting material to activated carbon and *p*-cresol loaded CSAC-SH: (a) Raw material (left: 1000x; right: 2500x); (b) Char-400 (left: 1000x; right: 2500x); (C) CSAC-$ZnCl_2$ (left: 1000x; right: 2500x); (d) CSAC-SH before adsorption (left: 1000x; right: 2500x); (e) CSAC-SH after adsorption of *p*-cresol (left: 1000x; right: 2500x).

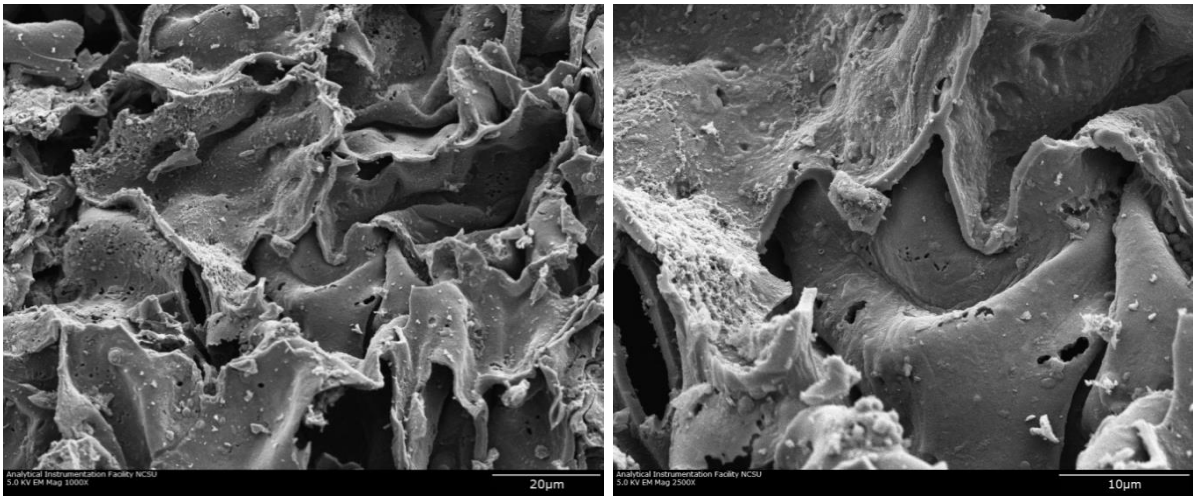
Analytical Instrumentation Facility NCSU
5.0 KV EM Mag 1000X
20µm
Analytical Instrumentation Facility NCSU
5.0 KV EM Mag 2500X
10µm

(c)

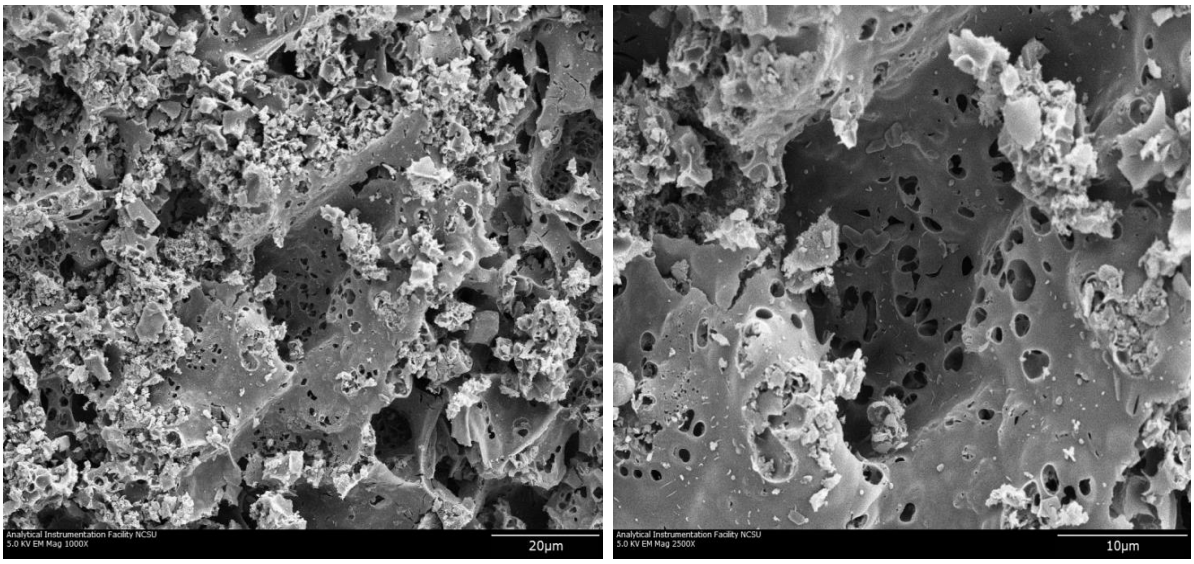
Analytical Instrumentation Facility NCSU
5.0 KV EM Mag 1000X
20µm
Analytical Instrumentation Facility NCSU
5.0 KV EM Mag 2500X
10µm

(d)

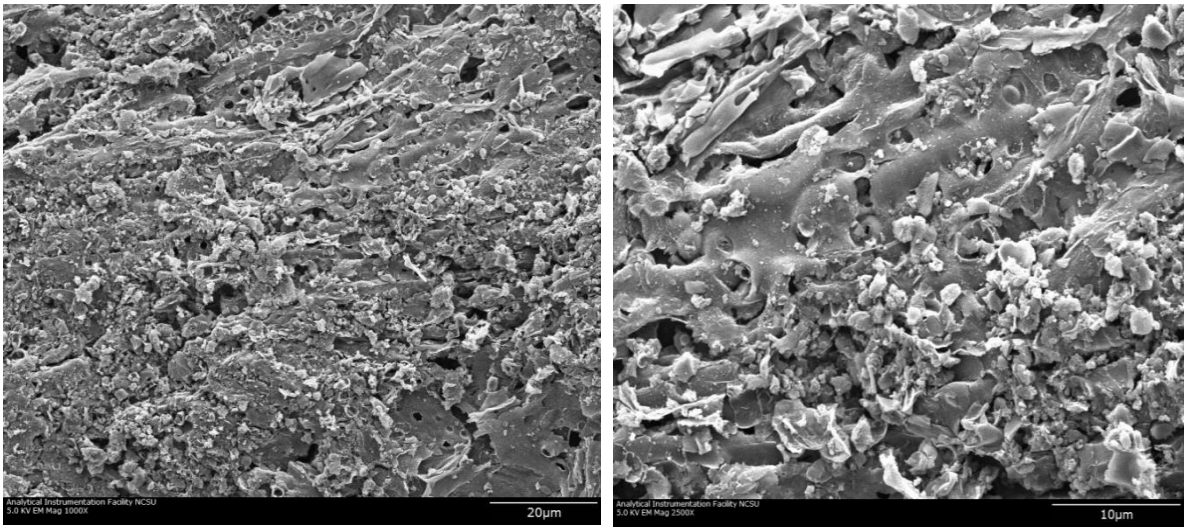
Analytical Instrumentation Facility NCSU
5.0 KV EM Mag 1000X
20µm
Analytical Instrumentation Facility NCSU
5.0 KV EM Mag 2500X
10µm

(e)

It is evident that the carbon treated by sodium hydroxide has a much higher degree of pore development than that processed by zinc chloride as can be seen from Fig. 4.2(c) and Fig. 4.2(d), which confirms the results of BET analysis. From the observation of the structure of the porosity of CSAC-SH, a distinct porous network was noted made up of a variety of micropores and mesopores developed along the channels of large open pores (macropores) on the surface which exhibited an approximate honeycomb shape. With this interrelated texture, macropores would assist with transport of adsorbates into the interior of carbon particles and facilitate the access of the adsorbates to micropores/mesopores for adsorption and enhance the trapping of more pollutants [16].

The SEM micrographs of Fig. 4.2(d) and Fig. 4.2(e) enable the direct observation of the changes of the micromorphology of CSAC-SH before and after adsorption of *p*-cresol. It is evident from Fig. 4.2(e) that the adsorbate molecules filled in the pores of the adsorbent.

4.3.1.3 FTIR analysis

The FTIR spectra of the raw material and activated carbon samples are given in Fig. 4.3. The broad band at around 3400 cm^{-1} for all samples is due to the hydroxyl (O-H) stretching vibration [10]. The band observed at around 2900 cm^{-1} is attributed to C-H stretching vibration for the raw material and Char-400, and the disappearance of this band for CSAC-SH and *p*-cresol loaded CSAC-SH suggests that the prepared activated carbon underwent full carbonization. The band near 1600 cm^{-1} is present in all samples and is assigned to carbonyl stretching vibration (C=O) in carboxyl and alkene groups [9,10]. The

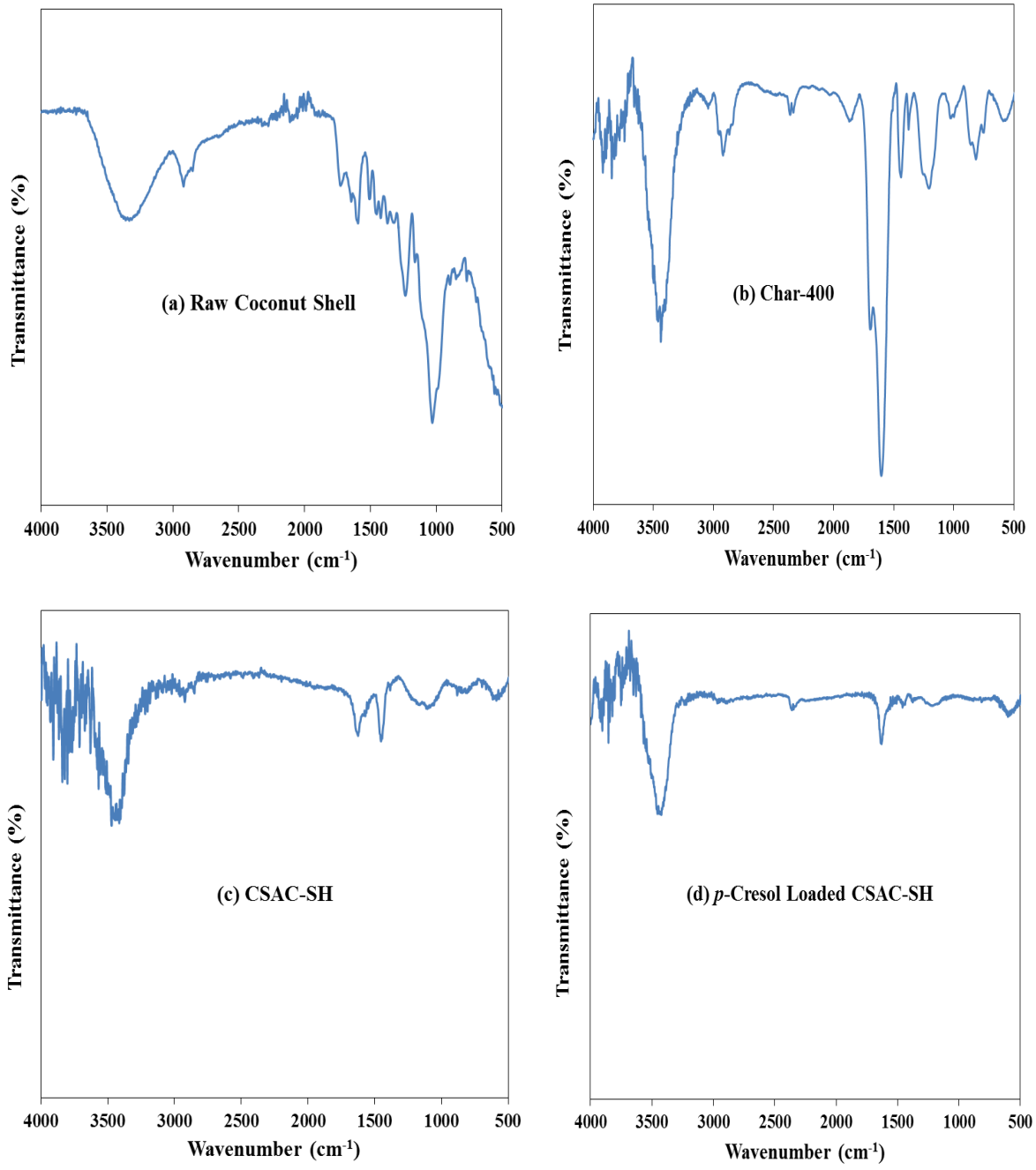

Fig. 4.3: FTIR spectra for precursor (a) and different activated carbon samples of (b), (c) and (d).

peaks observed in the spectra of CSAC-SH samples are less intense. Presence of aromatics can be observed through C=C bonds at wavenumber near 1450 cm^{-1} [10]. The decreased intensity of this band in the spectrum of CSAC-SH after adsorption may result from the reaction between the basic aromatic ring with *p*-cresol considering that basic functional groups are preferred for adsorption of phenolic compounds [18,20]. Similarly, the decrease of ketones, alcohol or ethers detected from the band located at around 1100 cm^{-1} of CSAC-SH spectrum after removal of *p*-cresol further confirmed the reaction between the adsorbent and adsorbate [10,21]. Additionally, the results of Boehm titration and the acid value of the adsorbent (Table 4.**3**) showed that CSAC-SH was rich in basic functional groups.

Table 4.3: Results of Boehm titration and acid value of CSAC-SH

Sample	Basic group (mmol g^{-1})	Acidic groups (mmol g^{-1})			Acid value
		Carboxylic	Lactonic	Phenolic	
CSAC-SH	1.65	0.95	0.1	0.03	9.9

4.3.2 Adsorption studies

4.3.2.1 Effect of contact time and initial adsorbate concentration on adsorption and kinetics

Fig. 4.4(a) presents adsorption of *p*-cresol onto CSAC-SH and percent removal with varying initial adsorbate concentrations ranging from 50 to 1000 mg L^{-1} for 24-h agitation time at 100 rpm at 298 K with 5g L^{-1} of CSAC-SH.

From this figure, the adsorption occurred much faster in the beginning and slowed down gradually over time until reaching equilibrium due to the effects of the availability of the activated sites and the strength of the driving force. Apparently it took shorter time (~ 4-10 h) for the lower initial adsorbate concentrations (50 to 300 mg L^{-1}) and much longer time (> 24 h) for higher initial concentrations (≥ 500 mg L^{-1}) to reach equilibrium.

The adsorption capacity increased with initial concentration as the higher concentration enabled more *p*-cresol molecules to be adsorbed. The adsorption efficiency increased slightly up to 98% when the initial concentration increased to 200 mg L^{-1}. However, a further increase in the initial concentration caused a reduction in percent removal of *p*-cresol since the number of the adsorbate ions exceeded the available sites for adsorption.

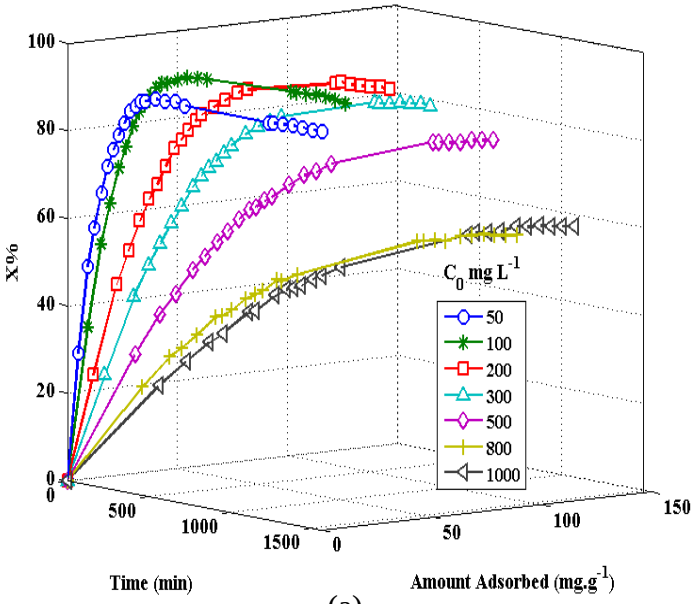

(a)

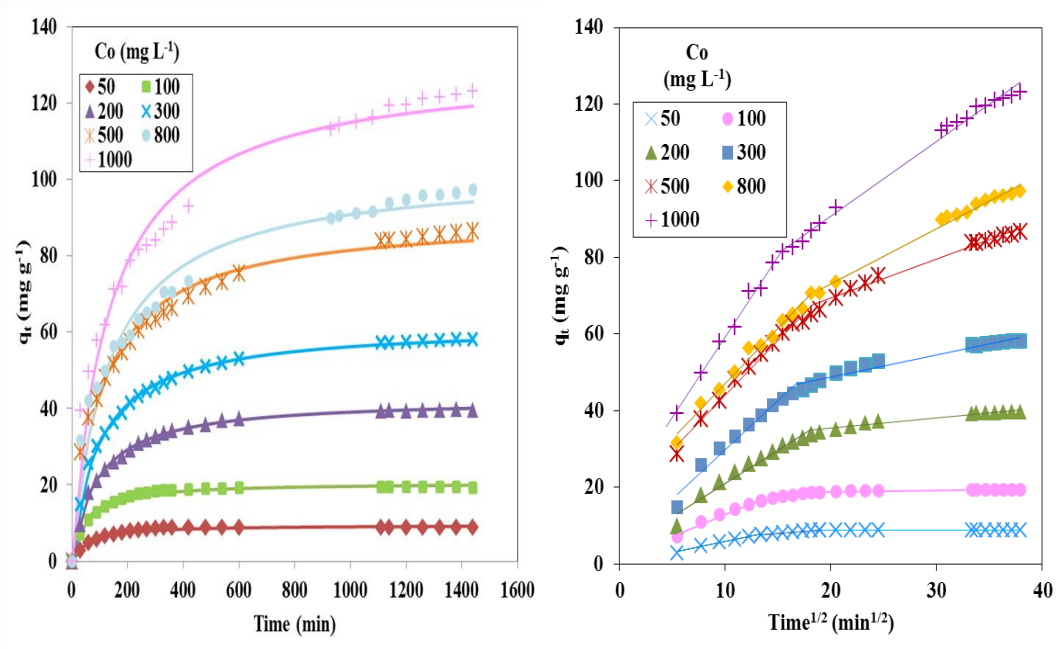

(b) (c)

Fig. 4.4: (a)Time evolution of the adsorption of *p*-cresol onto CSAC-SH and the percent removal with varying initial concentrations; (b) non-linear fit of the pseudo-second-order kinetic model for *p*-cresol removal; (c) intra-particle diffusion plots for adsorption of *p*-cresol with varying initial concentrations.

In order to study the adsorption of *p*-cresol on CSAS-SH, three kinetic models were tested (Table 4.4). The higher correlation coefficient (R2) values (> 97%) suggested that the pseudo-second-order kinetic model best represented the adsorption process and the non-linear fit of the second-order-kinetic model provided a good correlation for the experimental values (Fig. 4.4(b)). It is suggested that chemisorption was predominant in the adsorption process, which involved the valence forces through sharing or exchanging electrons between the adsorbate and adsorbent [10,22]. It is also noteworthy that the values of second order rate constant (K2) decreased from 2.057×10-3 to 5.79 ×10-5 g mg-1 min-1 as the initial concentration increased from 50 to 1000 mg L-1. This trend confirmed that the adsorption system was concentration dependent.

To identify the diffusion mechanism, the intra-particle diffusion model (Eq. (4-6) in Table 4.1) was applied to simulate the adsorption system and the results are shown in Fig. 4.4(c) and Table 4.5. The data from seven different initial concentrations showed two stages of linearity in Fig. 4.4(c), the first being the instantaneous adsorption and the second being the gradual adsorption phase with the controlling intra-particle diffusion. The higher K_{id1} values for the first phase were consistent with the higher *h* values at larger initial concentrations, demonstrating that the adsorption rate was higher. Moreover, neither of the two lines passed through the origin, suggesting that the rate-limiting step of the adsorption is not only governed by intra-particle diffusion [10].

Table 4.4: Kinetic constants for adsorption of *p*-cresol on CSAC-SH

Kinetic model names	Initial *p*-cresol concentration (mg L^{-1})						
	50	100	200	300	500	800	1000
Pseudo-first-order							
$q_{e,exp}$ (mg g^{-1})	8.77	19.23	39.72	58.06	86.56	97.28	123.13
$q_{e,cal}$ (mg g^{-1})	8.753	19.04	38.37	55.47	80.96	92.01	116.4
k_1 (min^{-1})	0.01175	0.01224	0.007501	0.006908	0.00634	0.005421	0.005407
R^2 (%)	99.67	99.17	97.7	96.39	92.34	92.09	92.77
Pseudo-second-order							
$q_{e,cal}$ (mg g^{-1})	9.455	20.57	42.61	61.84	90.31	102.7	130.2
k_2 (g mg^{-1} min^{-1})	0.002057	0.0009861	0.0002561	0.0001603	0.0001016	0.00007439	0.0000579
$h=k_2q_e^2$ (mg g^{-1} min^{-1})	0.1839	0.4172	0.4650	0.6130	0.8286	0.7846	0.9815
R^2 (%)	97.74	99	99.84	99.75	98.12	97.02	97.43

Table 4.4 Continued

Kinetic model names	Initial *p*-cresol concentration (mg L^{-1})						
	50	100	200	300	500	800	1000
Elovich $q_{e,cal}$ (mg g^{-1})	9.57	20.86	42.17	60.66	87.54	96.86	122.70
α (mg g^{-1} min^{-1})	1.961	4.891	1.719	2.137	3.038	2.661	3.245
β (g mg^{-1})	0.8078	0.378	0.1384	0.0933	0.06445	0.0553	0.04327
R^2 (%)	75.11	80.13	94.71	97.5	99.72	99.3	99.45

Table 4.5: Intra-particle diffusion parameters for adsorption of *p*-cresol on CSAC-SH

C_0 (mg/L)	Intra-particle diffusion model					
	K_{id1} (mg g^{-1} $min^{-0.5}$)	K_{id2} (mg g^{-1} $min^{-0.5}$)	R_1^2 (%)	R_2^2 (%)	C_1 (mg g^{-1})	C_2 (mg g^{-1})
50	0.5744	0.2233	97.76	95.64	0.0579	4.599
100	1.1615	0.4068	97.79	96.41	1.325	11.146
200	1.7514	0.2688	96.08	94.9	3.4033	30.044
300	2.567	0.5726	96.87	95.65	4.0548	37.397
500	2.86	1.0173	98.69	98.37	15.298	48.921
800	2.8846	1.4388	98.67	98.49	18.139	44.376
1000	4.2199	1.9464	99.12	99.16	16.865	51.832

4.3.2.2 Effect of adsorbent dosage

Adsorbent dosage has been reported as an influential factor in adsorption [4,14]. In the present research, its effect was also investigated by varying the amount of CSAC-SH from 1 g L^{-1} to 20 g L^{-1} for mitigation of 1000 mg L^{-1} *p*-cresol solutions agitated at 100 rpm at 298 K.

From Fig. 4.5, it is evident that an initial increase in adsorbent dosage induced larger percent removal of *p*-cresol perhaps due to the increased active sites for adsorption. After a certain dosage (8 g L^{-1}), 99% removal was achieved and thereafter the adsorption efficiency grew gently to ~100 % taken up when the adsorbent dosage reached 15 g L^{-1}. As reported by Singh et al. [4], after achieving 99% removal, adsorbent dosage is not that efficient and most of the vacant sites stay unoccupied. On the other hand, perhaps because of the unsaturation of the activated sites, the partial aggregation or the overlapping of the adsorbent, the amount adsorbed per unit mass of the adsorbent decreased with an increase in adsorbent dosage, as reported by Kilic et al. [3] and Demirbas et al. [14].

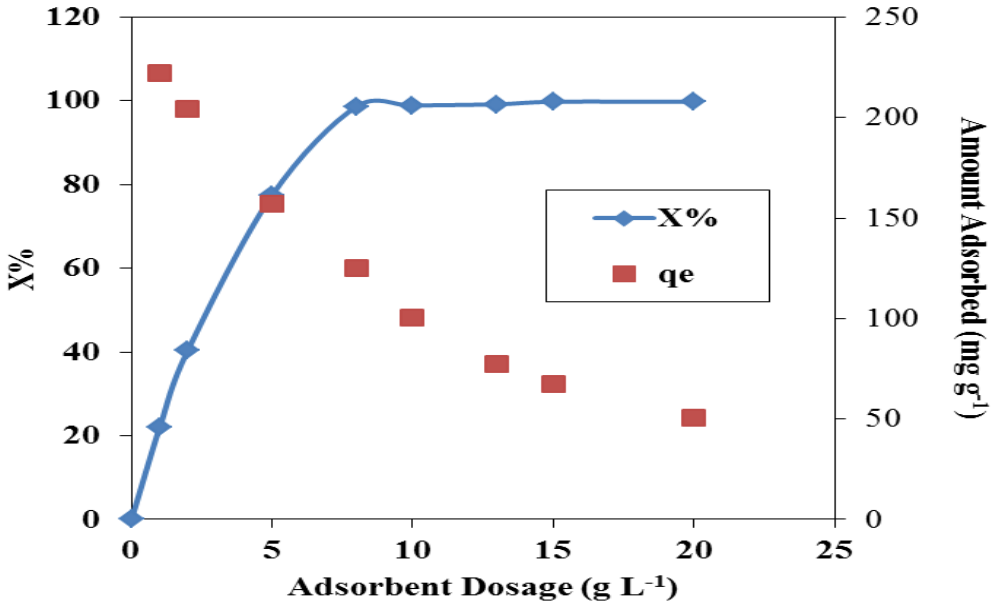

Fig. 4.5: Effect of adsorbent dosage on mitigation of *p*-cresol.

4.3.3 Adsorption isotherms

The results of the equilibrium study (Table 4.6) shows that Redlich-Peterson, Fritz-Schluender and Langmuir models are appropriate to represent the equilibrium data with the correlation coefficient R^2 being larger than 99%. Fig. 4.6 presents the non-linear plots of different isotherm models fitted to the equilibrium data. It is apparent that Redlich-Peterson model provided a better fit to the data than Freundlich, Temkin and Radke-Prausnitz models. Since Fritz-Schluender and Langmuir isotherm models closely simulated to the equilibrium data as that of the Redlich-Peterson isotherm, it suggested that they are also appropriate to describe the adsorption process. Besides, the equilibrium data were found to be well

represented by different studied isotherm models with high correlation coefficients (> 99%), Redlich-Peterson, Fritz-Schluender and Langmuir models, indicated the presence of more than one adsorption system for removal of *p*-cresol onto CSAC-SH [23]. Similar studies of the appropriate applicability of more than one isotherm model to equilibrium data was also reported by El Nemr et al. [23] on mitigation of chromium using marine red alga pterocladia capillacrea, Kilic et al. [3] on adsorption of phenol using tobacco residues-based activated carbon, and Singh et al. [4] on uptake of *p*-cresol using parthenium based activated carbon.

Table 4.6: Isotherm parameters for adsorption of *p*-cresol on CSAC-SH

Freundlich isotherm				Langmuir isotherm			Redlich-Peterson isotherm			
$q_e = K_F\, C_e{}^{1/n}$				$q_e = \frac{Q_O K_L C_e}{1 + K_L C_e}$			$q_e = \frac{AC_e}{1 + BC_e^{\beta}}$			
T(K)	K_F (mg g^{-1}) (L mg^{-1})$^{1/n}$	1/n	R^2 (%)	K_L (L mg^{-1})	Q_0 (mg g^{-1})	R^2 (%)	A (L g^{-1})	B (L mg^{-1})	β	R^2 (%)
298	32.37	0.295	96.32	0.0081	256.9	99.23	2.41	0.0137	0.945	99.37

Temkin isotherm				Fritz-Schluender isotherm					Radke-Prausnitz isotherm			
$q_e = \left(\frac{RT}{b_T}\right) In(\alpha C_e)$				$q_e = \frac{\alpha_1 C_e^{\beta_1}}{1 + \alpha_2 C_e^{\beta_2}}$					$\frac{1}{q_e} = \frac{1}{KC_e} + \frac{1}{kC_e^{1/n}}$			
T (K)	α (L g^{-1})	ϕ (J mol^{-1})	R^2 (%)	α_1 (mg g^{-1})/(mg L^{-1})$^{\beta_1}$	α_2 (mg L^{-1})$^{-\beta_2}$	β_1	β_2	R^2 (%)	K (L g^{-1})	k (mg g^{-1})(L mg^{-1})$^{1/n}$	1/n	R^2 (%)
298	0.0983	52.51	98.78	11.84	0.000636	0.515	1.037	99.36	119.1	32.73	0.294	96.4

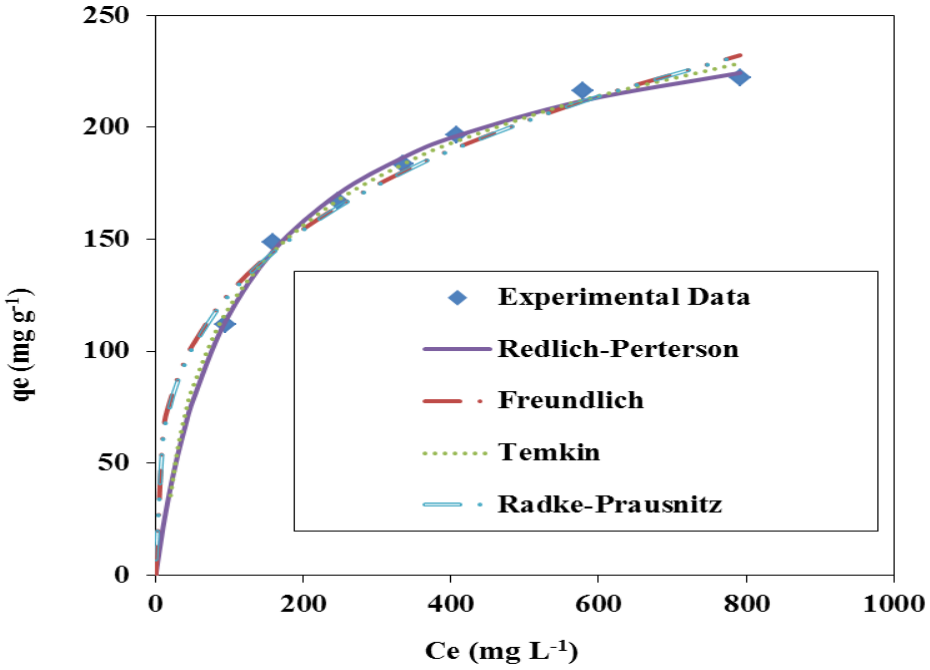

Fig. 4.6: Different non-linear isotherm plots of *p*-cresol adsorption onto CSAC-SH (conditions: 200, 300, 400, 500, 600, 800, 1000 mg L^{-1} of initial *p*-cresol solution, 1 g L^{-1} adsorbent dosage, 100 rpm and 298 K).

The Freundlich's parameter ($1/n$) was found to be 0.295, indicating the strong interaction between *p*-cresol and the prepared adsorbent [4]. In the Langmuir isotherm, a dimensionless separation factor R_L was determined from the Langmuir constant K_L (L mg^{-1}) [defined as $R_L = 1/(1 + K_L C_o)$] to ascertain the favorability of the adsorption, as described by [4]. The R_L was calculated to be between 0 and unity (0.11 to 0.38), suggesting the high favorability of the adsorption of *p*-cresol on CSAC-SH. The monolayer adsorption capacity of *p*-cresol was determined to be 256.9 mg g^{-1} on CSAC-SH, indicated that CSAC-SH had a

high adsorption capacity for *p*-cresol as compared to other selected adsorbents in literature (Table 4.7).

In addition, the adsorption capacity of CSAC-SH for *p*-cresol removal was found to be much larger than CSAC activated by $ZnCl_2$ from our previous work (Chapter 3) which may be contributed to their different physical and chemical properties. The parameters of CSAC-SH and CSAC were summarized in Table 4.9 for better comparison. From this table, it is obvious that NaOH treatment improved the physical and chemical characteristics of activated carbon much better than the $ZnCl_2$ treatment did, which may explain why CSAC-SH resulted in not only a larger adsorption capacity but also a higher initial adsorption rate.

Table 4.7: Comparison of the monolayer adsorption capacities of different adsorbents for *p*-cresol

Adsorbents	Adsorption Capacity (mg g^{-1})	Reference	Temperature (K)	Initial *p*-cresol concentration (mg L^{-1})	S_{BET} (m^2 g^{-1})
NaOH-coconut shell-activated carbon (CSAC-SH)	256.9	This work	298	200-1000	520.16
Parthenium based activated carbon (PAC)	62.91	[4]	301	500	260

Table 4.7 Continued

Adsorbents	Adsorption Capacity (mg g^{-1})	Reference	Temperature (K)	Initial *p*-cresol concentration (mg L^{-1})	S_{BET} (m^2 g^{-1})
Commercial activated carbon	98.93	[4]	301	500	686
Cork activated carbon (C8.750-23.CO2)	196.56	[24]	303	Up to 1000	647
Fir wood-activated carbon (FWKC1000)	253.8	[25]	303	200	1371
$ZnCl_2$-coconut shell-activated carbon (CSAC)	30.23	[6]	293	25-500	140.02
K_2CO_3-pine wood-activated carbon (PAC)	6.97	[26]	298	50-1000	21.23

Table 4.8: Comparison of the parameters between CSAC-SH and CSAC

	CSAC-SH	CSAC
Surface area ($m^2\ g^{-1}$)	520.16	140.02
Micropore area ($m^2\ g^{-1}$)	330.46	98.67
Total volume ($cm^3\ g^{-1}$)	0.31	0.079
Micropore volume ($cm^3\ g^{-1}$)	0.16	0.048
Basic group (mmol g^{-1})	1.65	0.52
Maximum monolayer adsorption capacity (mg g^{-1})	256.9 at 298K	30.23 at 293K 31.57 at 303K 32.77 at 313K
Initial adsorption rate h (mg g^{-1} min^{-1})	0.1839 for C_0 of 50 mg L^{-1} 0.4172 for C_0 of 100 mg L^{-1} 0.4650 for C_0 of 200 mg L^{-1} 0.8286 for C_0 of 500 mg L^{-1}	0.0677 for C_0 of 50 mg L^{-1} 0.1341 for C_0 of 100 mg L^{-1} 0.2155 for C_0 of 200 mg L^{-1} 0.3697 for C_0 of 500 mg L^{-1}

4.3.4 Thermodynamic study of the adsorption

Thermodynamic parameters were obtained from the plot between $\ln K_e$ versus $1/T$ as shown in Fig. 4.7 and the calculated values are listed in Table 4.9. The negative values of ΔG^o and ΔH^o suggested that the adsorption was spontaneous and exothermic, respectively. The adsorption efficiency of *p*-cresol decreased from 93.77% to 87.89% with the rise in temperature from 298 K to 328 K indicating that *p*-cresol uptake was favored at lower temperature. This might be due to the weakening of the adsorptive force between adsorbate and adsorbent, the distortion of the active sites or the increasing trend of desorption of the

adsorbed adsorbate molecules at higher temperatures [3,27]. The negative value of ΔS^o suggested the reduced randomness of adsorbate molecules on the solid adsorbent surface than in the solution due to the restricted mobility [3].

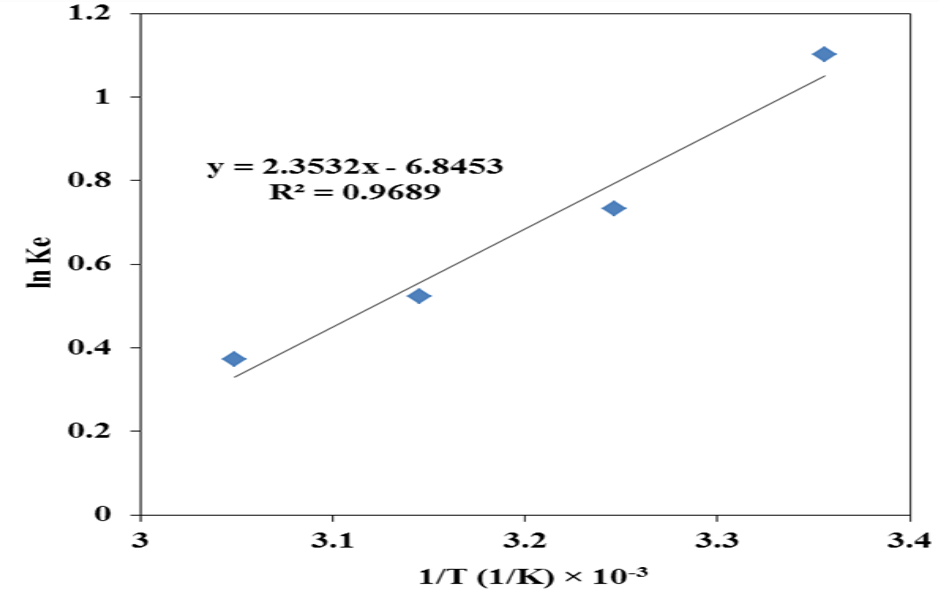

Fig. 4.7: Thermodynamic study of the *p*-cresol uptake using CSAC-SH.

Table 4.9: Thermodynamic parameters of the *p*-cresol adsorption onto CSAC-SH at different temperatures

T (K)	ΔG^0 (kJ mol^{-1})	ΔS^0 (J mol^{-1} K^{-1})	ΔH^0 (kJ mol^{-1})
298	-2.73	-56.91	-19.56
308	-1.88		
318	-1.38		
328	-1.02		

4.3.5 Desorption study

In the desorption study, it was found that the majority of *p*-cresol molecules were retained on the surface of the spent CSAC-SH, releasing only 12% of the adsorbed *p*-cresol back into solution even after 240 h as shown in Fig. 4.8. The low percentage of desorption suggests that the adsorbed *p*-cresol remains stable on the adsorbent, the adsorption is largely irreversible, and the adsorption is predominantly chemisorption type.

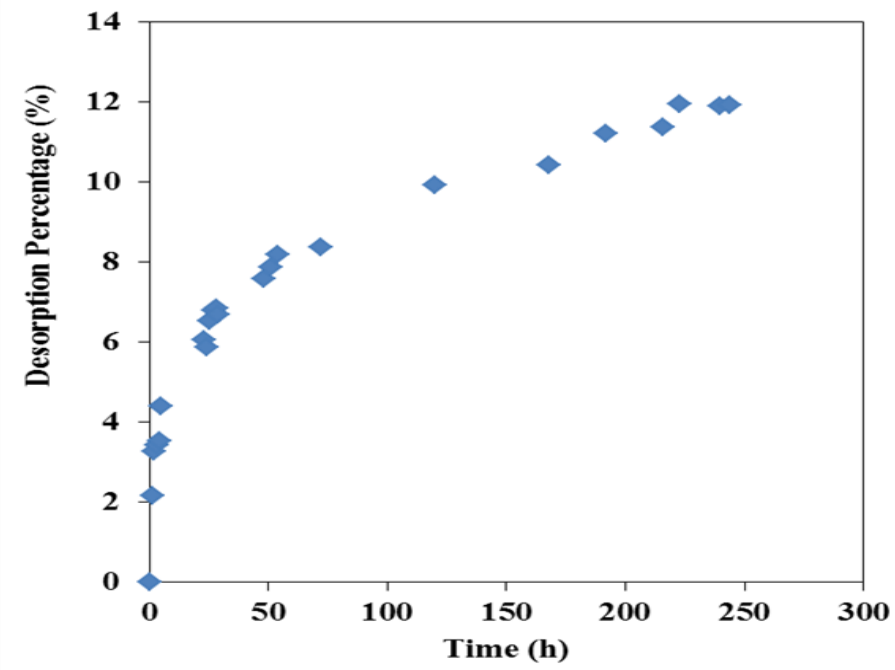

Fig. 4.8: Fraction of desorbed *p*-cresol from spent CSAC-SH by NaOH solution.

4.4 Conclusions

A coconut shell-based activated carbon (CSAC-SH) via NaOH-activation was tested for uptake of malodorous *p*-cresol from aqueous solutions. The characterization results revealed that CSAC-SH possessed a distinct microporous and mesoporous network and was composed mainly of basic functional groups. A pseudo-second-order kinetic model was found to describe the experimental data best. The equilibrium study showed that Redlich-Peterson, Fritz-Schluender and Langmuir isotherm models gave reasonably good fit to the experimental data. The maximum monolayer adsorption capacity of CSAC-SH was found to be 256.9 mg g^{-1}, suggesting that the prepared adsorbent is highly effective in mitigation of *p*-cresol. The desorption study demonstrated that the adsorbed *p*-cresol was mostly stable on the carbon surface due to chemisorption. The present research indicates that NaOH-activated carbon may be a promising adsorbent for removal of *p*-cresol from wastewater and hence can aid in cleaning the environment.

REFERENCES

[1] Parker DB, Gilley J, Woodbury B, Kim K, Galvin G, Bartelt-Hunt SL et al. Odorous VOC emission following land application of swine manure slurry. Atmos Environ 2013;66:91-100.

[2] Banat FA, Al-Bashir B, Al-Asheh S, Hayajneh O. Adsorption of phenol by bentonite. Environ Pollut 2000;107:391-8.

[3] Kilic M, Apaydin-Varol E, Pütün AE. Adsorptive removal of phenol from aqueous solutions on activated carbon prepared from tobacco residues: Equilibrium, kinetics and thermodynamics. J Hazard Mater 2011;189:397-403.

[4] Singh RK, Kumar S, Kumar S, Kumar A. Development of parthenium based activated carbon and its utilization for adsorptive removal of *p*-cresol from aqueous solution. J Hazard Mater 2008;155:523-35.

[5] Sayğılı H, Güzel F, Önal Y. Conversion of grape industrial processing waste to activated carbon sorbent and its performance in cationic and anionic dyes adsorption. J Clean Prod 2015;93:84-93.

[6] Zhu Y, Kolar P. Adsorptive removal of *p*-cresol using coconut shell-activated char. J Environ Chem Eng 2014;2:2050-8.

[7] Azevedo D, Araujo J, Bastos-Neto M, Torres AEB, Jaguaribe EF, Cavalcante CL. Microporous activated carbon prepared from coconut shells using chemical activation with zinc chloride. Micropor Mesopor Mater 2007;100:361-4.

[8] Mohd Din A, Hameed B, Ahmad A. Batch adsorption of phenol onto physiochemical-activated coconut shell. J Hazard Mater 2009;161:1522-9.

[9] Martins AC, Pezoti O, Cazetta AL, Bedin KC, Yamazaki DA, Bandoch GF et al. Removal of tetracycline by NaOH-activated carbon produced from macadamia nut shells: Kinetic and equilibrium studies. Chem Eng J 2015;260:291-9.

[10] Cazetta AL, Vargas AMM, Nogami EM, Kunita MH, Guilherme MR, Martins AC et al. NaOH-activated carbon of high surface area produced from coconut shell: Kinetics and equilibrium studies from the methylene blue adsorption. Chem Eng J 2011;174:117-25.

[11] Tan Y, Islam MA, Asif M, Hameed B. Adsorption of carbon dioxide by sodium hydroxide-modified granular coconut shell activated carbon in a fixed bed. Energy 2014;77:926-31.

[12] El-Sayed Y, Bandosz TJ. Adsorption of valeric acid from aqueous solution onto activated carbons: role of surface basic sites. J Colloid Interface Sci 2004;273:64-72.

[13] Boehm H. Chemical Identification of Surface Groups. Adv Catal 1966;16:179-274.

[14] Demirbas E, Dizge N, Sulak MT, Kobya M. Adsorption kinetics and equilibrium of copper from aqueous solutions using hazelnut shell activated carbon. Chem Eng J 2009;148:480-7.

[15] Rengaraj S, Moon S, Sivabalan R, Arabindoo B, Murugesan V. Removal of phenol from aqueous solution and resin manufacturing industry wastewater using an agricultural waste: rubber seed coat. J Hazard Mater 2002;89:185-96.

[16] Marsh H, Reinoso FR. Activated carbon. Elsevier; 2006.

[17] Yang K, Peng J, Srinivasakannan C, Zhang L, Xia H, Duan X. Preparation of high surface area activated carbon from coconut shells using microwave heating. Bioresour Technol 2010;101:6163-9.

[18] Dąbrowski A, Podkościelny P, Hubicki Z, Barczak M. Adsorption of phenolic compounds by activated carbon-a critical review. Chemosphere 2005;58:1049-70.

[19] Vargas AM, Garcia CA, Reis EM, Lenzi E, Costa WF, Almeida VC. NaOH-activated carbon from flamboyant (Delonix regia) pods: Optimization of preparation conditions using central composite rotatable design. Chem Eng J 2010;162:43-50.

[20] László K, Szűcs A. Surface characterization of polyethyleneterephthalate (PET) based activated carbon and the effect of pH on its adsorption capacity from aqueous phenol and 2,3,4-trichlorophenol solutions. Carbon 2001;39:1945-53.

[21] Yang J, Qiu K. Preparation of activated carbons from walnut shells via vacuum chemical activation and their application for methylene blue removal. Chem Eng J 2010;165:209-17.

[22] Tan I, Ahmad AL, Hameed B. Adsorption of basic dye on high-surface-area activated carbon prepared from coconut husk: Equilibrium, kinetic and thermodynamic studies. J Hazard Mater 2008;154:337-46.

[23] El Nemr A, El-Sikaily A, Khaled A, Abdelwahab O. Removal of toxic chromium from aqueous solution, wastewater and saline water by marine red alga Pterocladia capillacea and its activated carbon. Arabian J Chem 2015; 8.1: 105-117.

[24] Mourao P, Carrott P, Ribeiro Carrott M. Application of different equations to adsorption isotherms of phenolic compounds on activated carbons prepared from cork. Carbon 2006;44:2422-9.

[25] Wu F, Tseng R. Preparation of highly porous carbon from fir wood by KOH etching and CO_2 gasification for adsorption of dyes and phenols from water. J Colloid Interface Sci 2006;294:21-30.

[26] Das L, Kolar P, Classen JJ, Osborne JA. Adsorbents from pine wood via K2CO3-assisted low temperature carbonization for adsorption of *p*-cresol. Ind Crops Prod 2013;45:215-22.

[27] Hameed B, Rahman A. Removal of phenol from aqueous solutions by adsorption onto activated carbon prepared from biomass material. J Hazard Mater 2008;160:576-81.

CHAPTER 5

MITIGATION OF AQUEOUS AMMONIA USING AVOCADO-SEED ACTIVATED CARBON

Yiying Zhu [a], Praveen Kolar [a*], Sanjay B. Shah [a], Jay J. Cheng [a], P.K. Lim [b]

[a] Department of Biological and Agricultural Engineering, Campus Box 7625, North Carolina State University, Raleigh, NC, 27695-7625, USA.

[b] Department of Chemical and Biomolecular Engineering, Campus Box 7905, North Carolina State University, Raleigh, NC, 27695-7905, USA.

E-mail addresses: yzhu15@ncsu.edu, pkolar@ncsu.edu

[*] Corresponding author contact information: 278 Weaver Labs, Campus Box 7625, North Carolina State University, Raleigh, NC, 27695-7625, USA.

Phone: +1 919 513 9797; Fax: +1 919 515 7760.

E-mail address: pkolar@ncsu.edu

*** This chapter "MITIGATION OF AQUEOUS AMMONIA USING AVOCADO-SEED ACTIVATED CARBON" is currently under review at *Industrial Crops and Products Journal*.**

Abstract

An avocado seed-activated carbon prepared from methanesulfonic acid (AAC-MA) was tested as a novel adsorbent for removal of ammonia in aqueous solutions. Scanning electron microscopy (SEM) was employed to identify the structural and morphological properties of the prepared carbon. The effects of pH, adsorbent dosage, initial ammonia concentrations, and contact time on ammonia removal from aqueous solution were also investigated. Moreover, different kinetic and isotherm models were fitted to the experimental data to gain a better understanding of the efficiency and applicability of the adsorption system. The pseudo-second order kinetic model was found to best describe the ammonia adsorption. The equilibrium data were found to conform best to Langmuir isotherm model. The results demonstrated that the prepared activated carbon is promising in mitigating ammonia from aqueous solution with an adsorption capacity of 5.446 mg g^{-1} at 25 ^{o}C.

Key words

Ammonia adsorption; Equilibrium isotherm; Adsorption kinetics; SEM; Wastewater treatment

5.1 Introduction

Nitrogen compounds are biochemically interconvertible in terms of nitrate, nitrite, ammonia, organic nitrogen, as well as nitrogen gas, which are essential nutrients for life (APHA-AWWA-WPCF., 1981). However, excess nitrogen in receiving water bodies such as coastal seas, lakes, and rivers can cause eutrophication resulting in overgrowth of algae; excess algal growth can deplete the dissolved oxygen required by aquatic organisms for survival (Huang et al., 2010; Liu et al., 2013). Excessive nitrogen loading can also reduce soil productivity by increasing soil acidity, and form particulate matter particles or haze to impair atmospheric visibility and endanger public health (Love et al., 2011). Agricultural run-off, emissions from manure storage facilities in livestock farming operations, especially swine husbandry, release of fertilizer, decomposition of biological waste and industrial emissions have largely been blamed for these nitrogen pollution problems (Randall and Tsui, 2002; Love at al., 2012). As a result, nitrogen compounds are one of the most significant pollutants in industrial, agricultural, and domestic wastewaters and are in urgent need of control (Sharifnia et al., 2012). Among all the forms of nitrogen in water and wastewaters, ammonia nitrogen (NH_3-N), being toxic to fish and other living organisms, is the most frequently encountered nitrogenous compound (Jellali et al., 2011; Gupta et al., 2015). Moreover, the emission of ammonia, which is odorous, and an environmental stressor because it irritates eye, throat and nose as low as the breathing levels of 50-100 mg L^{-1} (Huang, Li and Chen, 2008). Hence, the removal of NH_3-N from wastewater prior to discharge is critical for nitrogen pollution reduction.

Ammoniacal nitrogen removal has been achieved by different technologies, such as biological treatment (nitrification-denitrification) (Peng and Zhu, 2006); ion-exchange by zeolite (Huang et al., 2010) and clinoptilolite (Vassileva and Voikova, 2009); air stripping (Bonmatí and Flotats, 2003); and adsorption by wheat straw based resins (Ma et al., 2011; Liu et al., 2013), composite materials (Halim et al., 2010) as well as activated carbon (Vassileva, Tzvetkova and Nickolov, 2009). Among these methods, adsorption is characterized by ease of application and establishment, wide range of operating conditions, high safety, low cost, as well as high effectiveness. Hence, adsorption of ammonia by different adsorbents is being increasingly explored. Of all the different kinds of adsorbents, activated carbons are of great interest because they are environmentally-friendly, simple, economical, easily-separable, rich in surface functional groups and allow recovery of ammonia as a fertilizer controlled release agent in farmland by desorption or phytotransformation (Vassileva et al., 2009; Love et al., 2011; Liu et al., 2013; Shi et al., 2013).

However, application of activated carbon for removal of ammonia nitrogen is still in need of further study. Generally, activated carbon does not exhibit high adsorption capacity for ammonia because it usually possesses a non-polar surface leading to a poor interaction with the polar adsorbate (Halim et al., 2010). Hence at present, the scientific literature is limited regarding ammonia removal by pristine or modified activated carbons because of their lower removal efficiencies compared to zeolite and other adsorbents (Shi, Wang and Zheng, 2013). It is widely recognized that both the nature of the raw materials and the

synthesis conditions are of great importance in determining the carbon adsorption performance (Zhu and Kolar, 2014).

With the recent interest in sustainable waste management, researchers are investigating renewable agricultural wastes as precursors for synthesis of adsorbents. Avocado seed, as an abundant agricultural residue from human consumption or food-processing plants, has not received adequate attention as an adsorbent (Elizalde-González et al., 2007). Up to date, only a few studies are available regarding use of avocado seed-activated carbons (AAC). For example, Elizalde-Gonzalez et al. (2007) studied one AAC prepared from phosphorous acid and Rodrigues et al. (2011) evaluated another AAC treated by physical activation for removal of phenol. The fresh avocado seed constitutes 10-13% of the fruit by weight (Rodrigues et al., 2011), and therefore, conversion of the avocado seeds to effective adsorbents will not only add value to the agricultural residue, solve the discharge problem, but will also provide a potential low-priced alternative to commercial activated carbons.

In order to enhance ammonia uptake capacity, the activated carbon surface should be modified to increase its affinity towards this polar adsorbate. It is well acknowledged that to attract positively charged species, the best activated carbons should be rich in acidic functional groups such as carbonyl, carboxyl, phenolic hydroxyl, lactone and quinine groups and using acids as activating agents will aid in the formation of these groups (Vassileva, Tzvetkova and Nickolov, 2009; Huang, Li and Chen, 2008). To the best of our knowledge,

methanesulfonic acid, a non-volatile strong acid, has never been applied for preparation of activated carbon for uptake of ammonia.

Hence, the goal of this research is to synthesize an acidic avocado seed-based activated carbon using methanesulfonic acid as an activating agent (AAC-MA). Specifically, we evaluated the adsorption capacity of AAC-MA for ammonia, and studied the effects of pH, reaction time, initial ammonia concentrations, and adsorbent dosages on the adsorption. In addition, the physical and chemical characteristics of the prepared activated carbon were examined by SEM, acid value and Boehm titration. Moreover, adsorption kinetics and equilibrium isotherms were studied in defining the efficiency and applicability of the adsorption of ammonia onto AAC-MA.

5.2 Materials and methods

5.2.1 Preparation of adsorbent

The feedstock for activated carbon synthesized in this research was procured from the local market. Avocado seeds were washed with deionized water to remove superficial impurities and dried at 50 ^{o}C overnight. Then the seeds were cut into small pieces of about 5 mm size. The size-reduced avocado seeds were impregnated with 70 wt.% methanesulfonic acid (Acros Organics) for 17 h with impregnation ratio (weight of acid/weight of avocado seed) of 0.8. Subsequently, the methanesulfonic acid treated sample was dried at 95 ^{o}C overnight and placed in a horizontal stainless steel reactor and carbonized at 700 ^{o}C for 1.5 h in a kiln (Sentry Xpress 4.0, Paragon) and cooled down to room temperature in a flowing

stream of nitrogen (2 L min^{-1}). The resulting activated carbon was repeatedly washed with deionized water to remove the acid residues, tar, fines and impurities and then dried in the oven at 75 ^{o}C to produce the final product, AAC-MA.

5.2.2 Adsorbent characterization

Various characterization methods were used to determine the physical and chemical properties of the prepared activated carbon.

5.2.2.1 Yield

The yield of the activated carbon was determined as the mass ratio of the produced activated carbon to precursor according to the following equation (Zhu and Kolar, 2014):

$$Yield\ (\%) = \frac{W_c}{W_o} \times 100 \qquad (5\text{-}1)$$

where W_c (g) and W_o (g) represent the dry weight of final AAC-MA and the starting material of avocado seeds used, respectively.

5.2.2.2 pH of the adsorbent

The acidity and basicity of the activated carbon surface was evaluated from the pH of the adsorbent suspension. After adding 0.4 g of prepared activated carbon sample to 20 mL deionized water, the solution was agitated at 400 rpm overnight to reach equilibrium and followed by filtration. Subsequently, pH of the filtrate was measured (Zhu and Kolar, 2014).

5.2.2.3 Surface chemistry characterization

The surface oxygen functional groups such as phenolic (-OH), carbonyl (C=O) and carboxylic groups (COOH) were determined by Boehm titration as described previously (Zhu and Kolar, 2014).

5.2.2.4 Scanning Electron Microscopic analysis

Scanning Electron Microscopy (SEM) was used to observe the surface morphology of the produced adsorbent. A Hitachi Model S-3200N apparatus was used to record the SEM images. Prior to analyses, the samples were dispersed on a diminutive aluminum disk with an adhesive, labeled and coated with gold for electron reflection, followed by vacuuming.

5.2.3 Batch adsorption of ammonia on AAC-MA

A 1000 mg L^{-1} stock solution of aqueous ammonia was prepared by dissolving 3.819 g anhydrous ammonium chloride salt (99.5%, extra pure, with anti-caking agent, Acros Organics) in 1 L deionized water. Working solutions (100 mL ea.) of different concentrations were prepared by stepwise dilution of the stock solution in 150 mL serum bottles. After loading 0.3 g of AAC-MA into the solution, the serum bottles were sealed with rubber stoppers and 20 mm aluminum air-tight caps and the batch adsorption was carried out at 125 rpm for 6 h at 25 ^{o}C. A control solution of ammonia under the same condition but with no AAC-WA was also tested simultaneously to confirm that the ammonia was neither volatilized nor adsorbed on the walls of the batch reactor.

The ammonia concentrations and variation in concentration with time were measured using the Nesslerization method (APHA-AWWA-WPCF., 1981). In this method, before analysis, Nessler reagent (a mixture of 100 g HgI_2, 70 g KI and 160 g NaOH dissolved in 1 L deionized water) and Rochelle salt solution (50 g $KNaC_4H_4O_6 \cdot 4H_2O$ dissolved in 100 mL deionized water) were prepared separately. Ammonia concentration was determined by reaction with an appropriate amount of Nessler reagent with a trace amount of Rochelle salt solution to prevent turbidity or precipitation to form a colored complex that varies from yellow to brown. The color in samples and standards were analyzed by a UV spectrophotometer (Genesys 10S, Thermo Scientific) at 425 nm and the intensity of the color was proportional to the ammonia concentration and the yellow color is characteristic of low ammonia nitrogen content. The amount of ammonia adsorbed onto AAC-MA, q_e (mg g^{-1}), and the removal efficiency (X %) of AAC-MA were calculated according to the following equations (Huang et al., 2010):

$$q_e = \frac{(C_o - C_e)V}{W} \tag{5-2}$$

$$X\,(\%) = \frac{C_o - C_t}{C_o} \times 100 \tag{5-3}$$

where C_o (mg L^{-1}), C_t (mg L^{-1}) and C_e (mg L^{-1}) are the initial, at time t, and equilibrium concentrations of ammonia in solution, respectively. V (L) is the volume of the solution, and W (g) is the mass of the dry AAC-MA used.

All the batch experiments were performed in duplicate and the mean values were used for analysis.

5.3 Results and discussion

5.3.1 Textural and chemical characteristics of AAC-MA

The yield (Eq. (5-1)) of AAC-MA was found to be 17%. The results of the chemical characterization including pH and Boehm titration of AAC-MA are tabulated in Table 5.1. The pH value of AAC-MA was 6.2 suggesting that the carbon was slightly acidic which was also corroborated by the results of Boehm titration that the adsorbent had more acidic groups than basic groups (Table 5.1). The abundance of acidic groups in AAC-MA will favor the adsorption of ammonia as Leuch and Bandosz (2007) reported that surface acidity plays a significant role in ammonia removal via acid-base interactions.

Table 5.1: Results of chemical characterization of AAC-MA

	Boehm titration					pH
	Acidic groups (mmol g^{-1})				Basic group	
Sample	Carboxylic	Lactonic	Phenolic	Total	mmol g^{-1}	
AAC-MA	0.25	0.10	0.25	0.6	0.1	6.2

The samples of precursor of avocado seeds and AAC-MA before and after adsorption were analyzed using SEM and the results are presented in Fig. 5.1. Three different types of morphology were observed among these three samples. As shown in Fig. 5.1(a), the raw material exhibited an irregular non-porous surface with a dispersion of avocado seed starch

granules. In contrast to Fig. 5.1(a), the carbon surface of AAC-MA (Fig. 5.1(b)) presents a high degree of cracks together with assorted size pores. This indicates that the pore structure of the prepared activated carbon was well developed and volatile compounds were released during the physiochemical activation. Not only were there large pores (macrospores), a large number of the smaller pores (mesopores and micropores) were also observed in AAC-MA. This feature favors the adsorption of ammonia since ammonia is a small molecule in size. In comparison with Fig. 5.1(b), in Fig. 5.1(c), the ammonia covered the pores of the adsorbent quite uniformly, leaving behind an almost non-porous surface of the adsorbed AAC-MA.

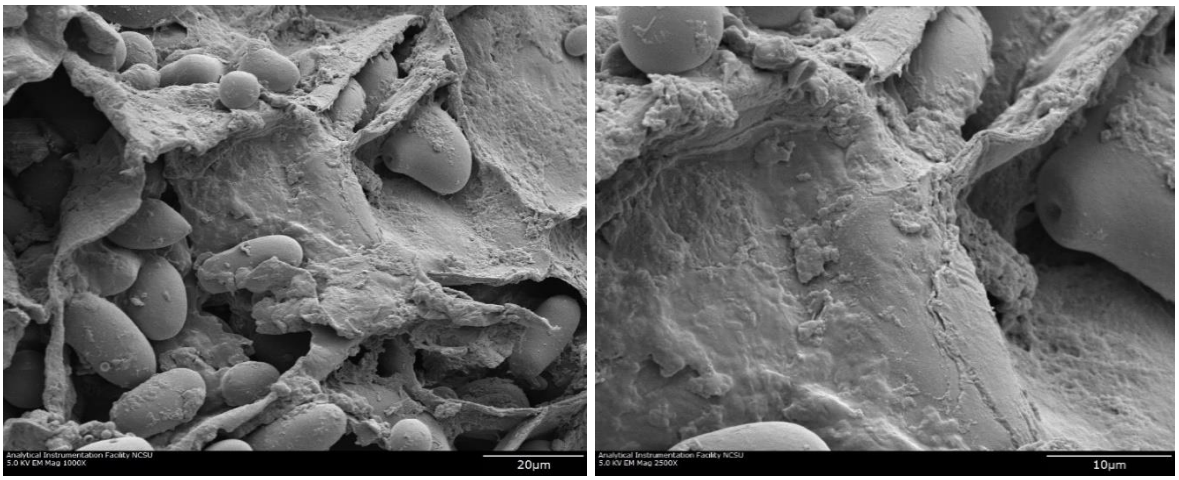

(a)

Fig. 5.1: (a) SEM images of (a) raw material of avocado seeds (left: 1000x; right 2500x), (b) AAC-MA before adsorption (left: 1000x; right 2500x), and (c) AAC-MA after adsorption (left: 1000x; right 2500x).

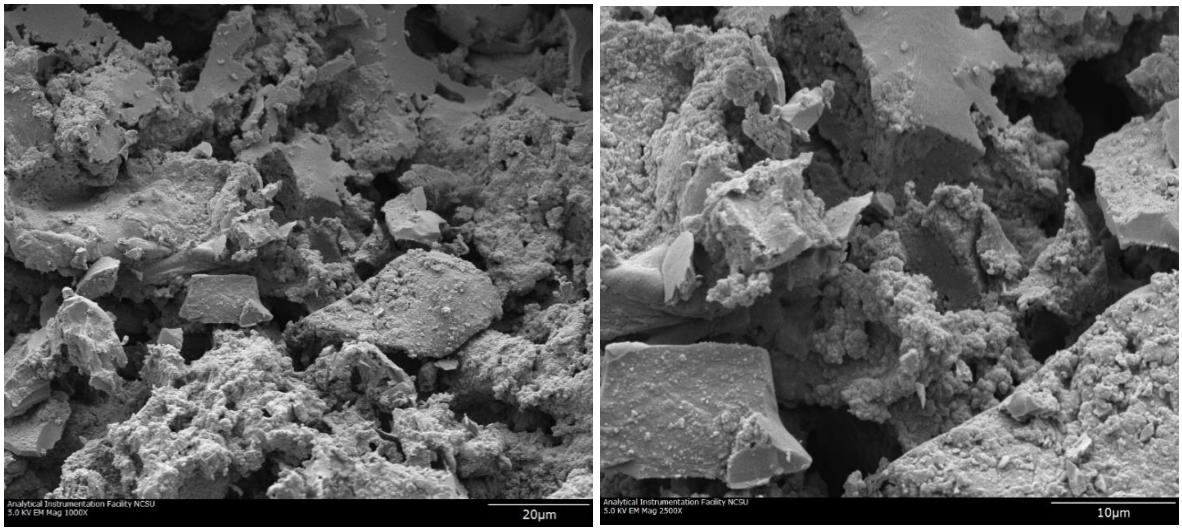
Analytical Instrumentation Facility NCSU
5.0 kV EM Mag 1000X
20µm
Analytical Instrumentation Facility NCSU
5.0 kV EM Mag 2500X
10µm

(b)

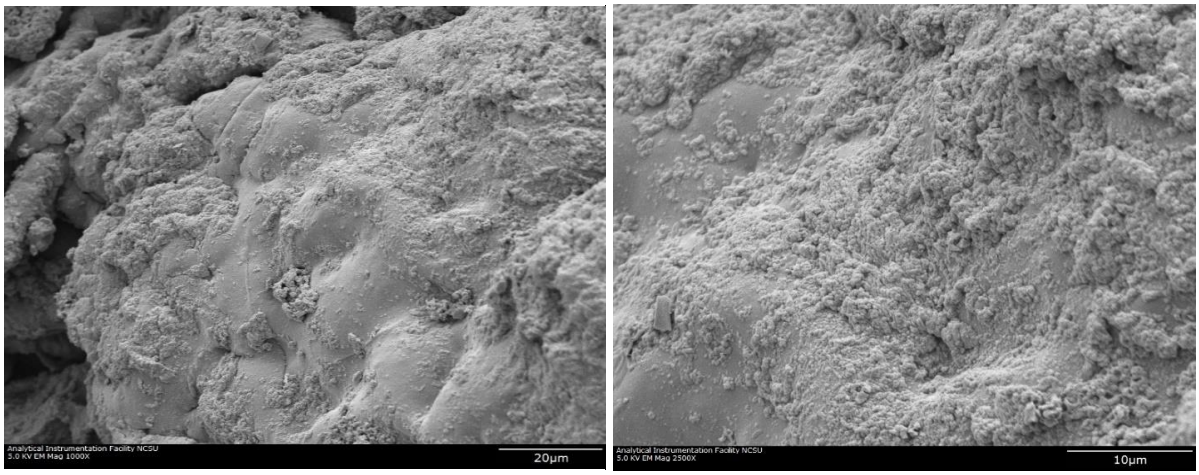
Analytical Instrumentation Facility NCSU
5.0 kV EM Mag 1000X
20µm
Analytical Instrumentation Facility NCSU
5.0 kV EM Mag 2500X
10µm

(c)

5.3.2 Effect of pH

pH is one of the controlling parameters in ammonia adsorption process which influences the adsorbent surface charge together with the degree of ionization and speciation of the adsorbate (Sharifnia et al., 2012; Boopathy et al., 2013). The effect of pH on uptake of ammonia by AAC-MA was studied at pH values ranging from 3-9 adjusted by diluted NaOH and HCl solutions for the initial concentration of 150 mg L^{-1} of ammonia and the results were presented in Fig. 5.2. Ammonia adsorption capacity reached a maximum value at pH value of 5 (Fig. 5.2). Reduced adsorption with increasing pH might be due to the fact that ammonia were gradually neutralized by hydroxyl ion at higher pH values rendering it uncharged and hence weakening the attraction of the charged adsorbent (Zheng and Wang, 2009; Sharifnia et al., 2012; Vassileva and Voikova, 2009). Additionally, ammonia might prefer to stay in solution than being adsorbed and higher pH. As can be seen in Fig. 5.2, a decrease in the pH value from 5 to 3 led to a drop in adsorption capacity as well. This is probably due to the intensified competition of H^+ and ammonia for exchange sites on the adsorbent surfaces which was also reported by other researchers (Huang et al., 2010; Sharifnia et al., 2012; Vassileva and Voikova, 2009). Another reason is probably because of the high protonation of the functional groups (C=O, COO^-) on the adsorbent surfaces that resulted in a partial positive charge that repelled the polar attraction of ammonia (Kizito et al., 2015). Zheng and Wang (2009) also found that the maximum ammonia adsorption capacity was obtained at pH value of 5 by a hydrogel composite. Therefore, the optimum pH value of 5 was used in the following experiments in this research.

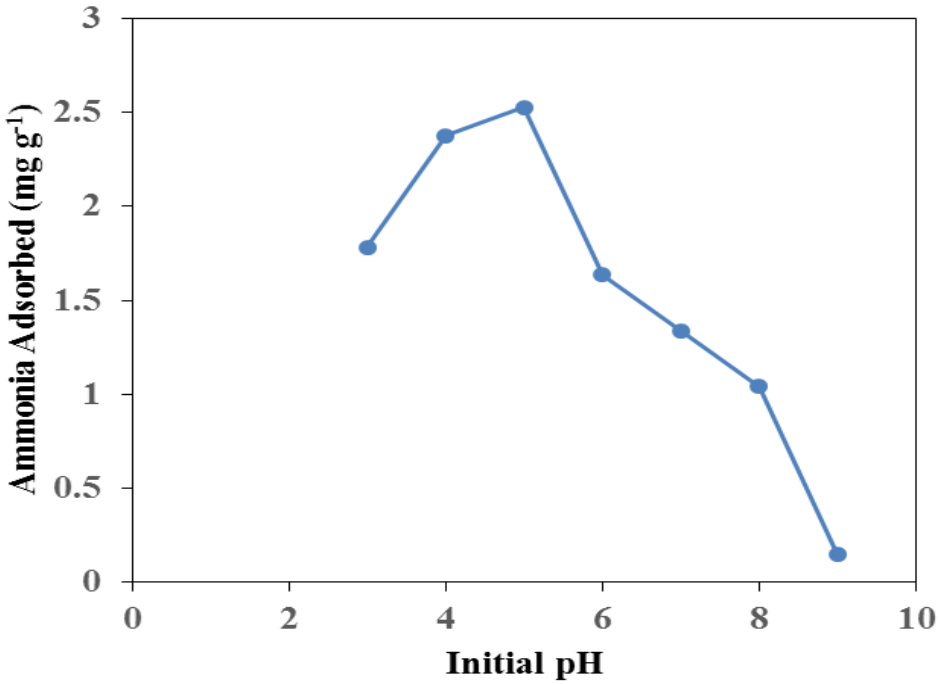

Fig. 5.2: Effect of pH on adsorption of ammonia onto AAC-MA (initial ammonia concentration: 150 mg L^{-1}; adsorbent dose: 3 g L^{-1}; agitation speed: 125 rpm; temperature: 25 ^{o}C).

5.3.3 Effect of adsorbent dosage

The adsorptive uptake of the ammonia from aqueous solution is highly dependent on the adsorbent dosage given that it determines the capacity of an adsorbent for a certain initial adsorbate concentration. The influence of AAC-MA dose on the adsorption of ammonia is given in Fig. 5.3.

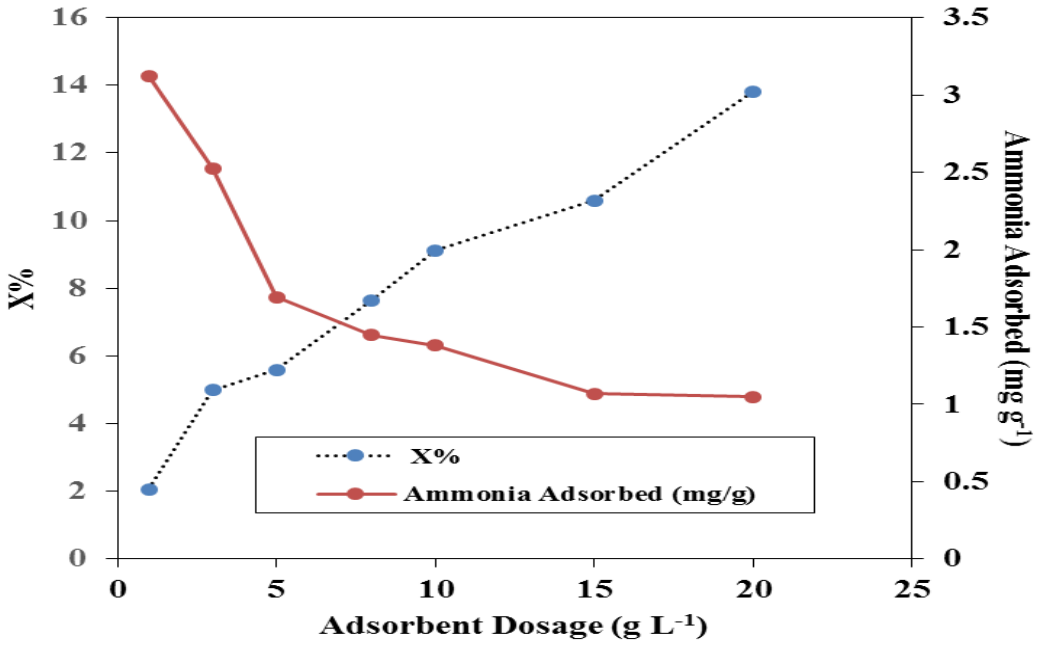

Fig. 5.3: Effect of adsorbent dosage on removal of ammonia on AAC-MA (initial ammonia concentration: 150 mg L^{-1}; pH: 5; agitation speed: 125 rpm; temperature: 25 ^{o}C).

The percentage removal of ammonia increased from 2.06 to 13.82% for the adsorbent dose from 1 to 20 g L^{-1} due to increased availability of active sites for adsorption. Inversely, as the adsorbent dosage increased from 1 to 20 g L^{-1}, the adsorbed amount of ammonia decreased from 3.12 to 1.05 mg g^{-1} that might be due to the increasing interface area for a limited number of ammonia. Similar trends of ammonia adsorption vs. adsorbent dosage were also observed by Vassileva and Voikova (2009) using NaCl pretreated Bulgarian clinoptilolite as an adsorbent and Ma et al. (2011) using a fertilizer controlled release agent prepared from wheat straw.

5.3.4 Effect of initial ammonia concentration and contact time

Contact time is a crucial factor because it affects the adsorption kinetics of an adsorbent for a given initial concentration of adsorbate (Zheng and Wang, 2009). Additionally, initial adsorbate concentration is another factor controlling the adsorption process. The relationship between the contact time and the ammonia adsorption amount at different initial adsorbate concentrations is shown in Fig. 5.4. There was faster ammonia uptake rate at the initial removal stage might be due to the availability of active sites for adsorption as well as the high solute concentration gradient, and this result is consistent with those reported by other researchers (Zhao et al., 2013; Zhang et al., 2011). Afterwards, the ammonia uptake decreased gradually and then remained constant and the equilibrium time for all concentrations were determined to be 4 h. Because ammonia uptake is a rapid process, most of the equilibrium time reported in earlier studies by other researchers was within 8 h (Zhao et al., 2013; Wahab, Jellali and Jedidi, 2010a; Sharifnia et al., 2012; Wahab, Jellali and Jedidi, 2010b). The equilibrium time for ammonia uptake varied in different studies since adsorption is a function of a number of factors, such as, experimental conditions, the material used, and agitation speed, as was also pointed out by Zhang et al. (2011). It was also noted in Fig. 5.4 that uptake capacity increased with increasing initial ammonia concentration, which might be ascribed to the higher availability of ammonia. With higher ammonia concentration, there is a stronger driving force to overcome the mass transfer resistance between the aqueous phase and the solid phase of the adsorbent and hence to increase the possibility of the collision between ammonia and the adsorbent so as to enhance the uptake

capacity, as described by Wahab et al. (2010b). For subsequent adsorption experiments, a minimum contact time of 4 h was chosen to ensure equilibrium adsorption.

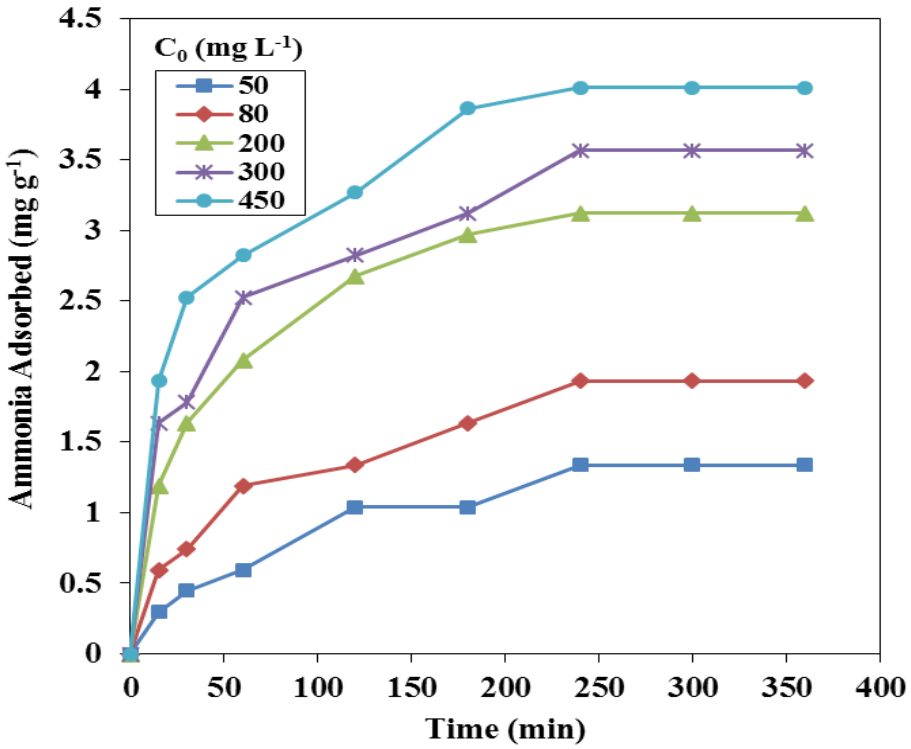

Fig. 5.4: Effect of contact time at different initial concentrations on ammonia removal by AAC-MA (adsorbent dose: 3 g L^{-1}; pH: 5; agitation speed: 125 rpm; temperature: 25 ^{o}C).

5.3.5 Adsorption kinetic modeling

Adsorption kinetics is a key tool for describing the efficiency of adsorption onto the adsorbent and the reaction pathways. Besides, it helps to provide the information of the

adsorption mechanism and identity the step governing the overall removal process. The most well-known models including Lagergren's pseudo-first-order (Eq. (5-4)) (Lagergren, 1898), Ho's pseudo-second-order (Eq. (5-5)) (Ho and McKay, 1998), Elovich (Eq. (5-6)) (Chien and Clayton, 1980) and intra-particle diffusion model (Eq. (5-7)) (Weber and Morris, 1963) were employed to test the obtained dynamic experimental data.

$$q_t = q_e[1 - e^{-k_1 t}] \tag{5-4}$$

where q_t (mg g^{-1}) and q_e (mg g^{-1}) are amounts of ammonia adsorbed at time t (min) and at equilibrium, respectively. $k_1(\min^{-1})$ is the rate constant of pseudo-first-order adsorption.

$$q_t = \frac{k_2 q_e^2 t}{1 + k_2 q_e t} \tag{5-5}$$

where q_t (mg g^{-1}) and q_e (mg g^{-1}) are amounts of adsorbate adsorbed at time t (min) and at equilibrium onto adsorbent, respectively. k_2 (g $mg^{-1}min^{-1}$) is the rate constant of pseudo-second-order adsorption.

$$q_t = \frac{1}{\beta} In(\alpha\beta) + \frac{1}{\beta} In(t) \tag{5-6}$$

where q_t (mg g^{-1}) is the adsorption amount at time t (min). α ($mg\ g^{-1}min^{-1}$) and β ($g\ mg^{-1}$) are the initial desorption rate and the desorption constant, respectively.

$$q_t = K_{id} t^{0.5} + C \tag{5-7}$$

where q_t (mg g^{-1}) is the amount of adsorbte adsorbed per unit mass of adsorbent at time t (min). $k_{id}(\text{mg g}^{-1}\text{min}^{-0.5})$ is the intraparticle diffusion rate constant. C (mg g^{-1}) is the thickness of the boundary layer.

The summary of the kinetic model parameters for uptake of ammonia are given in Table 5.2. Among all of the above-mentioned kinetics models fitted to the experimental data, the pseudo-second kinetic model gave a highest correlation coefficient (≥ 97.71%) implying that it explained the kinetic process best and it was the rate-limiting step. It can also be deduced that chemisorption occurred in the ammonia adsorption process using AAC-MA (Kizito et al., 2015). Observations in this study are similar to findings by others that showed that the pseudo-second order kinetic model gave better fitting results for uptake of ammonia than other kinetic models (Kizito et al., 2015; Jellali et al., 2011; Wahab, Jellali and Jedidi, 2010b). The non-linear fits of pseudo-second order kinetic model for the ammonia adsorption at different concentrations on AAC-MA are presented in Fig. 5.5.

Table 5.2: Kinetic constants for adsorption of ammonia on AAC-MA

Kinetic models	Initial ammonia concentration (mg L^{-1})				
	50	80	200	300	450
Experimental qe (mg g^{-1})	1.338	1.933	3.122	3.568	4.014
Pseudo-first-order model					
Calculated q_e (mg g^{-1})	1.367	1.887	3.049	3.366	3.813
k_1 (min^{-1})	0.01092	0.01504	0.02334	0.02687	0.03386
R^2 (%)	97.95	96.24	97.97	94.38	94.59

Table 5.2 Continued

Kinetic models	Initial ammonia concentration (mg L^{-1})				
	50	80	200	300	450
Pseudo-second – order model					
Calculated $q_{e,}$ (mg g^{-1})	1.731	2.252	3.464	3.785	4.212
k_2 (g mg^{-1} min^{-1})	0.006208	0.007651	0.008609	0.009313	0.01108
$h=k_2q_e^2$ (mg g^{-1} min^{-1})	0.018601	0.038802	0.103302	0.13342	0.19657
R^2 (%)	98.27	98.07	99.51	97.71	98.22
Elovich model					
$q_{e,cal}$ (mg g^{-1})					
α (mg g^{-1} min^{-1})	0.0446	0.09357	0.2784	0.423	0.7863
β (g mg^{-1})	2.756	2.168	1.526	1.484	1.447
R^2 (%)	96.17	97.15	98.22	97.33	97.62
Intraparticle diffusion model					
K_{id} (mg g^{-1} $min^{-0.5}$)	0.652	0.9234	1.535	1.621	1.838
C (mg g^{-1})	$8.206\times(10^{-7})$	0.09187	0.3418	0.5064	0.7026
R^2 (%)	97.99	98.2	95.7	92.92	90.44

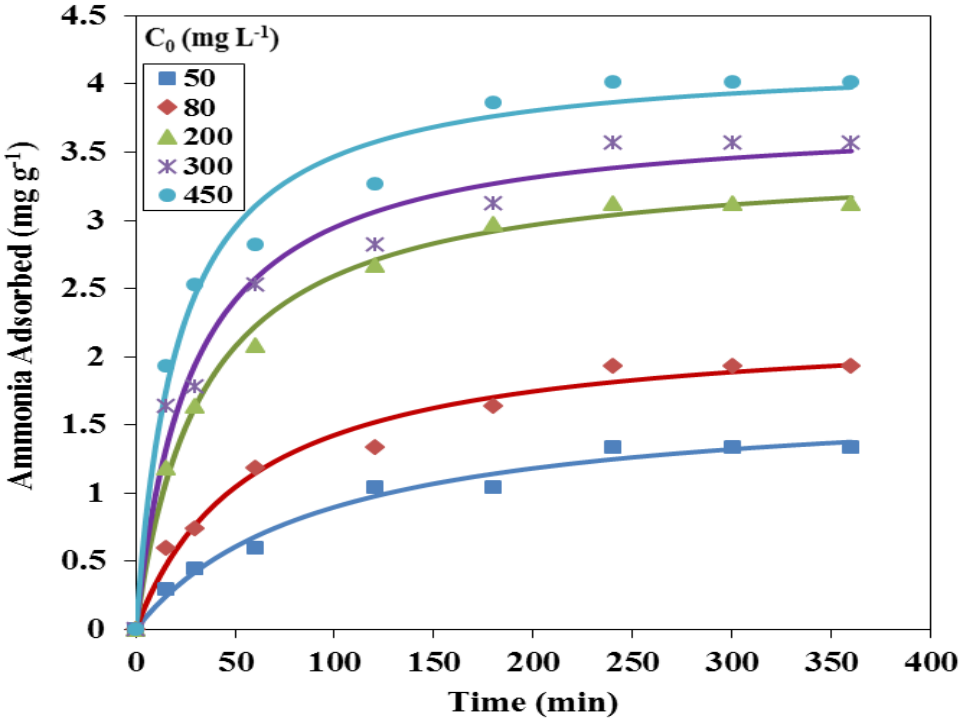

Fig. 5.5: Non-linear fits of pseudo-second order kinetic model for the ammonia adsorption on AAC-MA (initial ammonia concentration: 50, 80, 200, 300, 450 mg L^{-1}; adsorbent dose: 3 g L^{-1}; pH: 5; agitation speed: 125 rpm; temperature: 25 ^{o}C).

5.3.6 Adsorption isotherm modeling

Adsorption isotherms describe the interaction between adsorbent with adsorbate as well as how the adsorbate molecules distribute between the solid adsorbent phase (q_e [mg g^{-1}]) and the liquid phase (C_e [mg L^{-1}]) after reaching equilibrium. Finding a suitable isotherm model to represent the equilibrium isotherm data is of great importance for design purposes and optimization of the use of the adsorbent. Three non-linear isotherm models including the

two parameters isotherm models of Freundlich (1906) (Eq. (5-8)) and Langmuir (1918) (Eq. (5-9)) and three parameters isotherm model of Redlich-Perterson (1959) (Eq. (5-10)) were used to fit the equilibrium data. The Freundlich isotherm (1906) is expressed as:

$$q_e = K_F \, C_e^{\,1/n} \tag{5-8}$$

where K_F ($mg\ g^{-1}(L\ mg^{-1})^{1/n}$) and n are Freundlich adsorption isotherm parameters. The Freundlich model is an empirical isotherm model and it assumes a heterogeneous surface with a non-uniform distribution of adsorption heat over the surface. Additionally the model assumes that stronger binding sites have higher priority to be occupied (Freundlich, 1906).

The Langmuir isotherm (1918) is described as:

$$q_e = \frac{Q_0 K_L C_e}{1 + K_L C_e} \tag{5-9}$$

where Q_0 ($mg\ g^{-1}$) is the maximum monolayer adsorption amount of ammonia per unit mass of adsorbent. K_L ($L\ mg^{-1}$) is the Langmuir adsorption equilibrium constant. The Langmuir isotherm model assumes a homogeneous surface of the adsorbent with uniform binding energies of all the binding sites for monolayer adsorption (Langmuir, 1918).

The Redlich-Peterson isotherm (1959) is represented as:

$$q_e = \frac{AC_e}{1 + BC_e^{\beta}} \tag{5-10}$$

where A ($L\ g^{-1}$) and B ($L\ mg^{-1}$) are Redlich-Peterson isotherm constants. β is Redlich-Peterson exponent and its value is between 0 and 1. This isotherm model is reduced to Freundlich isotherm model at high concentrations following Henry's law when $\beta = 0$ while

it can be converted to Langmuir isotherm model in case $\beta = 1$ at low concentrations (Redlich and Peterson, 1959). Hence, it can be applied for either homogeneous or heterogeneous systems and can be used as a compromise between Langmuir and Freundlich models.

The results of the isotherm parameters for the adsorption of ammonia onto AAC-MA are tabulated in Table 5.3. The Langmuir isotherm model yields a better fit (R^2 = 99.5%) to the equilibrium data than the Freundlich isotherm model. The β value of unity in the Redlich-Peterson isotherm model converted it into the Langmuir isotherm which also verified that the Langmuir isotherm model was appropriate to describe the adsorption process. The good fit of the Langmuir isotherm model to experimental data is depicted in Fig. 5.6. Likewise, Vassileva and Voikova (2009), Jellali et al. (2011), Ma et al. (2011), Wahab et al. (2010a) reported that the equilibrium data conformed to Langmuir isotherm model and confirmed monolayer ammonia adsorption.

Table 5.3: Isotherm parameters for adsorption of ammonia on AAC-MA

Freundlich isotherm				Langmuir isotherm			Redlich-Peterson isotherm			
$q_e = K_F\ C_e{}^{1/n}$				$q_e = \frac{Q_O K_L C_e}{1 + K_L C_e}$			$q_e = \frac{AC_e}{1 + BC_e^{\beta}}$			
T (K)	K_F (mg g^{-1}) (L mg^{-1})$^{1/n}$	1/n	R^2 (%)	K_L (L mg^{-1})	Q_0 (mg g^{-1})	R^2 (%)	A (L g^{-1})	B (L mg^{-1})	β	R^2 (%)
298	0.2614	0.456	96.76	0.006525	5.446	99.5	0.03554	0.006525	1	99.5

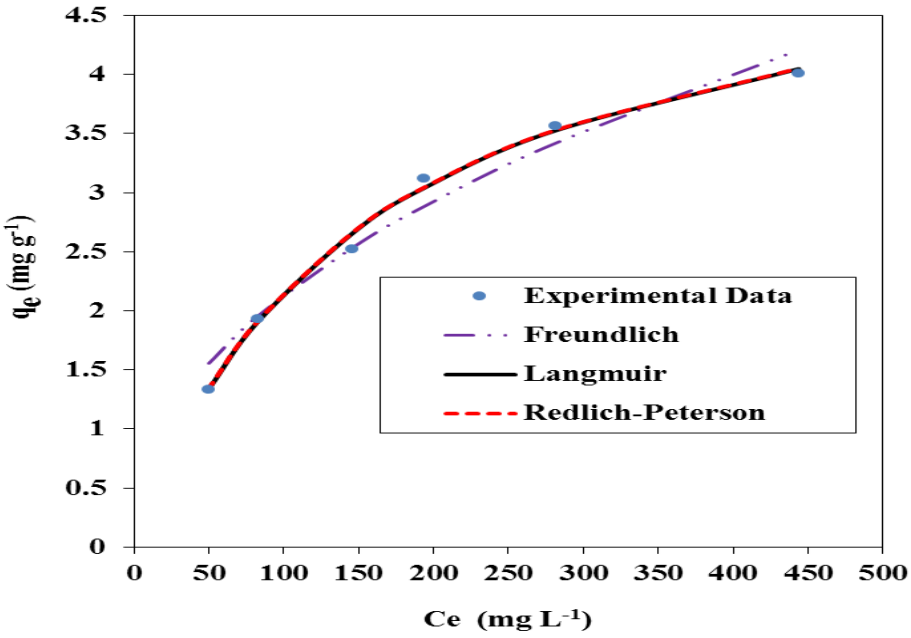

Fig. 5.6: Comparison of different isotherm models for ammonia adsorption on AAC-MA (initial ammonia concentration: 50, 80, 150, 200, 300, 450 mg L^{-1}; adsorbent dose: 3 g L^{-1}; pH: 5; agitation speed: 125 rpm; temperature: 25 ^{o}C).

The dimensionless constant separation factor (R_L) is given by $R_L = \frac{1}{1+K_L C_0}$ from Langmuir isotherm model parameter K_L and can be used to ascertain favorability of the adsorption (Langmuir, 1918). The R_L values were calculated to be between 0.254 to 0.754 in this study, indicating the favorable ammonia adsorption since the values were in the range of 0 and 1 (Zhang et al., 2011). Similarly, the value of 1/n (0.456) of Freundlich isotherm parameter was found to be between 0 and 1 implying favorable adsorption for ammonia (Zhao et al., 2013).

The monolayer adsorption capacity for ammonia was determined to be 5.446 mg g^{-1} at 25 ^{o}C in this study. Comparison of the adsorption capacity of AAC-MA to other selective adsorbents in literature is shown in Table 5.4. It is obvious from this table that AAC-MA has a strong ability for ammonia adsorption. A few adsorbents are even more efficient than AAC-MA to reduce ammonia, which may be attributed to their special surface chemical structure and/or the higher aqueous ammonia concentration employed as described by Jellali et al. (2011).

Table 5.4: A summary and comparison of the monolayer adsorption capacities of different adsorbents for ammonia

Number	Adsorbents	Adsorption capacity Q_o (mg g^{-1})	Temperature (^{o}C)	Initial ammonia concentration (mg L^{-1})	Reference
1	Avocado seed-activated carbon (AAC-MA)	5.446	25	50-450	Present work
2	Posidonia oceanica fibers (P. oceanica)	1.974	18	5-50	(Jellali et al., 2011)
3	Natural Bulgarian clinoptilolite (CL)	7.85	20	50-250	(Vassileva and Voikova, 2009)

Table 5.4 Continued

Number	Adsorbents	Adsorption capacity Q_o (mg g^{-1})	Temperature (°C)	Initial ammonia concentration (mg L^{-1})	Reference
4	Arene-sulphonic acid mesostructured material (AS-SBA-15)	14.9	20	50-700	(Rat - Valdambrini, Belkacemi and Hamoudi, 2012)
5	Ceramic adsorbent	112.4	25	2500-10000	(Zhao et al., 2013)
6	Ozonated activated carbon (OGAC)	1.12	25	200-800	(Love et al., 2011)
7	Sawdust	1.7	20	10-50	(Wahab, Jellali and Jedidi, 2010a)
8	Light expanded clay aggregate (LECA)	0.255	25	10-100	(Sharifnia et al., 2012)
9	Coconut shell-activated carbon (CSAC)	2.261	20	50-2000	(Boopathy et al., 2013)

5.4 Conclusions

Activated carbon prepared from avocado seeds using methanesulfonic acid as an activation agent (denoted as AAC-MA) was found to be effective in adsorbing ammonia from aqueous solutions. Adsorbent dosage, pH, initial ammonia concentration, and contact time were found to affect adsorption. The kinetic study showed that the best-fit kinetic model was a pseudo-second-order model. Langmuir adsorption model was found to be most accurate in representing the equilibrium data in the adsorption isotherm study. Our results suggest that the prepared activated carbon is an attractive adsorbent for removal of ammonia from aqueous solutions.

REFERENCES

APHA-AWWA-WPCF., 1981. Standard methods for the examination of water and wastewater. APHA Am. Publ. Health Assoc.

Bonmatí, A., Flotats, X., 2003. Air stripping of ammonia from pig slurry: characterisation and feasibility as a pre- or post-treatment to mesophilic anaerobic digestion, Waste Manage. 23, 261-272.

Boopathy, R., Karthikeyan, S., Mandal, A.B., Sekaran, G., 2013. Adsorption of ammonium ion by coconut shell-activated carbon from aqueous solution: kinetic, isotherm, and thermodynamic studies, Environ. Sci. Poll. Res. 20, 533-542.

Chien, S., Clayton, W., 1980. Application of Elovich equation to the kinetics of phosphate release and sorption in soils, Soil Sci. Soc. Am. J. 44, 265-268.

Elizalde-González, M.P., Mattusch, J., Peláez-Cid, A.A., Wennrich, R., 2007. Characterization of adsorbent materials prepared from avocado kernel seeds: Natural, activated and carbonized forms, J. Anal. Appl. Pyrolysis. 78, 185-193.

Freundlich, H., 1906. Over the adsorption in solution, J. Phys. Chem. 57, 385-470.

Gupta, V., Sadegh, H., Yari, M., Shahryari Ghoshekandi, R., Maazinejad, B., Chahardori, M., 2015. Removal of ammonium ions from wastewater: A short review in development of efficient methods, Global J. Environ. Sci. Manage. 1, 149-158.

Halim, A.A., Aziz, H.A., Johari, M.A.M., Ariffin, K.S., 2010. Comparison study of ammonia and COD adsorption on zeolite, activated carbon and composite materials in landfill leachate treatment, Desalination. 262, 31-35.

Ho, Y., McKay, G., 1998. Sorption of dye from aqueous solution by peat, Chem. Eng. J. 70, 115-124.

Huang, C., Li, H., Chen, C., 2008. Effect of surface acidic oxides of activated carbon on adsorption of ammonia, J. Hazard. Mater. 159, 523-527.

Huang, H., Xiao, X., Yan, B., Yang, L., 2010. Ammonium removal from aqueous solutions by using natural Chinese (Chende) zeolite as adsorbent, J. Hazard. Mater. 175, 247-252.

Jellali, S., Wahab, M.A., Anane, M., Riahi, K., Jedidi, N., 2011. Biosorption characteristics of ammonium from aqueous solutions onto Posidonia oceanica (L.) fibers, Desalination. 270, 40-49.

Kizito, S., Wu, S., Kirui, W.K., Lei, M., Lu, Q., Bah, H., Dong, R., 2015. Evaluation of slow pyrolyzed wood and rice husks biochar for adsorption of ammonium nitrogen from piggery manure anaerobic digestate slurry, Sci. Total Environ. 505, 102-112.

Lagergren, S., 1898. About the theory of so-called adsorption of soluble substances. K. Sven. Vetenskapsakad. Handl. 24, 1-39.

Langmuir, I., 1918. The adsorption of gases on plane surfaces of glass, mica and platinum. J. Am. Chem. Soc. 40, 1361-1403.

Le Leuch, L.M., Bandosz, T.J., 2007. The role of water and surface acidity on the reactive adsorption of ammonia on modified activated carbons, Carbon. 45, 568-578.

Liu, J., Su, Y., Li, Q., Yue, Q., Gao, B., 2013. Preparation of wheat straw based superabsorbent resins and their applications as adsorbents for ammonium and phosphate removal, Bioresour. Technol. 143, 32-39.

Love, C., Kolar, P., Classen, J., Das, L., 2011. Adsorption of ammonia on ozonated activated carbon, Trans. of the ASABE. 54, 1931-1940.

Ma, Z., Li, Q., Yue, Q., Gao, B., Li, W., Xu, X., Zhong, Q., 2011. Adsorption removal of ammonium and phosphate from water by fertilizer controlled release agent prepared from wheat straw, Chem. Eng. J. 171, 1209-1217.

Peng, Y., Zhu, G., 2006. Biological nitrogen removal with nitrification and denitrification via nitrite pathway, Appl. Microbiol. Biotechnol. 73, 15-26.

Randall, D., Tsui, T., 2002. Ammonia toxicity in fish, Mar. Pollut. Bull. 45, 17-23.

Rat-Valdambrini, M., Belkacemi, K., Hamoudi, S., 2012. Removal of ammonium cations from aqueous solution using arene-sulphonic acid functionalised SBA-15 as adsorbent, The Can. J. Chem. Eng. 90, 18-25.

Redlich, O., Peterson, D.L., 1959. A useful adsorption isotherm, J. Phys. Chem. 63, 1024-1024.

Rodrigues, L.A., da Silva, Maria Lucia Caetano Pinto, Alvarez-Mendes, M.O., dos Reis Coutinho, A., Thim, G.P., 2011. Phenol removal from aqueous solution by activated carbon produced from avocado kernel seeds, Chem. Eng. J. 174, 49-57.

Sharifnia, S., Khadivi, M.A., Shojaeimehr, T., Shavisi, Y., 2012. Characterization, isotherm and kinetic studies for ammonium ion adsorption by light expanded clay aggregate (LECA), J. Saudi Chem. Soc.

Shi, M., Wang, Z., Zheng, Z., 2013. Effect of Na impregnated activated carbon on the adsorption of NH 4-N from aqueous solution, J. of Environ. Sci. 25, 1501-1510.

Vassileva, P., Tzvetkova, P., Nickolov, R., 2009. Removal of ammonium ions from aqueous solutions with coal-based activated carbons modified by oxidation, Fuel. 88, 387-390.

Vassileva, P., Voikova, D., 2009. Investigation on natural and pretreated Bulgarian clinoptilolite for ammonium ions removal from aqueous solutions, J. Hazard. Mater. 170, 948-953.

Wahab, M.A., Jellali, S., Jedidi, N., 2010a. Ammonium biosorption onto sawdust: FTIR analysis, kinetics and adsorption isotherms modeling, Bioresour. Technol. 101, 5070-5075.

Wahab, M.A., Jellali, S., Jedidi, N., 2010b. Effect of temperature and pH on the biosorption of ammonium onto Posidonia oceanica fibers: equilibrium, and kinetic modeling studies, Bioresour. Technol. 101, 8606-8615.

Weber, W., Morris, J., 1963. Kinetics of adsorption on carbon from solution, J.Sanit.Eng.Div.Am.Soc.Civ.Eng. 89, 31-60.

Zhang, M., Zhang, H., Xu, D., Han, L., Niu, D., Zhang, L., Wu, W., Tian, B., 2011. Ammonium removal from aqueous solution by zeolites synthesized from low-calcium and high-calcium fly ashes, Desalination. 277, 46-53.

Zhao, Y., Yang, Y., Yang, S., Wang, Q., Feng, C., Zhang, Z., 2013. Adsorption of high ammonium nitrogen from wastewater using a novel ceramic adsorbent and the evaluation of the ammonium-adsorbed-ceramic as fertilizer, J. Colloid Interface Sci. 393, 264-270.

Zheng, Y., Wang, A., 2009. Evaluation of ammonium removal using a chitosan-g-poly (acrylic acid)/rectorite hydrogel composite, J. Hazard. Mater. 171, 671-677.

Zhu, Y., Kolar, P., 2014. Adsorptive removal of *p*-cresol using coconut shell-activated char, J. Environ. Chem. Eng. 2, 2050-2058.

CHAPTER 6

INVESTIGATION OF ADSORPTION OF *P*-CRESOL AND AMMONIA FROM AQUEOUS SOLUTION ON AVOCADO SEED-ACTIVATED CARBON

Yiying Zhu [a], Praveen Kolar [a*], Sanjay B. Shah [a], Jay J. Cheng [a], P.K. Lim [b]

[a] Department of Biological and Agricultural Engineering, Campus Box 7625, North Carolina State University, Raleigh, NC, 27695-7625, USA.

[b] Department of Chemical and Biomolecular Engineering, Campus Box 7905, North Carolina State University, Raleigh, NC, 27695-7905, USA.

E-mail addresses: yzhu15@ncsu.edu, pkolar@ncsu.edu

[*] Corresponding author contact information: 278 Weaver Labs, Campus Box 7625, North Carolina State University, Raleigh, NC, 27695-7625, USA.

Phone: +1 919 513 9797; Fax: +1 919 515 7760.

E-mail address: pkolar@ncsu.edu

Abstract

Avocado seed was used to prepare an activated carbon (AAC-MA) by physiochemical activation with methanesulfonic acid. Preliminary studies suggested that AAC-MA exhibited adsorptive properties for mitigation of ammonia and *p*-cresol. Hence, in this article, simultaneous adsorption of *p*-cresol and ammonia in a binary solute system was investigated at 25 ^{o}C with 3 g L^{-1} AAC-MA, agitated at 125 rpm and in the concentration range from 50 to 400 mg L^{-1}. The isotherms were investigated and extended Langmuir isotherm was found to be most suitable for the equilibrium data interpretation for adsorption of both *p*-cresol and ammonia on AAC-MA. The maximum adsorption capacities of *p*-cresol and ammonia in the double solute system on AAC-MA were found to be 87.79 and 3.393 mg g^{-1}, respectively. It can be deduced that the competition and interaction between *p*-cresol and ammonia for adsorption sites was negligible on AAC-MA. It is evident from this research that AAC-MA demonstrated good removal capacities for *p*-cresol and ammonia in both the single and double solute systems.

Key words

Methanesulfonic acid; Binary system; Simultaneous adsorption; Extended Langmuir isotherm; Kinetics

6.1 Introduction

In wastewater treatment, phenols are usually considered as one of the significant organic contaminants with high toxicity, carcinogenicity and environmental accumulation (Li et al., 2015; Mohd Din et al., 2009). They are extensively utilized in petroleum, chemicals, pharmaceuticals, plastics, and other industries and are detrimental to organisms even at low concentrations (Li et al., 2015). *p*-Cresol (4-methylphenol), as a malodorous volatile organic compound (VOC), is not only one of the most abundant phenolic compounds present in industrial effluents, but is also normally present in animal agriculture discharges (Das et al., 2013; Hadjar et al., 2011; Singh et al., 2008). *p*-Cresol can damage human kidney, liver, central nervous system as well as cardiovascular system, and will also react with NO_X and form atmospheric ozone to cause environmental and public health issues (CFR, 2008; Das et al., 2013; Singh et al., 2008).

Other than *p*-cresol, the industrial, agricultural and domestic wastewater pollution caused by ammonia has also posed a significant threat to the environment and public health. The presence of excess ammonia nitrogen in the receiving waters such as lakes and rivers has been blamed for eutrophication, excessive algae other microorganisms growth and increased dissolved oxygen depletion and fish toxicity (Huang et al., 2010). Ammonia nitrogen is the most frequently encountered nitrogenous species in wastewater and it will also give rise to nitrogen pollution resulting in corrosion and fouling (Boopathy et al., 2013; Jellali et al., 2011; Wahab et al., 2010). Animal agriculture, especially swine feeding operations, is also a major source for ammoniacal nitrogen pollution due to microbial decomposition of manure

and urine stored or treated in anaerobic lagoons, tanks, earthen basins, stockpiles and underground pits (Arogo et al., 2003). Ammonia in aqueous solution will impart unpleasant taste and the pungent smell of ammonia in the air can be smelt at minute concentrations in the atmosphere (Boopathy et al., 2013; Huang et al., 2008). Ammonia contributes to the formation of light-scattering aerosols as well as respirable aerosol particles that can impair visibility and respiration, and even can cause permanent injury or death under prolonged contact at a concentration higher than 300 ppm (Arogo et al., 2003; Huang et al., 2008).

In recognition of the adverse effects of *p*-cresol and ammonia, there is a need and an increasing interest to control and treat them before being released into the water bodies to protect aqueous ecosystem. The removal of pollutants by adsorption has been considered as a most versatile, simple and economical technology. Activated carbon is a widely employed adsorbent because of its microporosity, efficiency, special chemical nature, large surface area, large adsorption capacity and low operation cost (Bhatnagar et al., 2013; Mohd Din et al., 2009).

At present, several kinds of novel adsorbents have been successfully synthesized to mitigate *p*-cresol (Das et al., 2013; Hadjar et al., 2011; Singh et al., 2008; Zhu and Kolar, 2014) and ammonia (Boopathy et al., 2013; Huang et al., 2010; Jellali et al., 2011; Zhao et al., 2013), respectively. Nevertheless, to the best of our knowledge, there is no scientific literature has been reported in regard to successful simultaneous adsorption of *p*-cresol and ammonia, which are frequently exist together in wastewater. Multi-component adsorption bring about more complexity than single-component adsorption due to possible interactions

and competition between adsorbates and adsorbent and it involves more parameters that complicate adsorption (Noroozi et al., 2008). Another challenge facing simultaneous adsorption of *p*-cresol and ammonia using an activated carbon is that these two adsorbates are different in nature. Weakly acidic *p*-cresol is preferred for adsorption by activated carbon with basic functional groups (Ahmaruzzaman, 2008; Dąbrowski et al., 2005) while the polar alkaline ammonia is favored by an adsorbent with acidic property (Le Leuch and Bandosz, 2007; Vassileva et al., 2009). In this regard, a suitable activated carbon for uptake of *p*-cresol and ammonia simultaneously should have bi-functional characteristics of both acidic and basic features.

Avocado seeds have not received considerable attention as a raw material for activated carbon although there are substantial amounts of this biomass arising from human consumption or food-processing plants (Rodrigues et al., 2011). Therefore, more studies using the avocado seed-activated carbon (AAC) as an adsorbent are needed.

In our previous research, an avocado seed-activated carbon impregnated with methanesulfonic acid was synthesized (AAC-MA) and showed quite good adsorption behavior for ammonia. In the present research, the AAC-MA was further investigated for its ability to remove *p*-cresol from aqueous solution. Then, experiments were carried out to study the applicability of AAC-MA serving as a bi-functional adsorbent to simultaneously remove *p*-cresol and ammonia. The simultaneous adsorption isotherms for *p*-cresol and ammonia removal were thereafter studied.

6.2 Materials and methods

6.2.1 Preparation of AAC-MA

The preparation method for AAC-MA was described in Chapter 5. Briefly, avocado seeds were procured locally. Before use, avocado seeds were washed with deionized water, dried at 50 ^{o}C and then cut into small pieces. The seeds were impregnated with 70 wt.% methanesulfonic acid (Acros Organics) with weight ratio of acid to seeds of 0.8 for 17 h. After removing the supernatant, the charcoal was dried at 95 ^{o}C and then carbonized at 700 ^{o}C for 1.5 h in a kiln under a nitrogen flow. Finally, the obtained sample was repeatedly washed with deionized water and dried in the over at 75 ^{o}C overnight to produce the final activated carbon of AAC-MA. The AAC-MA was stored in an air-tight bottle for later experimental use.

6.2.2 Batch adsorption experiments

Single solute *p*-cresol adsorption experiments were performed in 150 mL serum bottles by contacting 100 mL 50-400 mg L^{-1} *p*-cresol solutions with 0.3 g AAC-MA as an adsorbent agitated at 125 rpm and 25 ^{o}C for 1 week to ensure achievement of equilibrium. Similarly, simultaneous batch adsorption experiments were carried out by mixing 100 mL of solutions containing 50-400 mg L^{-1} of *p*-cresol and 50-400 mg L^{-1} of ammonium chloride with 0.3 g AAC-MA as adsorbent agitated at 125 rpm and maintained at 25 ^{o}C for 1 week to ensure that equilibrium had been achieved. Aliquots of the solution samples were withdrawn at predetermined intervals and analyzed for residual *p*-cresol concentrations at 277 nm with a

UV spectrometer (Genesys 10S, Thermo Scientific) and ammonia concentrations using the automated phenate method (APHA-AWWA-WPCF., 1981). All the experiments were conducted in duplicate under identical conditions and the obtained mean values were used for analysis. The adsorption amount of *p*-cresol and ammonia per unit mass of the adsorbent at time t, respectively, q_t (mg g^{-1}), and the removal percentage, X (%), were calculated by:

$$q_t = \frac{(C_o - C_t)V}{W} \tag{6-1}$$

$$X\,(\%) = \frac{C_o - C_t}{C_o} \times 100 \tag{6-2}$$

where C_o (mg L^{-1}) and C_t (mg L^{-1})are the liquid-phase concentrations of *p*-cresol and ammonia at the initial time and at time t, respectively. V (L) is the volume of the aqueous solution and W (g) is the dry mass of AAC-MA used.

6.2.3 Kinetic studies of p-cresol adsorption onto AAC-MA

Adsorption kinetic studies of adsorption of *p*-cresol onto AAC-MA were carried out using different initial *p*-cresol concentrations of 50, 150, 200, and 400 mg L^{-1} at timed intervals with 3 g L^{-1} of AAC-MA at 125 rpm and 25 ^{o}C. Experiments were replicated twice under identical experimental conditions.

The experimental data were fitted with the pseudo-first-order (Eq. (6-3) (Lagergren, 1898), pseudo-second-order (Eq. (6-4) (Ho and McKay, 1998), Elovich (Eq. (6-5) (Chien and Clayton, 1980) and Avrami (Eq. (6-6) (Lopes et al., 2003) kinetics models, as listed below:

$$q_t = q_e[1 - e^{-k_1 t}] \quad (6\text{-}3)$$

$$q_t = \frac{k_2 q_e^2 t}{1 + k_2 q_e t} \quad (6\text{-}4)$$

$$q_t = \frac{1}{\beta}\ln(\alpha\beta) + \frac{1}{\beta}\ln(t) \quad (6\text{-}5)$$

$$q_t = q_e\left[1 - e^{(-k_{AV}t)^{n_{AV}}}\right] \quad (6\text{-}6)$$

where q_t (mg g^{-1}), q_e (mg g^{-1}) are the amount of *p*-cresol adsorbed on AAC-MA at time t (h) and at equilibrium. k_1(h^{-1}) and k_2(g $mg^{-1}h^{-1}$) are rate constants of pseudo-first-order and pseudo-second-order adsorption, respectively. α ($mg\ g^{-1}h^{-1}$) and β ($g\ mg^{-1}$) are Elovich constants related to the initial adsorption rate and desorption constant, respectively. k_{AV}(h^{-1}) and n_{AV} are Avrami constants.

6.2.4 Mechanism study of p-cresol adsorption onto AAC-MA

To determine the mechanism and rate limiting step of the adsorption process, an intraparticle diffusion model introduced by Weber and Morris (Weber and Morris, 1963) was used to analyze the experimental data as expressed below:

$$q_t = K_{id} t^{0.5} + C \quad (6\text{-}7)$$

where k_{id}(mg $g^{-1}h^{-0.5}$) represents the intraparticle diffusion constant. From the elucidation of this abovementioned model, the plot of q_t against $t^{1/2}$, should be linear if diffusion plays a role in the adsorption rate and the intercept is zero if intraparticle diffusion is the only rate limiting step (Dural et al., 2011). If the line does not pass through the origin, it shows that other kinetic models may be functioning simultaneously (Ma et al., 2011). Similarly, when

multi-linearity is observed, it is indicative of the involvement of different mechanisms with different rate constants in adsorption (Dural et al., 2011).

6.2.5 Adsorption equilibrium studies of p-cresol adsorption on AAC-MA

Adsorption isotherm studies were performed with seven different initial *p*-cresol concentrations of 50, 80, 150, 200, 300, 350 and 400 mg L^{-1} with a fixed AAC-MA dose of 3 g L^{-1} at 25 ^{o}C and agitated separated at 125 rpm. After equilibrium was achieved in 1 week, samples were withdrawn from the serum bottles and the residual concentrations of the *p*-cresol were determined. The adsorption experiments were run in duplicate. Adsorption isotherm of the uptake of *p*-cresol onto AAC-MA was determined by correlating the equilibrium data with Langmuir (Eq. (6-8)) (Langmuir, 1916), Freundlich (Eq. (6-9)) (Freundlich, 1906) and Redlich-Peterson (Eq. (6-10)) (Redlich and Peterson, 1959) isotherm models.

$$q_e = \frac{Q_0 K_L C_e}{1 + K_L C_e} \tag{6-8}$$

$$q_e = K_F \, C_e^{\,1/n} \tag{6-9}$$

$$q_e = \frac{A C_e}{1 + B C_e^{\beta}} \tag{6-10}$$

where q_e (mg g^{-1}) is the amount of adsorbate adsorbed onto unit weight of adsorbent at equilibrium. C_e (mg L^{-1}) is the liquid-phase concentration of adsorbate at equilibrium. Q_o(mg g^{-1}) and K_L(L mg^{-1}) are Langmuir constants in relation to the maximum monolayer adsorption capacity and adsorption energy. K_F (mg g^{-1}(L mg^{-1})$^{1/n}$) and $1/n$ are the

Freundlich constant and the dimensionless heterogeneity factor giving an indication of the adsorption intensity, respectively. $A(\mathrm{L\,g^{-1}})$ and $B(\mathrm{L\,mg^{-1}})$ are Redlich-Peterson isotherm constants while β is the isotherm exponent ranging between 0 and 1.

6.2.6 Adsorption equilibrium studies of simultaneous p-cresol and ammonia adsorption on AAC-MA in p-cresol + ammonia binary systems

In the *p*-cresol + ammonia binary adsorption systems, AAC-MA was used for simultaneous uptake of *p*-cresol and ammonia. Predetermined masses of 0.3 g AAC-MA was added to 150 mL serum bottles of 100 mL solutions containing 50, 150, 200, 300 and 400 mg L^{-1} equal mass concentrations of *p*-cresol and ammonium chloride at 125 rpm and 25 ^{o}C for 1 week to ensure equilibrium. The obtained equilibrium isotherm data of *p*-cresol and ammonia were correlated to different isotherm models including above-mentioned Langmuir (Eq. (6-8)) (Langmuir, 1916), Freundlich (Eq. (6-9)) (Freundlich, 1906), Redlich-Perterson (Eq. (6-10)) (Redlich and Peterson, 1959) and also extended Langmuir isotherm model (Eq. (6-11)) (Choy et al., 2000; Nouri et al., 2002) to attempt to predict the bi-components sorption systems.

$$q_{e,i} = \frac{K_i C_{e,i}}{1 + \sum a_{L,i} C_{e,i}} \tag{6-11}$$

where $q_{e,i}$ $(\mathrm{mg\,g^{-1}})$ is the amount of *p*-cresol or ammonia adsorbed onto unit weight of adsorbent at equilibrium in the *p*-cresol + ammonia binary system. $C_{e,i}$ $(\mathrm{mg\,L^{-1}})$ is the liquid-phase concentration of *p*-cresol or ammonia at equilibrium. K_i $(\mathrm{L\,g^{-1}})$ and $a_{L,i}$ $(\mathrm{L\,mg^{-1}})$ are Langmuir isotherm constants.

6.3 Results and discussion

6.3.1 Effects of contact time and initial concentration on p-cresol adsorption for single component removal

The results of *p*-cresol adsorption onto AAC-MA along with time at different *p*-cresol concentrations were depicted in Fig. 6.1(a). The maximum adsorption of *p*-cresol by AAC-MA at different concentrations studied were attained within 1 week. The adsorption process usually included three stages, of which *p*-cresol molecules first were transported to the outside of the adsorbent particle from external boundary layer film through mass transfer, and then they diffused from the internal boundary layer film onto the adsorbent surface and eventually the adsorbate molecules diffused to active sites for adsorption either by a pore diffusion via the liquid filled pores or by solid surface diffusion (Cheung et al., 2007; El Nemr et al., 2009). To achieve equilibrium, it could take long contact time especially considering that intraparticle diffusion is in a relatively slow manner since it occurs inside the activated carbon matrix (Mohd Din et al., 2009).

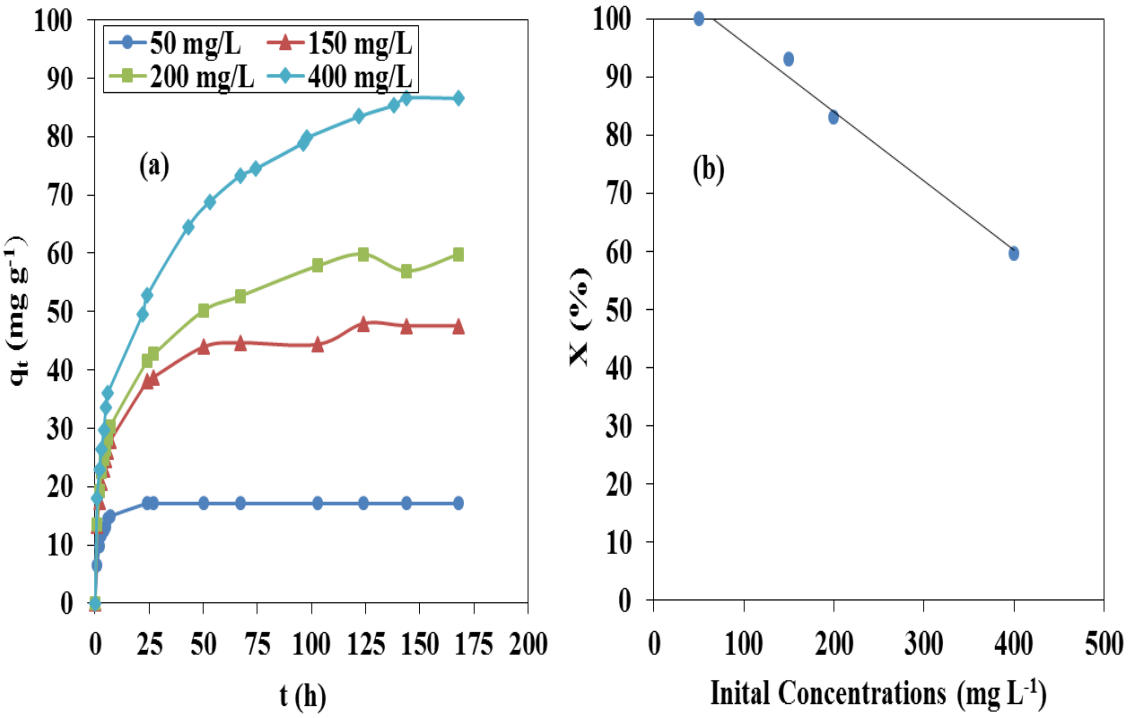

Fig. 6.1: (a) Adsorption profile of *p*-cresol at different initial *p*-cresol concentrations using AAC-MA (3 g L^{-1}); (b) *p*-cresol removal profile using AAC-MA (3 g L^{-1}).

As is evident from Fig. 6.1(a), for all initial *p*-cresol concentrations in this research, the *p*-cresol adsorption was rapid in the initial process due to the availability of large surface area of the adsorbent but it gradually slowed down with time until it reached equilibrium probably due to the hindrance or repulsion between charged adsorbates, the reduced availability of the adsorbate species as well as active sites, and slow diffusion from the exterior of the adsorbent to the interior sites. Similar findings were also reported by Sathishkumar et al. (2012) and El Nemr et al. (2009) for uptake of dyes.

It is also noticed in Fig. 6.1(a) that the amount adsorbed onto AAC-MA at a higher initial *p*-cresol concentration was larger than the corresponding amount when lower initial concentrations were used. Similar phenomenon was also observed by Mohd Din et al. (2009) on a coconut shell-activated carbon (CS850A) for removal of phenol, and it was explained that there was greater mass driving force at higher concentration and it allowed more adsorbate molecules to pass through the boundary layer to the adsorbent surface. With increasing initial *p*-cresol concentrations ranging from 50 mg L^{-1} to 400 mg L^{-1}, the adsorption capacity for *p*-cresol on AAC-MA increased from 17.12 to 86.57 mg g^{-1} in this study. However, as shown in Fig. 6.1(b), *p*-cresol removal percentage decreased from 100% to 59.6% as initial *p*-cresol concentration was increased from 50 mg L^{-1} to 400 mg L^{-1}. This trend was consistent with uptake of phenol on CS850A (Mohd Din et al., 2009), and copper on sawdust (Yu et al., 2000). Availability of the adsorptive sites on AAC-MA for uptake of *p*-cresol perhaps accounted for this phenomenon (Yu et al., 2000).

6.3.2 Single solute kinetic studies of p-cresol adsorption onto AAC-MA

The results of pseudo-first-order, pseudo-second-order, Elovich, and Avrami kinetic models fitted to the experimental adsorption data were tabulated in Table 6.1. The pseudo-second-order kinetic model was selected as the best-fit model as it has a high correlation coefficient R^2 (> 95%) for all concentrations, and the calculated q_e values from this model are closer to the experimental q_e values than other models. From Fig. 6.2, it is apparent that the experimental data displayed good compliance with the pseudo-second-order kinetic

model. Additionally, it is indicative of occurrence of the chemisorption in the adsorption process being a rate-controlling step (Mohd Din et al., 2009; Wahab et al., 2010).

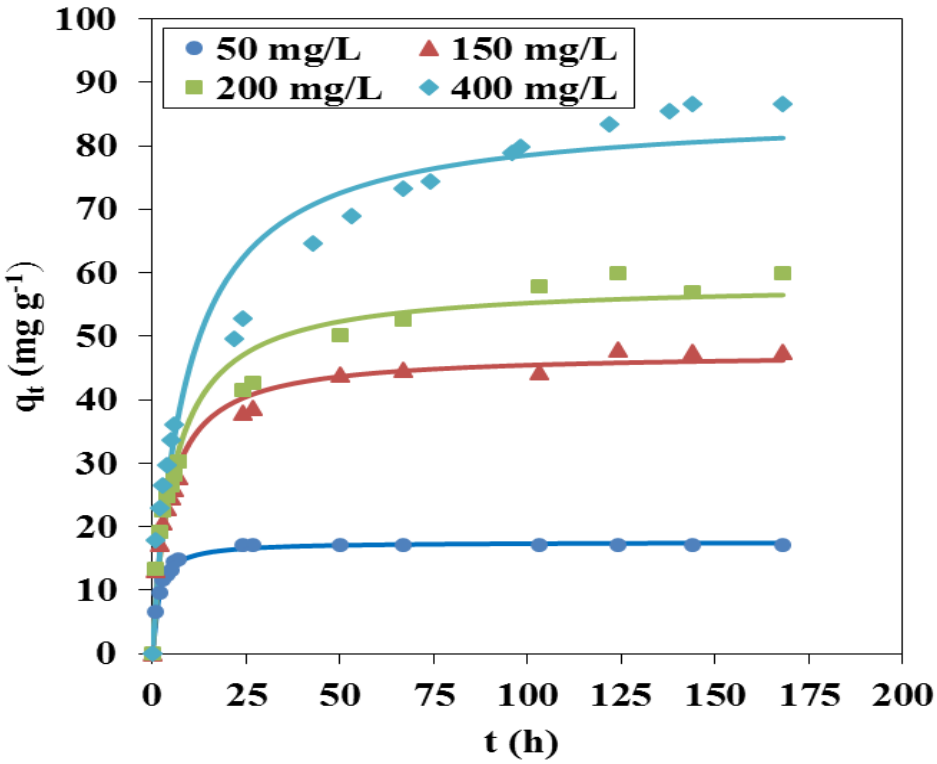

Fig. 6.2: Pseudo-second-order kinetic plot for the adsorption of *p*-cresol onto AAC-MA (3 g L^{-1}).

Table 6.1: Kinetic parameters for adsorption of *p*-cresol onto AAC-MA at different concentrations

Kinetic models	Initial *p*-cresol concentration (mg L^{-1})			
	50	150	200	400
Experimental qe (mg g^{-1})	17.115	47.578	59.868	86.565
Pseudo-first-order model				
Calculated q_e (mg g^{-1})	16.94	44.16	53.37	77.21
k_1 (h^{-1})	0.3666	0.1739	0.1391	0.08389
R^2 (%)	98.51	94.44	91.64	89.71
Pseudo-second –order model				
Calculated $q_{e,}$ (mg g^{-1})	17.62	47.4	58.48	85.58
k_2 (g mg^{-1} h^{-1})	0.03633	0.004928	0.002911	0.0013
R^2 (%)	99.53	98.41	97	95.75
Elovich model				
α (mg g^{-1} h^{-1})	470.1	47.46	34.02	31.57
β (g mg^{-1})	0.5763	0.1407	0.1054	0.06843
R^2 (%)	80.63	98.63	99.47	98.58
Avrami model				
qe (mg g^{-1})	16.94	44.16	53.37	77.21
k_{AV} (h^{-1})	1.809	0.5629	0.1611	0.09494
n_{AV}	0.2027	0.3089	0.8628	0.8835
R^2 (%)	98.29	94.44	91.64	89.71

6.3.3 Single solute mechanism study of p-cresol adsorption onto AAC-MA

The intraparticle diffusion model was employed to fit the experimental data of *p*-cresol removal and the analysis results are summarized in Table 6.2. The adsorbed amount of *p*-cresol (q_t) versus the square root of time ($t^{1/2}$) are plotted in Fig. 6.3. There are three linear segments in the plots for all concentrations suggesting three different steps (Shi et al., 2013). The initial linear part indicates the initial phase of external adsorption or instantaneous adsorption in which the adsorbate molecules were transferred to the external surface of adsorbent via film diffusion. The subsequent intermediate linear part represents the gradual adsorption stage, where the intraparticle diffusion is a rate-determining step. The final plateau describes the equilibrium of the adsorption. The linearity of the multi-linear plots in Fig. 6.3 reflects that intraparticle diffusion plays an important role in removing *p*-cresol by AAC-MA (El Nemr et al., 2009). Moreover, the second and third linear segments did not pass though the origin, implying that the intraparticle diffusion was not the only mechanism governing the whole adsorption process, and probably surface adsorption concurrently occurred (El Nemr et al., 2009; Martins et al., 2015)

Table 6.2: Parameters for intraparticle diffusion of *p*-cresol onto AAC-MA at different initial concentrations

Parameters	Initial *p*-cresol concentration (mg L^{-1})			
	50	150	200	400
$K_{id,1}$ (mg g^{-1} $h^{-0.5}$)	5.9063	10.315	11.285	14.426
$C_{i,1}$ (mg g^{-1})	0.5743	1.6949	1.597	1.5033
R^2 (%)	98.42	98.34	98.46	99.06
$K_{id,2}$ (mg g^{-1} $h^{-0.5}$)	1.0327	1.394	2.9583	4.812
$C_{i,2}$ (mg g^{-1})	12.067	32.128	27.799	31.09
R^2 (%)	99.15	86.36	98.57	96.5

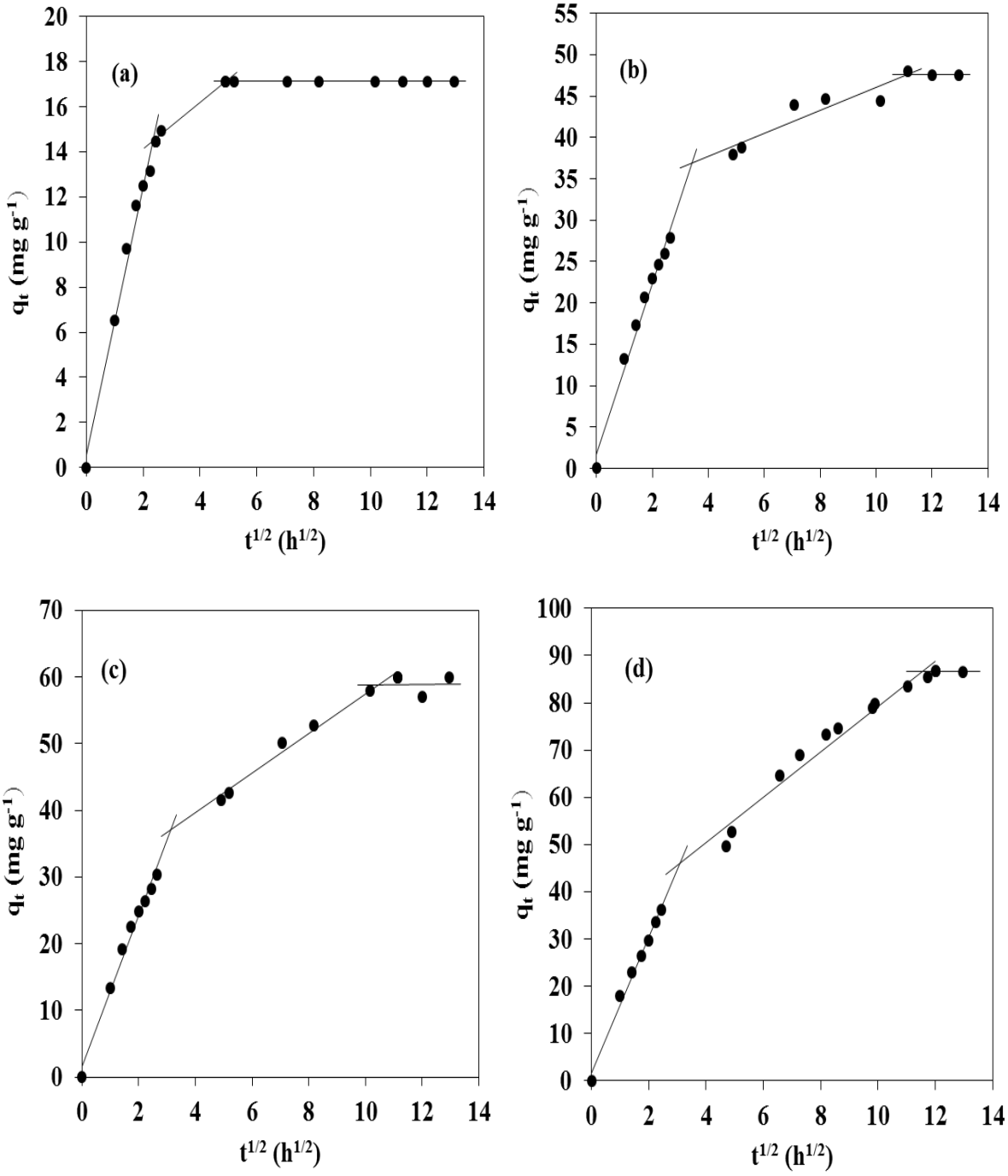

Fig. 6.3: Intraparticle diffusion model plots for adsorption of *p*-cresol onto AAC-MA (3 g L^{-1}) at different initial *p*-cresol concentration: (a) 50 ppm, (b) 150 ppm, (c) 200 ppm, (d) 400 ppm.

6.3.4 Single solute adsorption isotherm studies of p-cresol adsorption onto AAC-MA

Fig. 6.4 presents the comparative fits of Langmuir, Freundlich and Redlich-Peterson isotherm models with the equilibrium data for *p*-cresol adsorption on AAC-MA and Table 6.3 listed the fitted results and correlation coefficients were determined to judge the applicability of the isotherms equations. The highest correlation coefficient value (R^2) of 92.55% was achieved for Redlich-Peterson model in Table 6.3; this was also reflected in Fig. 6.4 where Redlich-Peterson isotherm yielded the best fit to the experimental data suggesting that the Redlich-Peterson model can best described the equilibrium data. The maximum monolayer adsorption capacity Q_0 for *p*-cresol by AAC-MA was determined to be 88.03 mg g^{-1} from Langmuir isotherm model which reveals that AAC-MA has a strong affinity towards *p*-cresol. The data for *p*-cresol adsorption suggests that AAC-MA is not only able for ammonia taken up from our previous research (Chapter 5), but is also applicable for *p*-cresol uptake. The dimensionless factor (R_L), calculated from $R_L = \frac{1}{1+K_L C_0}$, was between 0.0229 to 0.1577, indicating that the adsorption of *p*-cresol is favorable on AAC-MA since the R_L values were in the range of 0 to 1 (Singh et al., 2008). Additionally, the Freundlich's parameter (1/n) was determined to be 0.2582, which is less than the unity, suggesting favorable adsorption conditions (Huang et al., 2010; Shi et al., 2013).

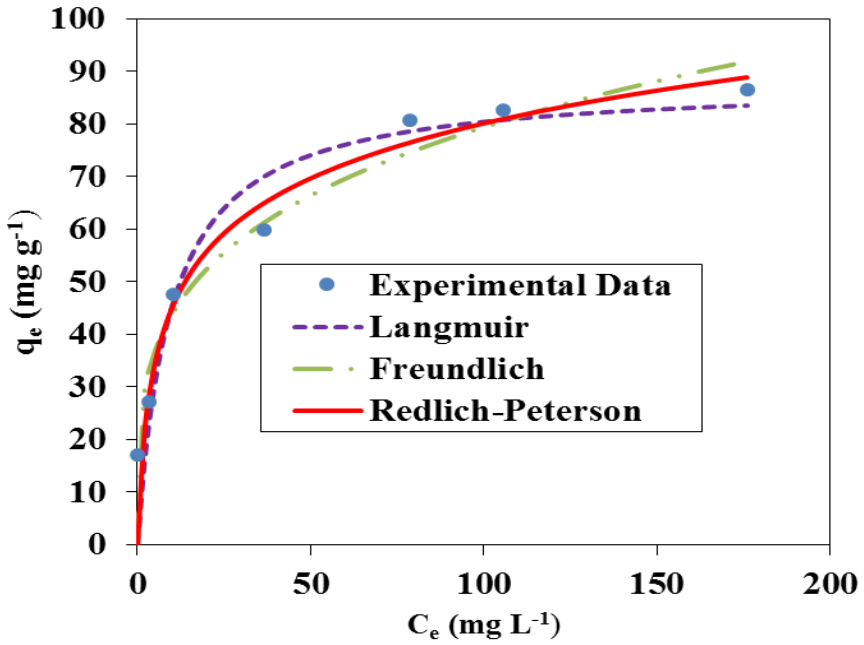

Fig. 6.4: Adsorption isotherm models for *p*-cresol adsorption on AAC-MA in single solute systems at 25 °C.

Table 6.3: Isotherm parameters for adsorption of *p*-cresol on AAC-MA

Isotherm models	Parameters
Langmuir $q_e = \frac{Q_O K_L C_e}{1 + K_L C_e}$	Q_0 = 88.03 mg g^{-1} K_L= 0.1068 L mg^{-1} R^2 = 90.63%
Freundlich $q_e = K_F\, C_e^{\,1/n}$	K_F = 24.2 mg g^{-1} (L mg^{-1})$^{1/n}$ $1/n$ = 0.2582 R^2 = 91.35%
Redlich-Peterson $q_e = \frac{AC_e}{1 + BC_e^{\beta}}$	A = 19.92 L g^{-1} B = 0.49 L mg^{-1} β = 0.8438 R^2 = 92.55%

6.3.5 Equilibrium studies of p-cresol and ammonia adsorption in binary solute systems

Equilibrium studies were carried out to determine the adsorption behavior of the simultaneous adsorption to analyze and design the adsorption systems. The characteristic parameters for different isotherms employed to fit the equilibrium data of adsorption of *p*-cresol and ammonia in the *p*-cresol + ammonia binary solute system were tabulated in Table 6.4.

Table 6.4: Results of different isotherm equations applied to the adsorption of *p*-cresol and ammonia on AAC-MA in double solute system

	p-Cresol adsorption	Ammonia adsorption
Isotherm models	Parameters	Parameters
Langmuir $q_e = \frac{Q_O K C_e}{1 + K C_e}$	Q_0 = 87.79 mg g^{-1} K_L= 0.05131 L mg^{-1} R^2 = 89.26 %	Q_0 = 3.393 mg g^{-1} K_L= 0.01074 L mg^{-1} R^2 = 93.14%
Freundlich $q_e = K_F\ C_e{}^{1/n}$	K_F = 23.87 mg g^{-1} (L mg^{-1})$^{1/n}$ $1/n$ = 0.2351 R^2 =87.84 %	K_F = 0.3156 mg g^{-1} (L mg^{-1})$^{1/n}$ $1/n$ = 0.3671 R^2 = 81.82%
Redlich-Peterson $q_e = \frac{A C_e}{1 + B C_e^{\beta}}$	A = 4.504 L g^{-1} B = 0.05131 L mg^{-1} β = 1 R^2 = 89.26%	A = 0.03643 L g^{-1} B = 0.01074 L mg^{-1} β = 1 R^2 = 93.14%
Extended Langmuir $q_{e,i} = \frac{K_i C_{e,i}}{1 + \sum a_{L,i} C_{e,i}}$	K = 4.5472 L g^{-1} $a_{L,p-cresol}$ = 0.05185L mg^{-1} $a_{L,ammonium}$ = 2.328×(10^{-6}) L mg^{-1} R^2 = 89.26%	K = 0.0234 L g^{-1} $a_{L,ammonium}$ = 0.008475 L mg^{-1} $a_{L,ammonium}$ = 0.002663 L mg^{-1} R^2 = 98.59%

The correlation coefficient values (R^2) showed that the *p*-cresol isotherm followed the Langmuir, Redlich-Peterson and extended Langmuir isotherms while ammonia adsorption data were correlated reasonably well with the extended Langmuir isotherm models in the binary systems. The three parameter Redlich-Peterson isotherm model was reduced to the two parameter Langmuir equation for *p*-cresol adsorption since β is 1 (Dąbrowski et al., 2005; Singh et al., 2008). The Langmuir and extended Langmuir isotherm models giving the best data correlation implies the homogeneous surface and equally available adsorption sites of AAC-MA for adsorption of *p*-cresol and ammonia (Choy et al., 2000). Furthermore, the extended Langmuir isotherm was suitable for describing adsorption of both *p*-cresol and ammonia suggesting that the interaction and competition between these two species for adsorption sites were negligible during simultaneous adsorption (Choy et al., 2000), which was probably attributed to the presence of both acidic and basic functional groups on AAC-MA for high adsorption capacity. Additionally, it can be presumed that the interaction between the adsorbed species of *p*-cresol and ammonia was insignificant and the adsorption sites had equal energy and were constant on the homogeneous carbon surface (Choy et al., 2000).

The maximum monolayer adsorption capacities were 87.79 and 3.393 mg g^{-1} for *p*-cresol and ammonia in the binary mixtures systems, respectively. Fig. 6.5 displays the equilibrium experimental data and fitted adsorption isotherm curves for both *p*-cresol and ammonia in the double solute systems. The comparisons of adsorption isotherm curves of *p*-cresol and ammonia adsorption between single and double solute systems are presented in

Fig. 6.6. It appeared that the adsorption capacity for both *p*-cresol and ammonia in single solute is slightly higher than that in double solute adsorption, which agrees with the reduced *p*-nitrophenol (PNP) uptake amount on a commercial activated carbon (GAC) in presence of *p*-cresol (PC) reported by Nouri probably (Nouri et al., 2002).

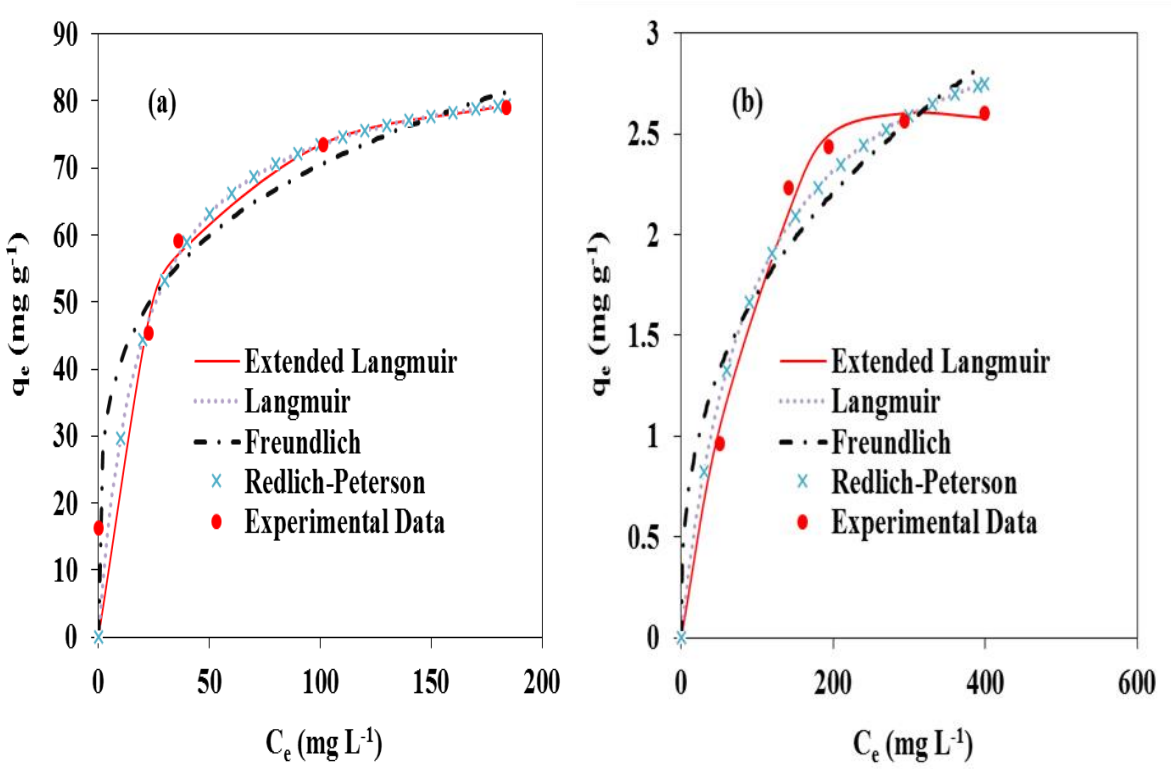

Fig. 6.5: Langmuir, Freundlich, Redlich-Peterson and extended Langmuir analyses for adsorption in the binary systems at 25 ^{o}C on 3 g L^{-1} AAC-MA: (a) *p*-cresol adsorption, (b) ammonia adsorption.

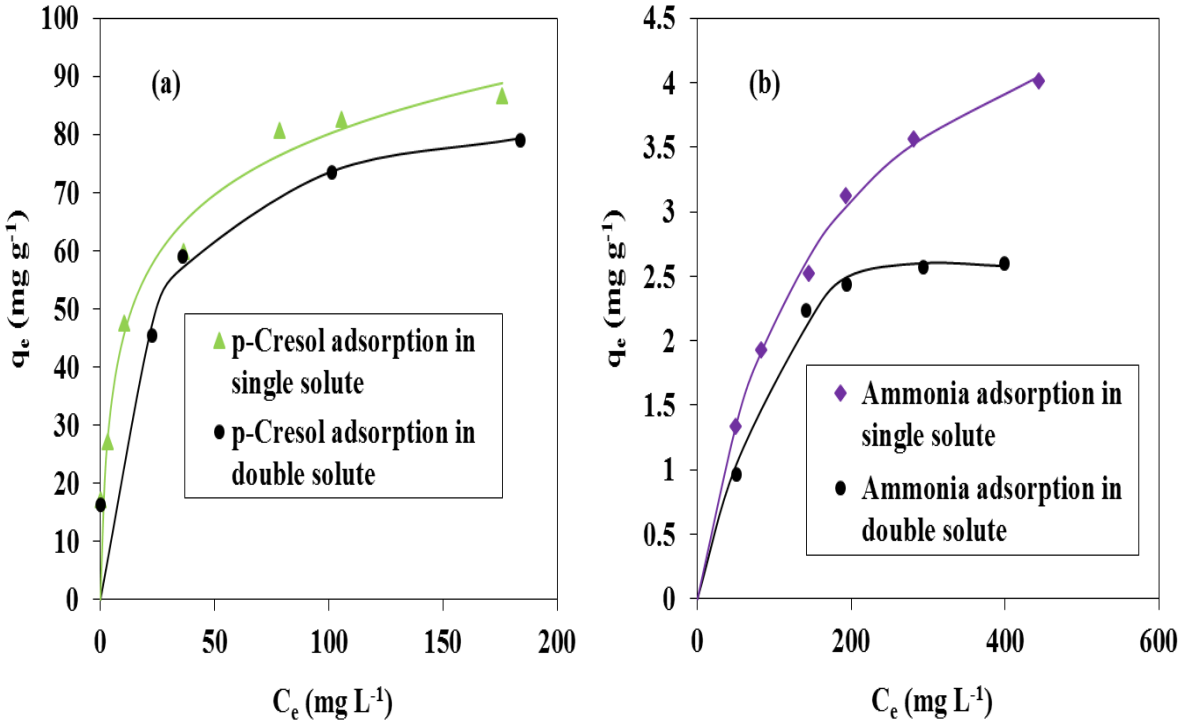

Fig. 6.6: Comparison of adsorption capacity for (a) *p*-cresol and (b) ammonia adsorption on AAC-MA in single and double solute system.

6.4 Conclusions

Activated carbon produced from avocado seeds and activated by methanesulfonic acid was tested in this study for *p*-cresol adsorption in a single-component system as well as simultaneous uptake of *p*-cresol and ammonia in a binary sorption system. In *p*-cresol adsorption from the single system, a pseudo-second kinetic model was found to best describe the kinetic data which also shows that the adsorption occurred mainly by chemisorption. In

addition, it was found that the isotherm data were best represented by the Redlich-Peterson isotherm model in the single solute system. In the binary system, Langmuir, Freundlich, Redlich-Peterson and extended Langmuir isotherms were employed to analyze the equilibrium data. When compared to different models studied, the extended Langmuir equation was found to establish a best correlation for the equilibrium curve for both *p*-cresol and ammonia. Additionally, the competition and interaction between these two species for active sites are insignificant for simultaneous adsorption of *p*-cresol and ammonia onto AAC-MA. Results showed in this research that *p*-cresol and ammonia can be effectively adsorbed from not only a single solute but also a double solute adsorption system by AAC-MA.

REFERENCES

Ahmaruzzaman, M., 2008. Adsorption of phenolic compounds on low-cost adsorbents: A review, Adv. Colloid Interface Sci. 143, 48-67. doi: 10.1016/j.cis.2008.07.002.

APHA-AWWA-WPCF., 1981. Standard Methods for the Examination of Water and Wastewater. APHA Am. Public Health Assoc.

Arogo, J., Westerman, P., Heber, A., 2003. A review of ammonia emissions from confined swine feeding operations, Trans. ASAE 46, 805-817.

Bhatnagar, A., Hogland, W., Marques, M., Sillanpää, M., 2013. An overview of the modification methods of activated carbon for its water treatment applications, Chem. Eng. J. 219, 499-511.

Boopathy, R., Karthikeyan, S., Mandal, A.B., Sekaran, G., 2013. Adsorption of ammonium ion by coconut shell-activated carbon from aqueous solution: kinetic, isotherm, and thermodynamic studies, Environ. Sci. Pollut. Res. 20, 533-542.

Cheung, W., Szeto, Y., McKay, G., 2007. Intraparticle diffusion processes during acid dye adsorption onto chitosan, Bioresour. Technol. 98, 2897-2904.

Chien, S., Clayton, W., 1980. Application of Elovich equation to the kinetics of phosphate release and sorption in soils, Soil Sci. Soc. Am. J. 44, 265-268.

Choy, K.K., Porter, J.F., McKay, G., 2000. Langmuir isotherm models applied to the multicomponent sorption of acid dyes from effluent onto activated carbon, J. Chem. Eng. Data 45, 575-584.

Code of federal regulations (CFR), 2008. National primary and secondary ambient air quality standards. 40CFR, Part 50. Office of the federal register, national archives, and records administration. Washington D.C: U.S. Government Printing Office.

Dąbrowski, A., Podkościelny, P., Hubicki, Z., Barczak, M., 2005. Adsorption of phenolic compounds by activated carbon—a critical review, Chemosphere 58, 1049-1070. doi: 10.1016/j.chemosphere.2004.09.067.

Das, L., Kolar, P., Classen, J.J., Osborne, J.A., 2013. Adsorbents from pine wood via K2CO3-assisted low temperature carbonization for adsorption of *p*-cresol, Ind. Crops Prod. 45, 215-222. doi: http://dx.doi.org/10.1016/j.indcrop.2012.12.010.

Dural, M.U., Cavas, L., Papageorgiou, S.K., Katsaros, F.K., 2011. Methylene blue adsorption on activated carbon prepared from Posidonia oceanica (L.) dead leaves: Kinetics and equilibrium studies, Chem. Eng. J. 168, 77-85.

El Nemr, A., Abdelwahab, O., El-Sikaily, A., Khaled, A., 2009. Removal of direct blue-86 from aqueous solution by new activated carbon developed from orange peel, J. Hazard. Mater. 161, 102-110.

Freundlich, H., 1906. Over the adsorption in solution, J. Phys. Chem. 57, 385-470.

Hadjar, H., Hamdi, B., Ania, C.O., 2011. Adsorption of *p*-cresol on novel diatomite/carbon composites, J. Hazard. Mater. 188, 304-310. doi: 10.1016/j.jhazmat.2011.01.108.

Ho, Y., McKay, G., 1998. Sorption of dye from aqueous solution by peat, Chem. Eng. J. 70, 115-124.

Huang, C., Li, H., Chen, C., 2008. Effect of surface acidic oxides of activated carbon on adsorption of ammonia, J. Hazard. Mater. 159, 523-527.

Huang, H., Xiao, X., Yan, B., Yang, L., 2010. Ammonium removal from aqueous solutions by using natural Chinese (Chende) zeolite as adsorbent, J. Hazard. Mater. 175, 247-252.

Jellali, S., Wahab, M.A., Anane, M., Riahi, K., Jedidi, N., 2011. Biosorption characteristics of ammonium from aqueous solutions onto Posidonia oceanica (L.) fibers, Desalination 270, 40-49.

Lagergren, S., 1898. About the theory of so-called adsorption of soluble substances. K. Sven. Vetenskapsakad. Handl. 24(4), 1-39.

Langmuir, I., 1916. The constitution and fundamental properties of solids and liquids. Part I. Solids. J. Am. Chem. Soc. 38, 2221-2295.

Le Leuch, L.M., Bandosz, T.J., 2007. The role of water and surface acidity on the reactive adsorption of ammonia on modified activated carbons, Carbon 45, 568-578. doi: 10.1016/j.carbon.2006.10.016.

Li, Y., Bi, H., Shi, X., 2015. Simultaneous Adsorption of Heavy Metal and Organic Pollutant onto Citrate-Modified Layered Double Hydroxides with Dodecylbenzenesulfonate, Environ. Eng. Sci. 32, 666-675.

Lopes, E.C., dos Anjos, F.S., Vieira, E.F., Cestari, A.R., 2003. An alternative Avrami equation to evaluate kinetic parameters of the interaction of Hg (II) with thin chitosan membranes, J. Colloid Interface Sci. 263, 542-547.

Ma, Z., Li, Q., Yue, Q., Gao, B., Li, W., Xu, X., Zhong, Q., 2011. Adsorption removal of ammonium and phosphate from water by fertilizer controlled release agent prepared from wheat straw, Chem. Eng. J. 171, 1209-1217.

Martins, A.C., Pezoti, O., Cazetta, A.L., Bedin, K.C., Yamazaki, D.A., Bandoch, G.F., Asefa, T., Visentainer, J.V., Almeida, V.C., 2015. Removal of tetracycline by NaOH-activated carbon produced from macadamia nut shells: Kinetic and equilibrium studies, Chem. Eng. J. 260, 291-299.

Mohd Din, A., Hameed, B., Ahmad, A., 2009. Batch adsorption of phenol onto physiochemical-activated coconut shell, J. Hazard. Mater. 161, 1522-1529.

Noroozi, B., Sorial, G.A., Bahrami, H., Arami, M., 2008. Adsorption of binary mixtures of cationic dyes, Dyes Pigments 76, 784-791. doi: http://dx.doi.org.prox.lib.ncsu.edu/10.1016/j.dyepig.2007.02.003.

Nouri, S., Haghseresht, F., Lu, G.M., 2002. Comparison of adsorption capacity of *p*-cresol & p-nitrophenol by activated carbon in single and double solute, Adsorption 8, 215-223.

Redlich, O., Peterson, D.L., 1959. A useful adsorption isotherm, J. Phys. Chem. 63, 1024-1024.

Rodrigues, L.A., da Silva, Maria Lucia Caetano Pinto, Alvarez-Mendes, M.O., dos Reis Coutinho, A., Thim, G.P., 2011. Phenol removal from aqueous solution by activated carbon produced from avocado kernel seeds, Chem. Eng. J. 174, 49-57.

Sathishkumar, P., Arulkumar, M., Palvannan, T., 2012. Utilization of agro-industrial waste Jatropha curcas pods as an activated carbon for the adsorption of reactive dye Remazol Brilliant Blue R (RBBR), J. Clean. Prod. 22, 67-75.

Shi, M., Wang, Z., Zheng, Z., 2013. Effect of Na impregnated activated carbon on the adsorption of NH 4-N from aqueous solution, J. Environ. Sci. 25, 1501-1510.

Singh, R.K., Kumar, S., Kumar, S., Kumar, A., 2008. Development of parthenium based activated carbon and its utilization for adsorptive removal of *p*-cresol from aqueous solution, J. Hazard. Mater. 155, 523-535. doi: http://dx.doi.org/10.1016/j.jhazmat.2007.11.117.

Vassileva, P., Tzvetkova, P., Nickolov, R., 2009. Removal of ammonium ions from aqueous solutions with coal-based activated carbons modified by oxidation, Fuel 88, 387-390.

Wahab, M.A., Jellali, S., Jedidi, N., 2010. Effect of temperature and pH on the biosorption of ammonium onto Posidonia oceanica fibers: equilibrium, and kinetic modeling studies, Bioresour. Technol. 101, 8606-8615.

Weber, W., Morris, J., 1963. Kinetics of adsorption on carbon from solution, J. Sanit. Eng. Div. Am. Soc. Civ. Eng. 89, 31-60.

Yu, B., Zhang, Y., Shukla, A., Shukla, S.S., Dorris, K.L., 2000. The removal of heavy metal from aqueous solutions by sawdust adsorption — removal of copper, J. Hazard. Mater. 80, 33-42. doi: http://dx.doi.org.prox.lib.ncsu.edu/10.1016/S0304-3894(00)00278-8.

Zhao, Y., Yang, Y., Yang, S., Wang, Q., Feng, C., Zhang, Z., 2013. Adsorption of high ammonium nitrogen from wastewater using a novel ceramic adsorbent and the evaluation of the ammonium-adsorbed-ceramic as fertilizer, J. Colloid Interface Sci. 393, 264-270.

Zhu, Y., Kolar, P., 2014. Adsorptive removal of *p*-cresol using coconut shell-activated char, J. Environ. Chem. Eng. 2, 2050-2058. doi: http://dx.doi.org/10.1016/j.jece.2014.08.022.

CHAPTER 7

CONCLUSIONS AND FUTURE DIRECTION

7.1 Conclusions

The present research was focused on synthesis of low-cost activated carbon prepared from agricultural by-products for removal of *p*-cresol and ammonia separately and simultaneously. The objectives were to: (1) synthesize an activated carbon possessing well developed porosity and basic oxygen functional groups for mitigation of *p*-cresol from aqueous single-solute systems, perform the characterization of the obtained activated carbon and carry out the batch experiments for kinetic and isotherm studies; (2) synthesize an activated carbon with adequate microspores and acidic functional groups for uptake of ammonia from aqueous single-solute adsorption systems, study the kinetics and isotherms of the adsorption systems; and (3) test a bi-functional activated carbon for simultaneous adsorption of *p*-cresol and ammonia in aqueous double-solute adsorption systems. The primary findings of this study are summarized below:

1) Findings from the studies to accomplish objective (1):
    - Activated carbons prepared from coconut shell-based activated carbon using zinc chloride (CSAC) and sodium hydroxide (CSAC-SH) as activating agents possess high structural stability with excellent physical strength, which is much better than activated carbon prepared from pine wood in preliminary studies.

- Physiochemical activation, in which chemical activation step is conducted after the thermal carbonization of the precursor, was found to be an effective technology for synthesis of reasonably good adsorbents.
- Adsorption on CSAC was found to be a function of initial adsorbate concentration, agitation speed, solution pH, and adsorbent dosage.
- Kinetic studies showed that adsorption of *p*-cresol on CSAC and CSAC-SH followed a pseudo-second order kinetic model and the adsorption proceeded via predominant chemisorption. Additionally, intrapraticle diffusion was rate controlling during the whole adsorption process.
- The comparison of the characterization results between CSAC-SH and CSAC demonstrated that NaOH improved the carbon properties better than $ZnCl_2$ with higher BET surface area, larger amount of microspores and measures, and more basic oxygen functional groups.
- CSAC-SH acquired a reasonably good maximum monolayer adsorption capacity Q_0 (256.9 mg g^{-1} at 298 K) for adsorption of *p*-cresol, which was much larger than that of CSAC (31.57 mg g^{-1} at 303 K) indicating that NaOH was a better activating agent than $ZnCl_2$ in this study.

2) Findings associated with studies to achieve objective (2):

- Avocado seed, being a rich agricultural by-product, can be converted into valuable activated carbon for mitigation of ammonia from aqueous solution with Q_0 of 5.446 mg g^{-1} at 298 K.

- Physiochemical activation process using methanesulfonic acid as activating agent helped modification of avocado seed-based activated carbon (AAC-MA) with well-developed porosity and sufficient acidic functional groups to attract polar ammonia.
- A pseudo-second order kinetic model was found to best describe the experimental kinetic data and Langmuir isotherm model was found to best represent the equilibrium data of the adsorption of ammonia from aqueous single-solute systems. Equilibrium of adsorption of ammonia on AAC-MA can be reached within a relative short time.

3) Findings from studies to accomplish objective (3):

- Effective *p*-cresol adsorption onto AAC-MA was observed with Q_0 of 88.03 mg g^{-1} at 298K from aqueous single-component systems.
- Being capable of uptake both of *p*-cresol and ammonia from single-solute systems, bi-functional AAC-MA was also found to be able to adsorb *p*-cresol and ammonia simultaneously from aqueous double-solute systems.
- The extended Langmuir isotherm is most suitable for representing equilibrium data of both *p*-cresol and ammonia for simultaneous adoption indicating negligible interaction and competition between these two species of adsorbates for adsorption sites. Additionally, homogeneous surface with regard of the energy of adsorption of AAC-MA was determined.

- Adsorption capacities in double-solute systems for was slightly lower than those in single-component systems with 87.79 and 3.39 mg g^{-1} for *p*-cresol and ammonia, respectively. However, the reduction amounts were insignificant, implying that AAC-MA was applicable for simultaneous uptake of *p*-cresol and ammonia.
- Specific porosity and chemical properties of containing both basic and acidic groups of AAC-MA might contribute to simultaneous adsorption.
- The synthesis process of AAC-MA from the lab-scale research may be scaled up for the practical use considering the activated carbon exhibits good quality and possess sufficient adsorption capacity for *p*-cresol and ammonia.

7.2 Future recommendations

Synthesis of effective activated carbon derived from a variety of other agricultural waste resources such as jackfruit peel, tobacco stalk, bagasse and peach seeds may also be considered for removal of *p*-cresol and ammonia separately and simultaneously. Other activating agents such as, *p*-toluenesulfonic acid should also be tested as activating agents for preparation of activated carbon. Additionally, synthesis of even better-performance activated carbon for adsorption of *p*-cresol and ammonia is still in need for further exploration, especially for improvement of ammonia uptake.

APPENDICES

Appendix A

Permissions to reuse copyright material

ELSEVIER LICENSE
TERMS AND CONDITIONS

Feb 06, 2016

This is a License Agreement between Yiying Zhu ("You") and Elsevier ("Elsevier") provided by Copyright Clearance Center ("CCC"). The license consists of your order details, the terms and conditions provided by Elsevier, and the payment terms and conditions.

All payments must be made in full to CCC. For payment instructions, please see information listed at the bottom of this form.

Supplier	Elsevier Limited The Boulevard,Langford Lane Kidlington,Oxford,OX5 1GB,UK
Registered Company Number	1982084
Customer name	Yiying Zhu
Customer address	2824 Avent Ferry RD RALEIGH, NC 27606
License number	3803110843845
License date	Feb 06, 2016
Licensed content publisher	Elsevier
Licensed content publication	Chemosphere
Licensed content title	Adsorption of phenolic compounds by activated carbon—a critical review
Licensed content author	A. Dąbrowski,P. Podkościelny,Z. Hubicki,M. Barczak
Licensed content date	February 2005
Licensed content volume number	58
Licensed content issue number	8

Number of pages	22
Start Page	1049
End Page	1070
Type of Use	reuse in a thesis/dissertation
Portion	figures/tables/illustrations
Number of figures/tables/illustrations	1
Format	both print and electronic
Are you the author of this Elsevier article?	No
Will you be translating?	No
Original figure numbers	Table 2
Title of your thesis/dissertation	Synthesis of bi-functional activated carbon for removal of p-cresol and ammonia
Expected completion date	Feb 2016
Estimated size (number of pages)	200
Elsevier VAT number	GB 494 6272 12
Permissions price	0.00 USD
VAT/Local Sales Tax	0.00 USD / 0.00 GBP
Total	0.00 USD
Terms and Conditions	Not attached

ELSEVIER LICENSE
TERMS AND CONDITIONS

Feb 06, 2016

This is a License Agreement between Yiying Zhu ("You") and Elsevier ("Elsevier") provided by Copyright Clearance Center ("CCC"). The license consists of your order details, the terms and conditions provided by Elsevier, and the payment terms and conditions.

All payments must be made in full to CCC. For payment instructions, please see information listed at the bottom of this form.

Supplier	Elsevier Limited The Boulevard,Langford Lane Kidlington,Oxford,OX5 1GB,UK
Registered Company Number	1982084
Customer name	Yiying Zhu
Customer address	2824 Avent Ferry RD RALEIGH, NC 27606
License number	3803111488131
License date	Feb 06, 2016
Licensed content publisher	Elsevier
Licensed content publication	Carbon
Licensed content title	The role of carbon materials in heterogeneous catalysis
Licensed content author	Francisco Rodríguez-reinoso
Licensed content date	1998
Licensed content volume number	36
Licensed content issue number	3
Number of pages	17
Start Page	159
End Page	175
Type of Use	reuse in a thesis/dissertation
Intended publisher of new work	other
Portion	figures/tables/illustrations
Number of figures/tables/illustrations	2

Format	both print and electronic
Are you the author of this Elsevier article?	No
Will you be translating?	No
Original figure numbers	Fig. 3 and Fig. 4
Title of your thesis/dissertation	Synthesis of bi-functional activated carbon for removal of p-cresol and ammonia
Expected completion date	Feb 2016
Estimated size (number of pages)	200
Elsevier VAT number	GB 494 6272 12
Permissions price	0.00 USD
VAT/Local Sales Tax	0.00 USD / 0.00 GBP
Total	0.00 USD
Terms and Conditions	Not attached

ELSEVIER LICENSE
TERMS AND CONDITIONS

Feb 06, 2016

This is a License Agreement between Yiying Zhu ("You") and Elsevier ("Elsevier") provided by Copyright Clearance Center ("CCC"). The license consists of your order details, the terms and conditions provided by Elsevier, and the payment terms and conditions.

All payments must be made in full to CCC. For payment instructions, please see information listed at the bottom of this form.

Supplier	Elsevier Limited The Boulevard,Langford Lane Kidlington,Oxford,OX5 1GB,UK
Registered Company Number	1982084
Customer name	Yiying Zhu
Customer address	2824 Avent Ferry RD RALEIGH, NC 27606
License number	3803120236943
License date	Feb 06, 2016
Licensed content publisher	Elsevier
Licensed content publication	Journal of Hazardous Materials
Licensed content title	Adsorption of p-cresol on novel diatomite/carbon composites
Licensed content author	H. Hadjar,B. Hamdi,C.O. Ania
Licensed content date	15 April 2011
Licensed content volume number	188
Licensed content issue number	1-3
Number of pages	7
Start Page	304
End Page	310
Type of Use	reuse in a thesis/dissertation
Intended publisher of new work	other
Portion	figures/tables/illustrations
Number of figures/tables/illustrations	1

Format	both print and electronic
Are you the author of this Elsevier article?	No
Will you be translating?	No
Original figure numbers	Adapted from Fig. 4
Title of your thesis/dissertation	Synthesis of bi-functional activated carbon for removal of p-cresol and ammonia
Expected completion date	Feb 2016
Estimated size (number of pages)	200
Elsevier VAT number	GB 494 6272 12
Permissions price	0.00 USD
VAT/Local Sales Tax	0.00 USD / 0.00 GBP
Total	0.00 USD
Terms and Conditions	Not attached

ELSEVIER LICENSE
TERMS AND CONDITIONS

Feb 06, 2016

This is a License Agreement between Yiying Zhu ("You") and Elsevier ("Elsevier") provided by Copyright Clearance Center ("CCC"). The license consists of your order details, the terms and conditions provided by Elsevier, and the payment terms and conditions.

All payments must be made in full to CCC. For payment instructions, please see information listed at the bottom of this form.

Supplier	Elsevier Limited The Boulevard,Langford Lane Kidlington,Oxford,OX5 1GB,UK
Registered Company Number	1982084
Customer name	Yiying Zhu
Customer address	2824 Avent Ferry RD RALEIGH, NC 27606
License number	3803120497679
License date	Feb 06, 2016
Licensed content publisher	Elsevier
Licensed content publication	Journal of Environmental Chemical Engineering
Licensed content title	Adsorptive removal of p-cresol using coconut shell-activated char
Licensed content author	Yiying Zhu,Praveen Kolar
Licensed content date	December 2014
Licensed content volume number	2
Licensed content issue number	4
Number of pages	9
Start Page	2050
End Page	2058
Type of Use	reuse in a thesis/dissertation
Intended publisher of new work	other
Portion	full article
Format	both print and electronic

Are you the author of this Elsevier article?	Yes
Will you be translating?	No
Title of your thesis/dissertation	Synthesis of bi-functional activated carbon for removal of p-cresol and ammonia
Expected completion date	Feb 2016
Estimated size (number of pages)	200
Elsevier VAT number	GB 494 6272 12
Permissions price	0.00 USD
VAT/Local Sales Tax	0.00 USD / 0.00 GBP
Total	0.00 USD
Terms and Conditions	Not attached

Appendix B

Supplementary material for Chapter 3

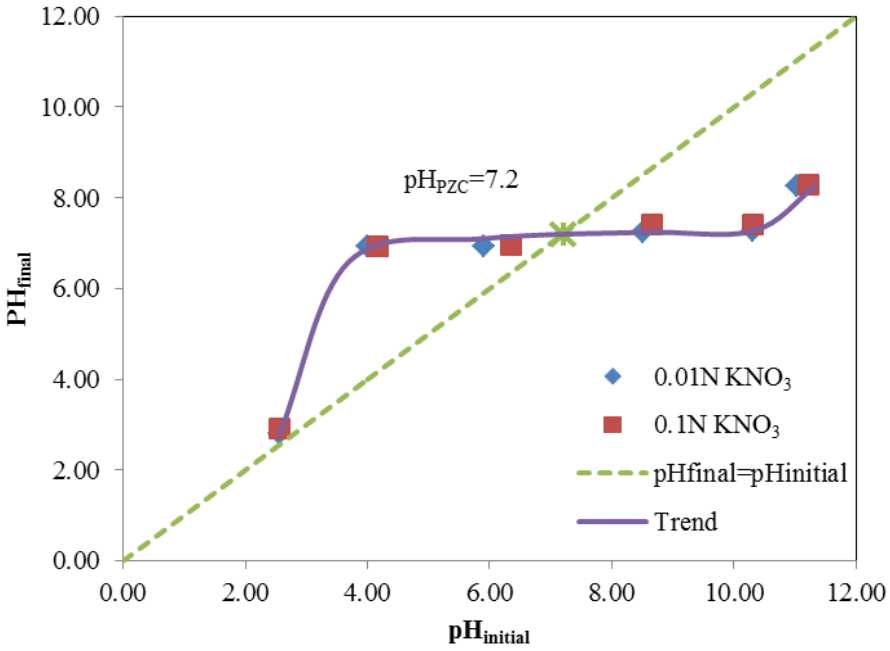

Supplementary Fig. B.1: Determination of pH_{pzc} of CSAC in KNO_3 solutions after equilibrium.

Supplementary Table B.1: Physical characterization of CSAC

Properties	CSAC
Total surface area (m^2/g)	140.02
Micropore area (m^2/g)	98.67
Total pore volume (cm^3/g)	0.0787
Miropore volume (cm^3/g)	0.048
Average pore diameter (nm)	2.249
Acid value	7.5
Yield %	25.38

Supplementary Table B.2: Boehm titration results for CSAC

Sample	Acidic groups (mmol g^{-1})				Basic group
	Carboxylic	Lactonic	Phenolic	Total	mmol g^{-1}
CSAC	0	0	0.13	0.13	0.52

Supplementary Table B.3: Pseudo-first, second order, and Elovich kinetic parameters for adsorption of *p*-cresol on CSAC

Parameter	Pseudoso first-order kinetics				Pseudo second-order kinetics				Elovich kinetic model			
	$q_{e,exp}$ (mg g^{-1})	$q_{e,cal}$ (mg g^{-1})	k_1 (min^{-1})	R^2	$q_{e,cal}$ (mg g^{-1})	k_2 (g mg^{-1} min^{-1})	$h=k_2q_e^2$ (mg g^{-1} min^{-1})	R^2	$q_{e,cal}$ (mg g^{-1})	α (mg g^{-1} min^{-1})	β (g mg^{-1})	R^2
Co (mg/L)												
25	2.18	2.091	0.0091	0.993	2.344	0.00433	0.0238	0.996	2.307	0.0561	2.256	0.988
50	4.78	4.650	0.0111	0.995	5.101	0.00260	0.0677	0.998	5.161	0.1715	1.083	0.984
100	9.34	9.006	0.0111	0.983	9.786	0.00140	0.1341	0.997	9.788	0.3648	0.5852	0.992
200	16.24	15.50	0.0107	0.976	17.30	0.00072	0.2155	0.993	16.67	0.6325	0.3449	0.987
500	24.14	23.28	0.0115	0.967	24.62	0.00061	0.3697	0.987	24.47	1.179	0.2467	0.990
pH												
2.7	21.70	21.01	0.0088	0.955	22.47	0.00051	0.2575	0.986	21.66	0.7291	0.2587	0.980
4.0	27.90	26.82	0.0089	0.937	28.56	0.00041	0.3344	0.978	26.52	1.087	0.2203	0.986
5.1	26.14	25.30	0.0086	0.946	27.03	0.00041	0.2996	0.980	24.86	0.9418	0.2312	0.967
6.1	24.53	23.46	0.0095	0.933	24.93	0.00051	0.3170	0.977	23.91	1.011	0.2459	0.989
7.0	24.14	23.28	0.0115	0.967	24.62	0.00061	0.3637	0.987	24.47	1.179	0.2467	0.990
8.3	23.84	23.34	0.0075	0.967	25.20	0.00036	0.2286	0.989	22.21	0.6682	0.2462	0.988
9.5	22.69	20.56	0.0122	0.862	21.81	0.00081	0.3853	0.948	22.05	1.517	0.2931	0.988
12.1	11.39	11.15	0.0069	0.924	12.04	0.00069	0.1000	0.952	8.79	0.4618	0.6985	0.875
Mass (g/L)												
5	30.49	28.92	0.0063	0.965	31.72	0.00023	0.2314	0.977	22.14	1.005	0.2695	0.940
10	24.14	23.28	0.0115	0.967	24.62	0.00061	0.3697	0.987	24.47	1.179	0.2467	0.990
15	23.01	22.65	0.0085	0.977	24.20	0.00045	0.2635	0.993	22.63	0.7685	0.2482	0.989
20	21.44	20.87	0.0112	0.948	21.91	0.00073	0.3504	0.984	22.54	1.147	0.2707	0.982
25	17.59	17.14	0.0123	0.944	17.94	0.00102	0.3283	0.985	19.09	1.086	0.3266	0.994
30	15.76	14.96	0.0219	0.945	15.89	0.00225	0.5681	0.997	20.87	1.437	0.3097	0.996
Agitation (rpm)												
0	18.35	18.58	0.0056	0.989	21.05	0.00028	0.1241	0.993	14.29	0.4251	0.3817	0.927
50	23.61	22.52	0.0085	0.963	24.18	0.00045	0.2631	0.984	21.09	0.9783	0.2842	0.977
100	24.14	23.28	0.0115	0.967	24.62	0.00061	0.3637	0.987	24.47	1.179	0.2467	0.990
200	26.51	25.71	0.0111	0.910	26.99	0.00060	0.4371	0.961	25.07	2.255	0.2704	0.982

Supplementary Table B.4: Kinetic parameters for adsorption of *p*-cresol for 1.5h adsorption

Experiment (Temp_Conc)	Pesudo 1st order		Pesudo 2ed order			Elovich			Intra-particle diffusion		
(K_mg/L)	R^2	K_1 (min^{-1})	R^2	K_2 (g mg^{-1} min^{-1})	$h=k_2q_e^2$ (mg g^{-1} min^{-1})	R^2	α (mg g^{-1} min^{-1})	β (g mg^{-1})	R^2	K_{id} (mg g^{-1} $min^{-0.5}$)	C
293_25	0.967	0.00603	0.968	0.00073	0.01706	0.856	0.0547	2.345	0.904	0.1087	3.544×10^{-8}
303_25	0.988	0.01164	0.988	0.00249	0.02123	0.956	0.0549	2.194	0.931	0.112	8.167×10^{-10}
313_25	0.989	0.01343	0.989	0.00264	0.02852	0.975	0.0702	1.748	0.939	0.1419	5.161×10^{-7}
293_50	0.980	0.00581	0.980	0.00037	0.02683	0.971	0.0759	1.213	0.874	0.1724	5.916×10^{-7}
303_50	0.995	0.01559	0.997	0.00189	0.06221	0.969	0.1546	0.959	0.971	0.2855	1.399×10^{-6}
313_50	0.998	0.0176	0.998	0.00231	0.06736	0.984	0.1588	0.9444	0.974	0.2913	7.474×10^{-7}
293_100	0.990	0.01748	0.990	0.00141	0.10793	0.971	0.2535	0.583	0.964	0.4685	7×10^{-7}
303_100	0.996	0.02527	0.997	0.00257	0.16300	0.994	0.3463	0.5611	0.990	0.5525	2.318×10^{-8}
313_100	0.997	0.02125	0.998	0.00171	0.15264	0.986	0.3436	0.5028	0.986	0.5853	1.161×10^{-8}
293_200	0.993	0.03062	0.996	0.00232	0.31542	0.993	0.6535	0.3746	0.992	0.9073	0.02815
303_200	0.989	0.02957	0.994	0.00217	0.31509	0.981	0.6813	0.3728	0.996	0.9237	0.04366
313_200	0.980	0.0311	0.988	0.00231	0.35461	0.966	0.7894	0.3687	0.994	0.9662	0.1805
293_500	0.99	0.0235	0.993	0.00110	0.32429	0.967	0.7441	0.2768	0.993	1.15	4.055×10^{-9}
303_500	0.986	0.03764	0.994	0.00225	0.61852	0.985	1.329	0.27	0.988	1.373	0.6168
313_500	0.982	0.04441	0.991	0.00272	0.85311	0.979	1.913	0.2607	0.971	1.519	1.182

Supplementary Table B.5: Intrapartical diffusion parameters for adsorption of *p*-cresol on CSAC

Parameter	Intraparticle diffusion model			
	K_{id1} (mg g^{-1} $min^{-0.5}$)	K_{id2} (mg g^{-1} $min^{-0.5}$)	R_1^2	R_2^2
Co (mg/L)				
25	0.1566	0.0175	0.9816	0.9987
50	0.3589	0.029	0.9972	0.9594
100	0.6025	0.0593	0.9873	0.9869
200	0.9152	0.0862	0.9902	0.9352
500	1.2563	0.1678	0.9847	0.9685
Mass (g/L)				
5	1.1300	0.2962	0.9298	0.7881
10	1.2563	0.1678	0.9847	0.9685
15	1.2263	0.1657	0.9756	0.9849
20	1.1165	0.1246	0.9575	0.9970
25	0.9335	0.1073	0.9856	0.9999
30	0.9720	0.0462	0.9612	0.9955
Agitation (rpm)				
0	0.8215	0.1884	0.9716	0.8492
50	1.0834	0.1881	0.9879	0.9611
100	1.2563	0.1678	0.9847	0.9685
200	1.1252	0.1667	0.9678	0.9811